Enabling Fairness in Cloud Computing Infrastructures

by

Ram Srivatsa Kannan

A dissertation submitted in partial fulfillment
of the requirements for the degree of
Doctor of Philosophy
(Computer Science and Engineering)
in The University of Michigan
2019

Doctoral Committee:

Assistant Professor Jason Mars, Co-Chair
Assistant Professor Lingjia Tang, Co-Chair
Associate Professor Karthik Duraiswamy
Professor Trevor N. Mudge

Ram Srivatsa Kannan

ramsri@umich.edu

ORCID iD: 0000-0003-1089-9008

To my family, Dasrath Srivatsa, Narasimhan Kannan, Mithra Kannan and Vineetha Govindaraj

ACKNOWLEDGEMENTS

To my life-coach and my undergraduate advisor Venkateswaran Nagarajan: because I owe it all to you. Many Thanks!

First and foremost I would like to express my sincere gratitude to my advisors, Jason and Lingjia. Jason, for being patient with me and trusting me. Your passion has profoundly impacted me to pursue the things I want. Lingjia, for teaching me how to articulate my thoughts with scientific rigor. Lavanya Subramanian, my mentor who traveled with me along my Ph.D. You were always there to support me throughout my Ph.D. I really owe you a lot. I thank my dissertation committee Lingjia, Jason, Trevor, Karthik - for their guidance in constructing this dissertation.

I want to thank Jeongseob. He was the first person I would approach if I had an idea. He was really critical and pushed me really hard. I would also like to thank Animesh for teaching me how to write papers. His feedback really helped me shape my papers. Mike, I am really going to miss your feedback. He helped me out right from my first project all the way up to my defense talk. Clarity Lab has been a great source of encouragement and feedback for shaping my research. Yunqi, Vini, Parker, Johann, Yiping, Chang-Hong, Shih-Chieh, Austin, Matt, Steve, Md, Hailong, and Quan were great colleagues. It was through the collaboration and discussion with you all that I grow and improve tremendously and become a better scientist. Thanks for being there during my successes and failures.

I would like to thank Davide Bergamasco from the performance engineering team of VMware for being a great mentor during my internships. His experience in data-

center research helped me identify problems for my Ph.D. I also thank Eric Schkufza from VMware research for being a great mentor. He made me look at his research with awe and taught me what it takes to be a great researcher.

Grad school is indeed a tiring journey. In this process, I am very thankful for having blessed with a great roommate – Bikash. He was there throughout my entire journey. My great moments with him will never be forgotten. I thank Srayan Datta for being a great friend. Dada started his Ph.D. with me and had also graduated with me. I had a great time at EECS 470 which continued forward with Thomas, Salsa, Karthik, and Walter. I also thank Ann Arbor's tamil gumbal Balaji, Prasanna Kumar, John Titus, Prashipa Selvaraj, Rahul, Karthik, Naveen, Maddy, UV, Ezhil, Keshav, Sandeep, Devi, Rashmi, Veena, Sandipp, Kavin, Anand, Suresh, and Subbu for helping me feel home by recreating Tamil Nadu. I also thank my other Ann Arbor friends Akshitha, Subarno, Arun, Amen, Desing, Ankush, Jana, Mani, Ananda, Javad, Naveen, Vaishnav, Nilmini, Pallavi and Digna. I had a great time during your stay at Ann Arbor.

I am very thankful to all my teachers from school and professors from undergrad for strengthening my fundamentals to deal grad school with courage. Special thanks to Uma mam and Shivakumar Sir from my school days Pughazendhi Sir and Radha Senthilkumar mam from MIT, Anna University.

Carnatic music was a great stress buster during my grad school days. I thanks my beloved guru Vidwan Vijayan Bhaskar for teaching me to play mridangam during my childhood days. He was one of the most passionate teachers, and I am fortunate to be acquainted with me. I owe him and Guru Kaaraikudi Mani a lot. I also thank Michigan Sahana for helping me rediscover Carnatic music during my grad school days. Special thanks to Krithika, Shalini, Srihari (thin one), Srihari (gym body) and Sandeep.

My first step towards my research career was initiated by Prof Venateswaran Na-

garajan (Waran). I feel I am the luckiest person in the world to have been acquainted with him. Waran is the greatest guru I can ever get and I owe my entire professional success to him. I am proud to be holding the legacy of being his student. I thank my WARFT colleagues Thina, Vinesh, Ramprakash, SR, Rajagopal, and Vignesh. I am also grateful to A Vignesh and Aswin for being great mentors at WARFT. I'm also happy to have been close with my batchmates Prashanth and Abullu from MIT, Anna University. They were great friends and mentors with whom most I have had my most elongated conversations.

I'd also like to thank my two greatest friends Mahesh and Vignesh. I feel it's incredible to have such great friends where there is absolutely no career overlap. Whenever I travel back to India, I am as excited to see Mahesh and Vignesh as my family. Living away with family for graduate education is really stressful. Having such friends back home makes one feel better. My career and personal life trajectory have been shaped with great detail because of Vignesh and Mahesh. I owe them a lot.

My family has been my biggest source of support. Thanks to my mother, Mithra and my father Kannan for supporting my educational career both financially and morally. My father's work ethic, sincerity, and commitment has been a great influence in my life. He was there to make sure I did not fall. My mother's love, affection, and commitment to my family took our family to the next level. My family is happy and prosperous because of her sincere efforts in raising her kids. I had a really happy and fun childhood which I owe entirely to my brother. He was really really awesome. I'd also thank my grandma, uncle, Abhishek and aunt, Anu for their fun times. Also my paternal aunt, Kowsalya and her daughter Jaya for their great support.

Finally, I'd like to thank my great wife, Vineetha. She had always believed in me. My life started taking a positive trajectory after her arrival. I envision her as my luckiest charm. My last days of my Ph.D. was the most stressful. She was

instrumental in making me hang in there. I am lucky to have been married to an extremely smart significant other. I am also grateful to Vineetha's parents Vedha and Shrikanth for helping us build and start our family on our own.

TABLE OF CONTENTS

LIST OF FIGURES

Figure

LIST OF TABLES

Table

ABSTRACT

Cloud computing has emerged as a key technology in many ways over the past few years, evidenced by the fact that 93% of the organizations is either running applications or experimenting with Infrastructure-as-a-Service (IaaS) cloud. Hence, to meet the demands of a large set of target audience, IaaS cloud service providers consolidate applications belonging to multiple tenants. However, consolidation of applications leads to performance interference with each other as these applications end up competing for the shared resources violating QoS of the executing tenants.

This dissertation investigates the implications of interference in consolidated cloud computing environments to enable fairness in the execution of applications across tenants. In this context, this dissertation identifies three key issues in cloud computing infrastructures. We observe that tenants using IaaS public clouds share multi-core datacenter servers. In such a situation, we identify that the applications belonging to tenants might compete for shared architectural resources like Last Level Cache (LLC) and bandwidth to memory, slowing down the execution time of applications. This necessitates a need for a technique that can accurately estimate the slowdown in execution time caused due to multi-tenant execution. Such slowdown estimates can be used to bill tenants appropriately enabling fairness among tenants.

For private datacenters, where performance degradation cannot be tolerated, it becomes critical to detect interference and investigate its root cause. Under such circumstances, there is a need for a real-time, lightweight and scalable mechanism that can detect performance degradation and identify the root cause resource which

applications are contending for (I/O, network, CPU, Shared Cache).

Finally, the advent of microservice computing environments, calls for a need to rethink resource management strategies in multi-tenant execution scenarios. Specifically, we observe that the visibility enabled by microservices execution framework can be exploited to achieve high throughput and resource utilization while still meeting Service Level Agreements (SLAs) in multi-tenant execution scenarios. To enable this, we propose techniques that can dynamically batch and reorder requests propagating through individual microservice stages within an application.

CHAPTER I

Introduction

The design choice of datacenters revolves around the use of homogeneous high-performance hardware including SSDs for storage, high bandwidth network, CPUs and compute heavy GPUs [123]. In this design style, a management service layer like a hypervisor is provisioned for enabling efficient utilization of underlying infrastructure, streamlined processing of applications, and cost-effective growth of datacenters resources [41, 65, 16, 118]. Such an approach unifies high-performance datacenter resources together with state-of-the-art hypervisor technologies for optimizing the execution of a wide variety of applications. An execution environment with such capabilities enables co-location of applications belonging to multiple tenants on a single system, improving resource utilization of the entire datacenter.

However, co-location degrades the performance of users' applications in many situations [71, 37, 133, 27, 95, 97, 84, 103]. Hence, the issues germinating from co-location might spawn a variety of problems creating an unfair execution scenario. For example, tenants co-located in the same server in an Infrastructure-as-a-Service public cloud might share microarchitectural resources like Last Level Cache (LLC) and bandwidth to memory [71, 22, 103]. This situation slows down the execution of these applications. As a result, such a slowdown will increase the cost incurred by each tenant giving rise to an unfair execution scenario.

Motivated by these limitations, there has been a wealth of prior work aiming to improve the execution efficiency of datacenters [71, 37, 133, 27, 95, 97, 84, 103]. These include a wide variety of hardware enabled approaches and software-based approaches that are existing either as standalone runtime systems or integrated as a part of the operating system/hypervisor. This dissertation argues that the key to enabling harmonious application execution in consolidated datacenters is to realize a mechanism for detecting, identifying, estimating and mitigating interference. Such a mechanism should incur low-performance overhead, should be platform-agnostic, highly accurate and should be compatible with previous, existing and future generation architectures. Towards this end, we identify and characterize such unfair execution scenarios and provide solutions categorically based on the nature and requirement of each datacenter (public clouds, private datacenters, and serverless computing infrastructures).

1.1 Motivation

This section motivates the need for techniques to enable fairness in cloud computing infrastructures. Towards this end, we compartmentalize challenges that exist in current generation clouds based on the type of datacenter and provide solutions based on the requirements of tenants utilizing a specific datacenter type.

1.1.1 Interference Estimation

Infrastructure as a Service (IaaS) cloud computing enables users to take advantage of the computing resources under the pay-as-you-go scheme by paying an hourly price per running application [11]. Customers renting IaaS public clouds now can choose resource fragments at varying granularity – the number of virtual CPUs, the amount of memory and storage size, based on their usage requirements. Cloud service providers utilize virtualization to instantiate Virtual Machines (VMs) that hosts tenant applications based on their requested configurations.

In light of the significant potential for improving resource utilization, cloud service providers consolidate VMs belonging to different tenants into a single server. This causes applications to slow down due to the sharing of specific architectural resources like Last Level Cache (LLC) and DRAM bandwidth [71, 37, 133, 27, 79]. The increased execution time that applications are subjected due to slowdown reflects directly on the price paid by the users under the pay-as-you-go scheme creating an unfair pricing scenario in IaaS public clouds.

In order to enable fair pricing in public clouds, a solution is needed to quantify slowdown of an application due to its co-runners [22, 104]. The slowdown is generally quantified as the ratio of the execution time of an application when it is running along with the co-runner to the ratio of the execution time of the application when it is running alone. In this work, we design a runtime system that can accurately estimate the slowdown exhibited by individual applications on shared cloud infrastructures.

1.1.2 Interference Detection and Mitigation

The design of private datacenters centers is centered around utilizing high-performance hardware including SSDs for storage, high bandwidth network, CPUs and compute heavy GPUs all in a single datacenter infrastructure. Such private datacenter infrastructures when coalesced with state of the art virtualization technologies offer users with isolated fragments of high-performance computing resources suited for housing a wide variety of applications.

However, there exist many situations where the performance of users applications might be degraded [95, 97, 84, 103]. For example, in VSAN (Virtual Storage Area Network), the virtual disks of a VM (Virtual Machine) are split into chunks which are then replicated and distributed to multiple physical disks on different hosts in order to provide high data availability. Under such circumstances, several VMs will end up sharing the same physical disk, which may potentially lead to a noisy neighbor

scenario. In such a scenario, a VM running a particular I/O heavy workload, causing significant contention with other VMs at disk I/O, will affect the neighboring VMs latency/throughput.

Similarly, in many instances, hypervisor software may oversubscribe server resources in order to increase resource utilization. In such situations, it is common to observe CPU, Last Level Cache, Memory Bandwidth and Network contention due to noisy neighbors. The effect of interference can be avoided by scheduling potentially contentious VMs on different machines. However, this requires datacenter providers/hypervisor software to identify problematic VMs (VMs that affect the performance of co-running applications) and also to determine the root cause of contention for each of the affected VMs.

In order to abstract private datacenter users from the effect of contention, we need a solution to detect contention and investigate its root causes during runtime. In other words, we need a system that can pinpoint an antagonistic VM and identify the root cause resource at which contention occurs (CPU, I/O, Network, Storage). In this work, we design a real-time system that utilizes system software telemetry to detect contentious VMs and identify the root cause resource at which contention occurs.

1.1.3 Guaranteeing QoS for Latency Critical Applications

Multi-tenant execution has been explored actively in the context of traditional datacenters and cloud computing frameworks towards improving resource utilization. Prior works that study multi-tenant execution have proposed to co-locate high priority latency sensitive applications with other low priority batch applications [71, 126]. However, multi-tenant execution in a serverless computing framework would operate on a fundamentally different set of considerations/assumptions. Firstly, execution scenarios in serverless computing frameworks house multiple latency critical appli-

cations belonging to different tenants [47, 120]. This is uncommon in virtualized public clouds where there is limited knowledge of the executing application. As a result, guaranteeing user defined SLAs under such execution environments becomes extremely difficult. Secondly, serverless computing framework is priority agnostic, in contrast to traditional datacenters where batch applications are given low priority while latency sensitive applications are given a higher priority. In a serverless computing framework, meeting the service level agreements (SLA) of every individual tenant is critical. Lastly, resource sharing in multi-tenant serverless execution scenarios happens at a microservice level granularity. This is in contrast to traditional datacenters where resource sharing is characterized by contention at LLC, CPU, I/O, and network.

These fundamentally unique characteristics of serverless computing frameworks motivate us to rethink the design of runtime systems that drive multi-tenancy in such frameworks. For this purpose, we design a system that enables consolidated execution of queries belonging to multiple tenants in a serverless computing framework.

1.2 Enabling Fairness in multi-tenant Cloud Computing Infrastructures

The goal of this dissertation is to enable fairness in multi-tenant cloud computing infrastructures. This section gives a brief introduction of the techniques used for enabling fairness in cloud computing infrastructures.

1.2.1 Caliper

Accurately estimating slowdown at runtime can be utilized to enable fair pricing in IaaS public clouds. Towards this end, there have been many efforts that try to estimate slowdown of applications at runtime [76, 31, 22, 40, 108, 126, 102, 84, 71].

Prior software approaches [22, 40, 126, 108] utilize an online runtime system that periodically pauses all the applications except one for a short time, thus allowing the running application to monopolize the computing resources on the system during those pause periods. The performance of the running application during such pause periods is used to determine slowdown.

A few other hardware enabled approaches [76, 31, 30, 102] designed to estimate slowdown are based on a methodology that aims at modeling interference bottom up as an aggregate of interference across multiple processor subsystems. However, this may prove to be prohibitively difficult as core counts increase and processor architectures accrue performance improvement mechanisms that are ever larger in number and complexity. These approaches leave several challenges that pose barriers to its adoption:

1. **Low accuracy:** The most recent state-of-the-art technique addressing this problem [22] **neglects the notion of application phases** and pauses co-running applications periodically at millisecond granularity. This methodology shows estimation errors of up to 40% leaving significant room for improvement in accuracy.

2. **High overhead:** It has been reported that datacenter providers tolerate no more than 1% to 2% degradation in performance to support dynamic monitoring approaches in production [92]. However, the execution time overhead of the state-of-the-art software interference estimation technique can be as significant as 12% [22].

3. **Non-reliable (or less scalable):** The accuracy and the overhead of prior approaches [22, 102, 40, 76, 31] deteriorate as the number of co-running applications increases. As the number of cores on modern servers keeps increasing, deploying a technique that inadequately supports current and future levels of

multi-tenancy would not be a preferred choice.

4. **Priori knowledge:** Another class of static techniques requires *a priori* [71, 37] knowledge about all workloads and the profiling for each type of workload. This requirement limits the types of workloads for which such a technique can be applied and, more broadly, the kind of datacenters that can adopt the approach (e.g., public clouds).

To overcome these challenges, we design a mechanism called *micro-experiments* – short-lived measurements of application performance under different conditions – to accurately estimate the interference experienced by applications due to performance degradation. On top of this mechanism, we introduce **Caliper** to estimate slowdown of an application at runtime with high accuracy and negligible overhead. To enable *Caliper*, one of the most significant challenges is to accurately, efficiently, and continuously detect phases within applications. In this work, we design a solution to identify all such phases by leveraging performance monitoring units (PMUs).

1.2.2 Interference Detection and Inestigation

Private clouds are critical for tenants that require high-performance datacenter infrastructure. In such infrastructures, it becomes the responsibility of the cloud service provider to abstract its users from noisy neighbors who contend for shared resources. An important step towards solving this problem is to pinpoint each noisy neighbor and the resource for which contention occurs. However, there exist three major challenges while tackling the datacenter contention problem.

1. **Absence of Apriori Application Profile.** New applications are getting executed in the cloud infrastructure, for which the datacenter operators do not have any prior performance profile. This makes the Detection task challenging

as there is no baseline performance to compare against to detect a change in the QoS metric.

2. **Multiple Sources of Contention.** Different applications exert stress on different subsystems of the stack (one application might only stress network while other application might have a large number of I/O requests stressing I/O system stack), requiring Investigation task to handle multiple sources of contention.

3. **Low Runtime Overhead.** The technique needs to perform both these tasks with very low-performance overhead in order to quickly adapt to the application runtime environment.

Prior relevant body of work solves these challenges partially. Bubble-up [72] and Cuanta [37] require a priori knowledge of application behavior restricting its applicability in the Detection task. While Application Slowdown Model (ASM) [103], Geiko [97], and Seawall [95] detect performance degradation, they are unable to identify the source of contention, restricting its applicability in the Investigation task. Finally, the third category of work, Deepdive [84] and CPI^2 [130], have very high overhead in performing these two tasks, making it difficult to deploy them at runtime systems.

To tackle these challenges, we present Proctor, a runtime system that continuously monitors, automatically detects and investigates a wide range of performance issues directly affect- ing the Quality of Service of VMs running in a cloud-scale datacenter, with high accuracy and low-performance overhead.

1.2.3 Guaranteeing QoS at microservice computing frameworks

Improving the resource utilization of serverless computing infrastructures is a critical and unsolved problem. There are several steps that we undertook towards

identifying and solving this problem.

- **Analysis of microservice execution scenarios.** Our investigation observes the key differences between traditional and microservice-based computing platforms – primarily in the context of visibility into the underlying microservices that exist providing exposure to application specific QoS metrics.
- **Accurate estimation of completion time at individual microservice stages.** We provide insights towards building a model that could estimate with high accuracy the completion time of individual requests at the different microservice stages and hence, the overall time of completion.
- **Guarantee end-to-end SLAs by exploiting stage level SLAs.** By utilizing the completion time predictions from the model, we derive individual stage SLAs for each microservice/stage. We then combine this per-stage SLA requirement with our understanding of end-to-end latency and slack. This enables an efficient request scheduling mechanism towards the end goal of maximizing server throughput without violating the end-to-end SLA.

Using these techniques, we built GrandSlam, a holistic runtime framework that enables consolidated execution of queries belonging to multiple tenants in a serverless cloud computing framework. GrandSlam does so by providing a prediction based on identifying "safe" consolidation to deliver satisfactory QoS (latency) while maximizing throughput simultaneously.

1.3 Summary of Contributions

The specific contributions of this dissertation are as follows.

1. **Caliper:** This dissertation presents Caliper, a novel *phase aware interference estimation* technique that is accurate, lightweight and can be used to estimate slowdown of applications belonging to multiple tenants running in public clouds.

This, in turn, can be utilized to enable fair pricing among tenants using IaaS public clouds.

2. **Proctor:** This dissertation presents Proctor, a runtime system, continuously monitors VMs in a datacenter to automatically detects and identify the sources of contention, with low overhead and high accuracy. We envision Proctor as a guide, that can direct the corrective measures for mitigating interference.

3. **GrandSlam:** This dissertation presents GrandSlam, a runtime system to guarantee SLAs among applications utilizing microservices in a serverless computing platform. This enables an efficient request scheduling mechanism towards the end goal of maximizing server throughput without violating the end-to-end SLA.

CHAPTER II

Background and Related Work

In this Chapter, we give a background and survey the related literature to the topics covered in this dissertation. These include prior efforts in estimating slowdown due to interference online, as well as techniques that have been used to enable co-location to improve datacenter server utilization and techniques to detect interference due to contention at I/O, network, CPU and Last Level Cache.

2.1 Interference Estimation

There have been many prior studies to detect performance interference in a variety aspects of architectural resources. We look first into the hardware enabled approaches and then address the prior work that utilizes system and OS level approaches for detecting interference.

Hardware techniques: There are several approaches that try to estimate slowdown due to contention in shared caches, memory controller and bandwidth [83, 31, 105, 90]. Nesbit et al. employed the network fair queuing model in the memory scheduler to meet the fairness [83]. Mutlu and Moscibroda focused on DRAM specific architectural features such as row buffers and DRAM banks [76]. They utilized memory scheduling techniques to ensure the fairness between multiple threads. Ebrahimi et al. extended the fairness problem in memory subsystems by including shared last

level cache and memory bandwidth [31]. This work focused on the source incurring performance interference and proposed throttling mechanism by controlling injection rates of requests to alleviate the contention of shared resources. Suh et al. firstly discussed the cache partitioning scheme to efficiently use the shared resources [105]. Qureshi et al. proposed utility based cache partitioning technique to achieve high performance [90].

Software/Systems approaches: There are many efforts introducing software frameworks and proposing the new designs of operating systems [37, 71, 126, 108, 82, 86, 68]. Q-Cloud measures the resource capacity for satisfying QoS in a dedicated server called as a staging server and then performs placement decisions based on choosing the right server that will be profitable to minimize interference [82]. To accurately estimate the performance interferences without profiling on a dedicated server, Bubble-up [71] and Cuanta [37] designed the synthetic workloads to understand the degree of interference when co-locating applications. Meanwhile, Soares et al. studied the concept of pollute buffer in shared last level caches to prevent filling the shared caches as non-reusable data. Their work focused on improving the utilization of shared caches through OS-level page allocation [98]. Zhuravlev et al. extended the CPU scheduler to alleviate the some of the interferences. The goal of this work is to schedule the threads by evenly distributing the load intensity to caches [133]. Blagodurov et al. proposed that the scheduler needs to consider the effects of NUMA [21]. Also, there are numerous prior studies to solve the contention problems such as shared last level cache and NUMA by scheduling virtual machines [6, 91, 69].

2.2 Interference Detection and Mitigation

In this section we discuss work relevant detection and mitigation of interference causing application/VM behavior and diagnosing its root causes. We present related work that attempts to mitigate CPU, I/O and network contention.

VM Management: State-of-the-art VM management tools such as vSphere [41], XenServer [124] or resource management tools utilized in IaaS public clouds like Microsoft Azure [67] and Amazon Web Services [11] performs VM placements naively using primitive factors and metrics. For example, VMware's Distributed Resource Management (DRM) [39] takes into account factors like load balancing and power management as factors for optimal placement of VMs. However, this is agnostic towards performance issues due to disk failures, congestion in the network or contention by neighboring VMs. Proctor can complement such systems by informing datacenter providers information pertaining to problematic VMs and its root causes. This can motivate smart VM placement strategies.

Contention Detection Techniques Major classes of contention detection techniques focus on a particular aspect present in the system rather than providing an integrated approach. Zhuravlev et al.extended the CPU scheduler to alleviate the degree of interferences in a native system. The goal of this work is to schedule the threads by evenly distributing the load intensity to caches[134]. Shieeh et.al [95] tries to eliminate disk contention by utilizing a log-structured design for disk arrays. Parda [38] and IOFlow [110] tries to address contention at the disk level by observing latency of I/O requests and re-ordering disk queues. Seawall [96], EyeQ [55] and Hadrian [15] focus mainly on isolating interference in network in multi-tenant environments. However, all these techniques fail to provide an integrated solution for hyperconverged environments where contention exists at storage, network and in CPUs.

A Priori Knowledge Another class of applications observe correlation between various system parameters to detect performance issues in runtime and its root causes [4][119][125][77][63]. Typically, these techniques leverage baseline performance from a set of training applications and provide predictive solutions at runtime for unknown applications. However, the hyper-parameters present in current day systems

are too complex to create a generalized model for prediction. Moreover, in current generation datacenters, we observe system configurations to be highly dynamic which is directly reflected on the application's performance. Hence, in addition to being agnostic towards the nature of the application, it becomes mandatory for our solution to be adaptable towards changing characteristics of system as well as newer systems.

2.3 Guaranteeing Response Latencies in Microservice Execution Frameworks

Prior literature on guaranteeing response latency fall into two primary categories: Improving QoS without violating latency constraints, managing SLAs in multi-stage applications.

2.3.1 Improving QoS without Violating Latency Constraints

Prior work on addressing response latency variation and providing quality of service (QoS) guarantees have primarily been in the context of traditional datacenters [111, 71, 126, 28, 70]. Bubble-Up [71] and Bubble-Flux [126] quantify contention for last level cache capacity and memory bandwidth towards enabling co-location of a latency critical application alongside batch applications. However, these techniques prioritize the latency critical user-facing application and end up significantly hurting the performance of the co-running batch applications. Paragon [28] and Whare-Map [70] utilize runtime systems using machine learning techniques like collaborative filtering and sensitivity analysis towards identifying the right amount of resources required for guaranteeing QoS in heterogeneous datacenters. However, these techniques are designed for traditional datacenter applications like Memcached, Web Search etc. There is some prior literature that attempts to estimate performance at co-located situations in accelerator environments [56, 25, 24, 64, 5, 109, 113, 112]. Baymax [25]

predicts the behavior of tasks executing in a GPU accelerator context. Prophet [24] models the interference across accelerator resources in co-located execution scenarios. However, neither of these techniques cater to the needs of a microservice execution framework, as they do not tackle the challenge of providing solutions for guaranteeing latency for applications containing multiple stages. A small body of prior work also focusses on batch processing OLD requests [43, 74]. In addition to that, none of these techniques have attempted to perform dynamic batching which is critical in improving the throughput when DNN based artificial intelligence applications are being executed.

2.3.2 Managing SLAs in Multi-Stage Applications

Recent prior works have identified the advantages of architectures/applications that are composed of multiple stages, especially its ease of deployment [53, 59, 115, 89, 48, 106, 54, 46, 32, 58]. Under such scenarios, support for multi-tenancy as well as schemes to abstract users from the impact of multi-tenancy would be critical. However, explorations in this direction by companies such as Facebook [60], Microsoft [53, 89] and academic institutions neglect multi-tenant execution scenarios [116, 127]. However, the most relevant prior works that have looked into multi-stage applications from the academic standpoint are as follows:

TimeTrader. [116] addresses the problem of meeting application specific latency targets for multi request execution in Online Data Intensive applications (OLDIs). Towards meeting that objective, they employ a mechanism that tries to reorder requests that contain varying slack using merely an **Earliest Deadline First** scheduling methodology. However, this technique assumes that the applications contain a single processing stage and fails to acknowledge the intrinsic latency variance across multiple stages. Hence, it deprioritizes requests assuming to contain relaxed latency constraints, however, would be subjected to a bulk of compute at its later stages.

This leads to diminished effectiveness in mitigating response latency for multi-stage applications, as we quantitatively show in Section 5.3.

PowerChief. [127] seeks to identify the bottleneck stages present in multi-stage voice and image based intelligent personal assisstant applications towards employing dynamic voltage frequency scaling to boost partial execution stages. However, PowerChief does not strive to guarantee SLAs at a user/request level. Furthermore, the proposed solution is not generalized for a microservice execution framework which handles requests from multiple tenants and focuses on a particular class of applications.

CHAPTER III

Caliper: Interference Estimator for Multi-tenant Environments Sharing Architectural Resources

One of the major drawbacks of datacenter co-location is the slowdown caused to the execution of applications. Under such circumstances, it is essential to have the ability to estimate the slowdown of applications accurately. Such slowdown estimates could enable resource allocation of shared resources to each application in a slowdown aware manner motivated towards providing strong Quality-of-Service (QoS) guarantees. Also, in Infrastructure-as-a-Service (IaaS) clouds, such a mechanism could be used to bill its customers appropriately based on the amount of slowdown that their applications have been subjected to by the co-running applications [102, 22].

In this study, we design a mechanism called *micro-experiments* – short-lived measurements of application performance under different conditions – to accurately estimate the interference experienced by applications due to slowdown. On top of this mechanism, we introduce **Caliper** to estimate slowdown of an application at runtime with high accuracy and negligible overhead. A micro-experiment is a period during which the performance of an application is abstracted from the interference incurred by co-runners, using which an accurate estimate of its slowdown can be obtained. One of the most crucial challenges while utilizing micro-experiments for estimating the slowdown is to determine when micro-experiments should be performed. We ob-

serve that interference does not change significantly within a single application phase. Thus, the problem of identifying when to perform a micro-experiment boils down towards identifying phases of applications at runtime while executing with co-runners. Triggering a micro-experiment on the application at each of its phases once allows the runtime to estimate co-runner interference with negligible overheads accurately.

To enable *Caliper*, one of the most significant challenges is to accurately, efficiently, and continuously detect not only phases within applications but also phases in application's co-runners. In this work, we design a solution to identify all such phases by leveraging performance monitoring units (PMUs). Since each application has different sensitivities towards architectural resources, we identify the right set of PMU types that can differentiate phase changes across a wide variety of unknown applications. We perform cross-validation on these selected PMU types on a spectrum of application workloads to demonstrate generality.

With *Caliper*, we are able to estimate the slowdown at multi-tenant execution scenarios accurately with a mean absolute error of 4% and negligible overhead of less than 1% for a broad spectrum of workload scenarios when executing 16 applications, making it readily deployable in current and future datacenters.

3.1 Motivation

In this section, we introduce key challenges that are present while co-locating multiple batch applications in multi-core systems. We then illustrate the state-of-the-art techniques that try to address these challenges and their limitations.

3.1.1 Multi-tenant Execution of Batch Applications

Modern computer systems host a wide range of applications of varying nature. These applications are broadly classified into two types (1) batch applications and (2) user-facing applications. Applications which are of batch type are throughput

oriented and not user-facing. This type of application represents today's workloads that execute in datacenters and clouds. Consolidation of such applications to increase the resource utilization of the system is a common trend [11, 13]. On the other hand, another class of applications like Memcached and Web Search is latency critical/user-facing and hence is required to meet strict Quality of Service (QoS) guarantees. As a result, the consolidation of such latency critical applications with other applications is generally avoided as co-location will affect the latency of these applications significantly [132, 1, 73]. These applications are typically housed in private datacenters or run on dedicated machines that guarantee Service Level Agreements (SLAs).

Although the consolidation of batch applications onto a single server increases the resource utilization, it has a direct impact on individual application performance. State-of-the-art virtualization technologies try to provide performance isolation at some levels. Current hypervisors perform:

1. Strict CPU reservations by disallowing sharing of CPU cores among different applications [65, 16].

2. Statically partitioning DRAM memory and disk space among different applications [65, 16].

3. Static partitioning of I/O and network bandwidth proportionally among applications using SR-IOV [57, 87].

However, applications are still slowed down mainly due to contention at the last-level cache (LLC) and main memory bandwidth. The resource contention at the LLC and main memory bandwidth increases the overall memory access latency, significantly slowing down the execution of different applications. Hence, it becomes critical to identify and gauge the slowdown applications are subjected to when they are housed at multi-tenant execution scenarios. As a major step towards solving this

problem, prior approaches try to precisely estimate the amount of slowdown each application which is subjected to in multi-tenant execution scenarios [102, 22].

3.1.2 Limitations of the State-of-the-art Approach

Broadly, state-of-the-art approaches that try to estimate slowdown are classified into two different categories – **static approaches** that require a priori knowledge about the applications executing and **dynamic approaches** which can perform slowdown estimation for unknown applications. In this section, we enumerate the limitations of the state-of-the-art static and dynamic approaches that try to solve this problem.

3.1.2.1 Static Approaches

Prior static approaches like Bubble-Up [71] and Cuanta [37] have shown to be effective at generating precise performance predictions at co-located execution scenarios with high accuracy. However, there exist several primary limitations of the work, including requiring a priori knowledge of application behavior and the lack of adaptability to changes in application dynamic behaviors. These limitations restrict the possibility of deploying such static approaches for a variety of datacenter infrastructures which encounter unknown applications on a regular basis. (e.g., private datacenters and public clouds)

3.1.2.2 Dynamic Approaches

Another class of prior works, that does not require a priori knowledge, has attempted to estimate slowdown of applications due to shared cache capacity and/or memory bandwidth interference [22, 126, 102]. The most recent prior work by Breslow et al. [22] is software based that utilizes a technique called *POPPA*. The main motivation behind POPPA towards estimating slowdown is based on modeling interference

as a ratio of solo and co-located execution performance. While co-located application performance can be directly measured at runtime, it is challenging to estimate solo performance of an application while running with co-runners simultaneously. Towards obtaining an estimate of solo performance, POPPA periodically pauses all co-running applications for a very short time except one application repeatedly at fixed time intervals as depicted in Fig 3.1a. The pause periods allow it to monopolize system resources and (briefly) match its solo performance. POPPA has several limitations as it suffers severely from low accuracy and high overheads especially as the number of application contexts increases.

On the other hand, there is a class of literature that has attempted to tackle the problem of estimating slowdown at runtime by utilizing novel hardware to track application interference among individual processor subsystems, which are taken together to model the overall interference of the applications [76, 30, 31, 102]. The most recent work by Subramanian et al. presents Application Slowdown Model (ASM). This work is based on the hypothesis that performance of each application is proportional to the rate at which it accesses the shared cache. Hence, in order to identify the shared cache access rate, it maintains an auxiliary tag store for each application, which tracks the state of the cache in a situation where the application would have been running alone. Every application that is co-located within the system utilizes this specialized hardware periodically in a round robin fashion to collect its corresponding shared cache access rates, which in turn is utilized by ASM to estimate its corresponding slowdown. One of the key limitations of ASM is that it requires additional hardware support precluding it from being used as a solution on existing commodity servers [76, 30, 31, 102, 101, 35, 34].

The combination of the poor accuracy, overhead, inadequate support for multi-tenancy, deployability, requirement of additional hardware support significantly limits the applicability of the prior approaches. Towards satisfying these shortcomings, we

	Bubble-Up [71]	POPPA [22]	ASM [102]	FST [31]	Caliper
Low overhead	✓				✓
No additional hardware	✓	✓			✓
No offline profile			✓	✓	✓
Estimation error	7%	45%	20%	30%	4%

Table 3.1: Comparison between Caliper and other interference estimation techniques

design a technique that can be deployed readily in production-grade datacenters. **Our technique can accurately estimate slowdown in executions scenarios that encounter a wide class of unknown applications**, unlike prior static approaches [71, 37] that require a priori knowledge of the executing applications. Table 3.1 presents a comparison between Caliper and sever other interference estimation techniques.

Later in Section 3.5.3, we experimentally evaluate each of these scenarios to illustrate the shortcomings of the prior dynamic approaches [22, 102]. Then, we show how our proposed phase aware interference estimation technique is able to estimate slowdown accurately with negligible overhead even when the number of simultaneously executing applications is up to 16 contexts as existing in modern datacenters.

3.2 Overview of Caliper

In this section, we describe **Caliper**, a runtime system for estimating interference at multi-tenant execution environments.

Goal. The design goal of Caliper is to accurately estimate the slowdown of an application at runtime. To achieve this, we need to gauge the performance of the application running with co-runners, $Perf_{(co-run)}$, as well as the performance of the application when it is running alone, $Perf_{(solo-run)}$. Using these quantities, the slowdown of the applications can be easily estimated by the following Equation 3.1.

$$slowdown = Perf_{(co-run)}/Perf_{(solo-run)} \tag{3.1}$$

We have utilized Instructions Per Cycle (IPC) as the metric to quantify performance. $Perf_{(co-run)}$ from equation 3.1 is the IPC of the application during co-location and is directly measured when the application is running along with the co-runners. $Perf_{(solo-run)}$ is the solo execution performance of the application. IPC can be measured easily and cheaply on commodity processors. A wide body of prior interference estimation techniques utilizes IPC as their primary metric to quantify performance [102, 22, 40]. For even latency-sensitive applications, a prior study from Google leveraged the CPI (Cycles Per Instructions) metric as a performance indicator [131]. Although the metric may not be highly accurate for some applications, it is used to only guide the performance estimation.

Approach. The primary objective of this study is to be able to precisely estimate $Perf_{(solo-run)}$ even during the presence of co-runners. To achieve this goal, we introduce a software technique, called *micro-experiment*. **A micro-experiment is a short-lived runtime period for a few milliseconds during which an experiment is run to collect a measurement of interest.** Our runtime system performs micro-experiments by opportunistically pausing the execution of an application's co-runners for a small amount of time so that the resource contention is eliminated temporarily in the system. The result of such a micro-experiment represents an accurate estimate of the application's solo execution performance and this estimation along with $Perf_{(co-run)}$ (direct performance measurement of an application when it is run together with other applications) can be used as a basis to obtain the slowdown at runtime.

Challenges. To keep the cost of the estimation process low, we need to address a key challenge. A recent prior study that periodically pauses co-running applications

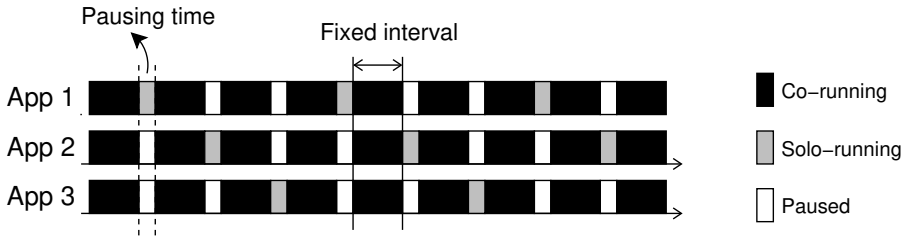

(a) POPPA [22]

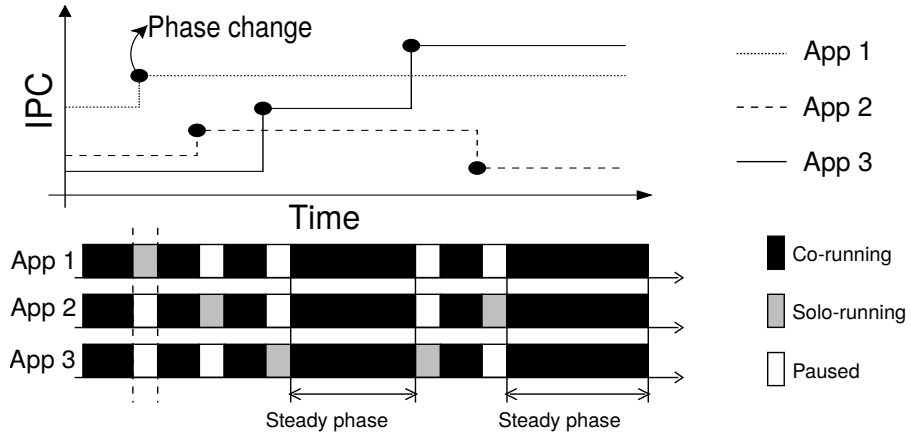

(b) Caliper

Figure 3.1: Interference estimation by *POPPA* [22] vs. *Caliper*

to estimate the performance degradation has been shown to cause non-negligible overheads [22]. This is due to the following reasons:

1. Frequent pausing can disturb forward progress of the applications due to the execution stalls.

2. Pausing an application evicts its entries present in hardware caches, TLBs, BTBs, etc. This exacerbates the performance overhead problem.

3. As the number of cores in a server increases, more applications (or VMs) can be housed in servers. Under such circumstances, periodically pausing every co-running application will increase the effective time for which individual applications is paused. Hence, a naive technique like periodic pausing becomes an unsuitable solution for operation at scale.

Thus, it is essential to identify when micro-experiments need to be triggered. In

this study, we overcome this challenge by utilizing phase boundaries as the triggers for conducting micro-experiments. The key observations that led towards utilizing phase boundaries as triggers are as follows. First, the execution behavior of applications does not drastically change within a single phase. This means that we do not need to estimate slowdown by performing micro-experiments within a steady phase. Second, we observe that the number of phase changes is not large in most applications, as also observed by previous works [94, 29, 42]. The majority of applications have a very few phases spanning over an execution time which range from a few minutes up to half an hour [81]. It gives us an opportunity to opportunistically conduct our micro-experiments technique so that we are able to avoid excessive pauses for the common case where applications have very few phase changes.

Fig 3.1b illustrates how Caliper estimates the slowdown by using micro-experiments. Whenever there is a phase change, we perform a micro-experiment by pausing all the co-running applications giving an opportunity for the un-paused applications to eliminate the resource contention. Then, we are able to measure $Perf_{(solo-run)}$ for the application without the resource contentions. However the most recent work that ties to estimate slowdown during runtime [22], pauses the co-running applications in a periodic fashion as shown in Fig 3.1a. We have conducted micro-experiments using 75 milliseconds as a pause period. The parameter is empirically determined in our testbed to monopolize architectural resources during that time. Section 3.5.2 talks in detail about the choice of our pause period. As a result, we can estimate the slowdown with negligible overheads of less than 0.5% for most of the situations. We will discuss the parameter sensitivity in the evaluation section.

While performing micro-experiments, our runtime estimates $Perf_{(solo-run)}$ of an application at every phase boundary. We aggregate the estimation of slowdown at every these individual phases of the application to calculate the slowdown for the entire execution of the application as shown by Equation 3.2.

$$Perf_{(solo-run)} = \frac{IPC_{(1)} \times T_{(1)} + IPC_{(2)} \times T_{(2)} + ... + IPC_{(n)} \times T_{(n)}}{T_1 + T_2.... + T_n} \tag{3.2}$$

where, $Perf_{(solo-run)}$ is the estimated IPC of solo execution of an application, $IPC_{(i)}$ is estimated IPC of solo execution of the application during phase i, $T_{(i)}$ is the time for which the application remains in phase i and n is the total number of phases in the application.

3.3 Application Phase Behaviors

In this section, we describe phase behaviors of applications in multi-tenant execution environments. Traditionally, phases can be defined as intervals within the execution of a program with similar behavior [42]. Phase changes typically manifest themselves as observable changes in execution behavior of applications. Although there have been many efforts to detect phase changes of a single application via performance monitoring units (PMUs) [52, 94, 42, 29], it is challenging to precisely identify phase boundaries in multi-tenant environments. This is because the PMU-based measurements of individual applications in multi-tenant environments are affected by the behavior of co-running applications. Prior techniques are unreliable when multiple applications are simultaneously running and hence cannot be directly applicable to our runtime system.

3.3.1 Two Classes of Phase Changes

As a first step towards detecting phase changes in co-located environments, we taxonomize phases detected by PMUs (e.g., as shifts in an application's CPI) as falling into one of two classes – *endogenous* phase changes that result from an application's innate behavior and *exogenous* phase changes that result from co-running applica-

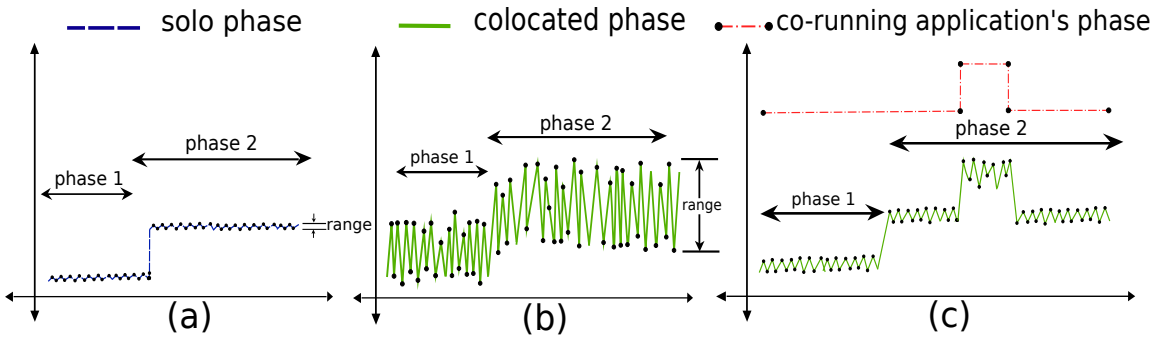

Figure 3.2: (a) Solo Execution of application. (b) Fluctuations in PMU type during co-location. (c) Co-phase interference during co-location

tions. Thus, the goal of our runtime system is to accurately identify endogenous phase changes while minimizing the detection of exogenous phase changes. This is critical as exogenous phase changes are false positives incurring unnecessary micro-experiments. It results in increasing the overhead of our runtime system. In the next subsection, we investigate the causes of exogenous phase changes in further detail.

3.3.2 Characteristics of Exogenous Phase Changes

To study the characteristics of exogenous phase changes, we observe PMUs when an application is executing along with its co-runners. Through these observations, we identify two critical reasons contributing to exogenous phase changes.

Fluctuation. PMU-based measurements of a single phase are a set of discrete, time series based, numerical quantities that lie between a range possessing minuscule variation as shown in Fig 3.2 (a). However, in the presence of co-runners, PMU-based measurements belonging to a single phase of the same application fluctuate a lot. In such scenarios, some of the PMU-based measurements lie in the range of a different phase, making it challenging to determine phase boundaries. Fig 3.2 (a) represents the execution of an application when it is running alone. Fig 3.2 (b), represents the execution of an application when it is executing along with a co-runner. From Fig 3.2 (b), we can clearly see that some PMU measurements from phase 1 lie in the range

of the PMU measurements from phase 2 and vice versa. This makes it challenging to identify phase boundaries. We have observed this phenomenon especially with PMU measurements corresponding to micro-architectural entities like last-level cache misses that are shared by multiple cores.

Co-phase interference. Phase changes in one application can cause changes to other co-running applications. We call this phenomenon as co-phase interference. Fig 3.2 (c), again represents the execution of an application when it is executing along with a different co-runner. From Fig 3.2 (c), we can clearly see that the change in PMU measurements corresponding to co-phase interference is difficult to be distinguished from endogenous phase changes.

Our goal here is to build a robust **phase aware runtime system** that detects endogenous phase changes while minimizing the detection of exogenous phase changes. This is because triggering micro-experiments during exogenous phase changes is undesired as they will result in increasing the performance overhead due to pausing of co-runners.

3.4 Identifying Phase Changes during Co-location

The primary goal of Caliper's phase detection approach is to detect endogenous phases (true positives) while ignoring exogenous phases (false positives) at runtime. For this purpose, we propose a PMU-based mechanism. The primary objective of our mechanism is to identify the representative PMU types which accurately detect every single endogenous phase change while neglecting all exogenous phases. In addition to that, the extracted PMU types should be generic. In other words, it should be able to detect endogenous phase changes even for an unknown application whose phase behavior has not been witnessed before. For this purpose, we first assess each PMU type, to detect phase changes for a training set of applications. We then **cross validate** to examine its ability to detect endogenous phases and ignore exogenous

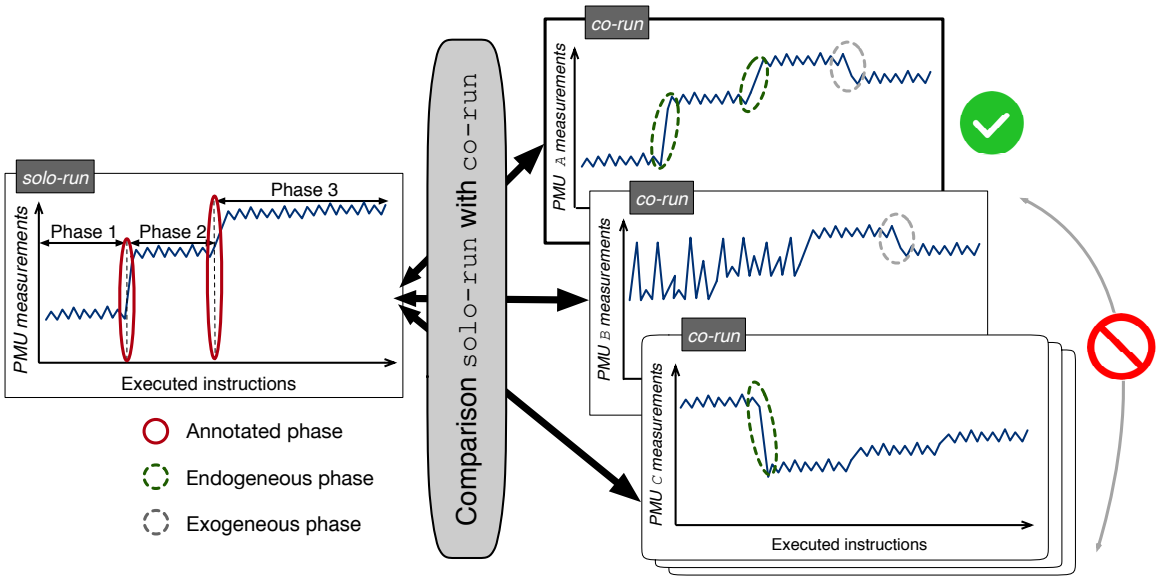

Figure 3.3: Comparing phases during co-located execution with phases present in solo execution

phases for unknown applications. This determines the generality of each PMU type. Based on the ability of each PMU type, we choose the best PMU type.

The initial step in this process is to carefully choose our training set of applications to cover a wide range of contentiousness, sensitivity and phase changing attributes [107]. The list of training applications is shown in the first column of Table 3.2. We use `astar` as our training co-runner which is cross-validated in our evaluation under section 4.4. The application `astar` from SPEC CPU2006 is known to be both contentious and to have numerous and rapidly changing phases [107], which can train our model to be resistant against both fluctuations as well as co-phase interference. With these pointers, we undertake the following three-step approach to extract the set of PMU types that can be utilized for phase detection.

(1) Comparing PMU measurements during co-run with solo execution. We execute the training set of applications alone to obtain PMU measurements during solo execution. We manually annotate the endogenous phases present in each of the training set of applications.

We then collect PMU measurements for each application present in training set

during co-location. By using the PMU measurements during co-location, we verify for each PMU type its ability to detect endogenous phases by comparing the timestamps corresponding to the actual phase changes that happen during solo execution (from the annotated phases during previous step). This process is illustrated in Fig 3.3 as we observe that the measurements for PMU `A` detect all the two endogenous phases present which are confirmed by the annotated solo execution of the application. However, the measurements for PMU `B` could not detect any endogenous phase changes. It just detects an exogenous phase change which is not desired. With the PMU `C`, it detects only an endogenous phase chase, but misses the other endogenous phase. So, the PMU type `A` is resilient for the application to detect phase changes in multi-tenant environments. We performed above process for 18 different PMU types.

(2) Obtaining PMU scoreboard. We then quantify the effectiveness of each PMU type that was successful in identifying phase changes during the previous step (1). This quantification helps in selecting the best PMU type that detects every possible phase change present in the system. This is done by obtaining the PMU scoreboard which will be discussed in detail at Section 3.4.1.

(3) Selecting the final set of PMU types. From observing the best PMU type for every single application present in the training set, we obtain a single set of PMU type(s). Those PMU types can be utilized to detect phase changes across a diverse class of application. We describe this step in the Section 3.4.2.

3.4.1 Obtaining PMU Scoreboard

The motivation of PMU scoreboarding is to quantify the effectiveness of each PMU type. Using this quantification, we obtain a common set of PMUs that can work effectively towards identifying phase changes. Our PMU scoreboarding quantifies PMU types by gauging how steep change in PMU measurements are at each phase boundary. We use a technique called step detection to quantify steepness at each

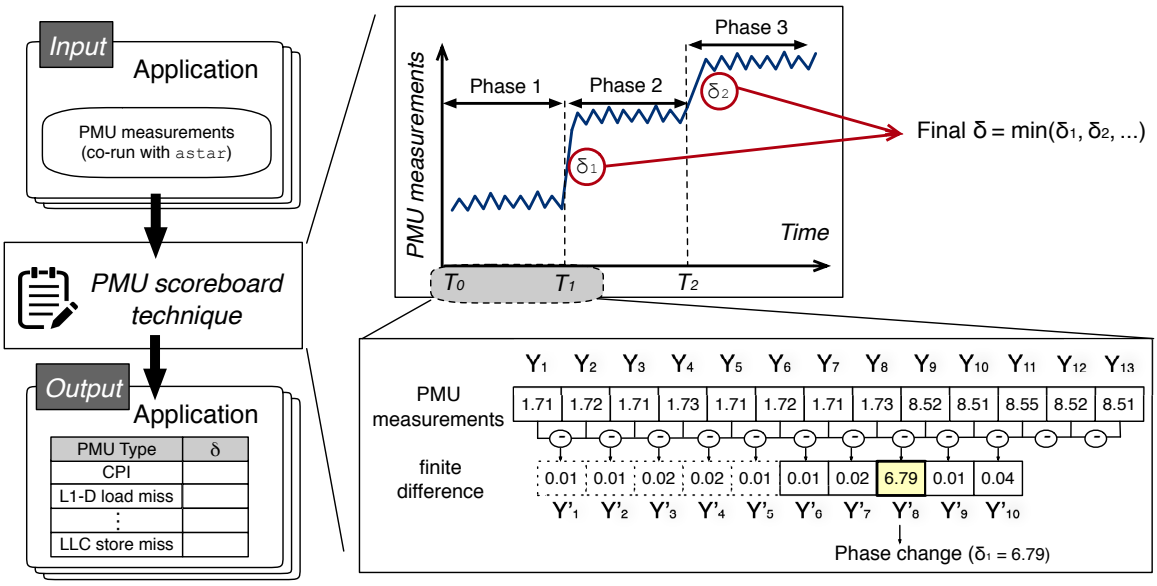

Figure 3.4: Overview of PMU scoreboard technique

phase boundary. Fig 3.4 shows the overall flow for obtaining the PMU scoreboard.

Inputs. Application and training dataset of time series PMU measurements during co-location.

Output. Threshold of separation (δ, described below) quantifying the steepness of a PMU type at phase boundary for an application.

Objective function. To quantify the effectiveness of a PMU type we assess the steepness magnitude expressed by PMU measurements during phase change (higher variation means PMU type distinguishes phase boundaries significantly better).

Methodology. The steepness is obtained by performing the step detection scheme. The step detection scheme is a process of finding abrupt changes in a time series signal and internally uses a technique called finite difference method for identifying abrupt changes. The fundamental hypothesis of finite difference method for identifying abrupt changes is based on the fact that the absolute difference between subsequent time-series measurements is very high at the exact point where the abrupt changes occur.

Mathematically, the finite difference of a time series signal is the rate of change

Workloads	PMU rank		
	1st	2nd	3rd
astar	**CPI**	branch	L1-D load miss
bzip2	**LLC store miss**	CPI	L1-D load miss
cactusADM	**L1-D load miss**	L1-D load	CPI
dealII	**CPI**	L1-D load	branch
mcf	**L1-D load miss**	CPI	LLC load
milc	**LLC store miss**	L1-D load	branch
xalancbmk	**LLC store miss**	LLC load	L1-D load
tonto	**L1-D load miss**	branch	CPI

Table 3.2: PMU types ordered by their effectiveness

in the individual elements. We implement the finite difference method by performing pair wise difference of subsequent elements present in the time series using the following formula :-

$$Y' = \frac{Y_{j+1} - Y_j}{2\Delta T} \qquad\qquad Y'_j = Y_j \ (for\ 1 < j < n-1)$$

where Y_j is the j^{th} points present in the time series, n being the number of points, ΔT being the difference between the number of timestamps for time series values. The result highlights the drastic change by showcasing a high value for Y'. Figure 3.4 clearly illustrates this where we can see a sharp increase in the PMU measurement at time T_1 (at the point Y_9). Its corresponding finite differential value is very high at point Y'_8, which is utilized to indicate a phase change at that timestamp T_1.

Based on statistical analysis by prior studies, abrupt changes are defined as points that are higher than three standard deviations above or below mean. The lowest numerical value of each such abrupt change obtained by step detection is returned as the threshold of separation δ for a PMU type that is being utilized to perform phase detection for an application. For the example given at Fig 3.4, the value of δ is the minimum of the value of δ_1 and δ_2.

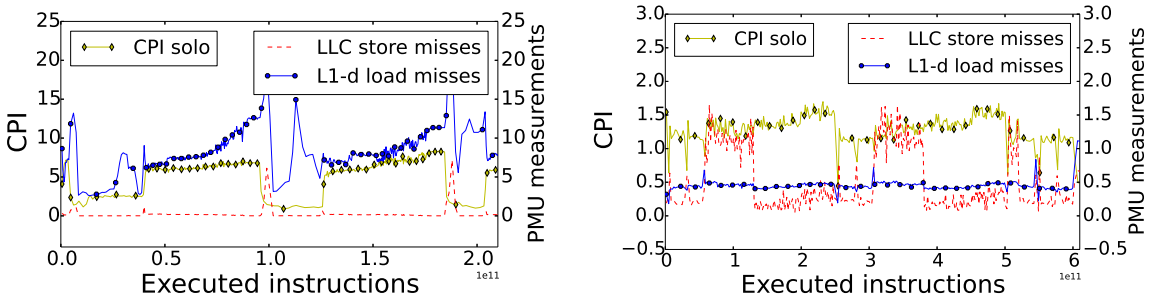

(a) `mcf` (b) `milc`

Figure 3.5: Phase changes triggered by PMU types when running with `astar`. Single PMU type is insufficient to detect phase changes

3.4.2 Ranking and Selecting PMU Types

In order to choose appropriate PMU types for identifying endogenous phase changes, we rank PMU types for every single application using the δ value (threshold of separation) obtained from the PMU scoreboarding technique. From that, we choose the PMU type that is capable of detecting endogenous phases across all the applications. In this paper, we have shown the top 3 PMU types in Table 3.2 for each application that are ranked using the δ value.

However, an observation from our training experiments whose results as depicted in Table 3.2 shows that no single PMU type can detect phase changes across all the training set of applications. In other words, there can be a situation where an architectural resource that can detect phase changes on an application could fail to detect phase changes completely on a different application. We illustrate this hypothesis based on a real-world example.

Fig 3.5 shows an example where a single PMU type will not be able to identify phase boundaries across two different applications. Each application requires different PMU types to precisely detect phase changes. In other words, `mcf` requires *L1-d load misses* while `milc` requires *LLC store misses* and vice versa fails. The x-axis indicates the cumulative number of instructions executed as time progresses. The left y-axis featured as yellow (diamond) line shows the CPI of the applications when running

alone and the right y-axis and the blue (circle) and red (dashed) line show the selected hardware performance monitors for the application when running with three instances of `astar` as co-runners.

From Fig 3.5 (a), we find out that the PMU type, *L1-d cache load misses*, can effectively detect phase changes of `mcf` in co-located environments. This is not true for the application `milc` as the same PMU type *L1-d cache load misses* fails to detect phase changes as shown in Fig 3.5 (b). These results motivate the need for multiple PMU types to capture phase changes across a variety of applications. To achieve this, we undertake an approach where we observe a set of architectural resources (*CPI*, *LLC store miss*, and *L1-D load miss*) in contrast to a single resource. Moreover, to avoid missing endogenous phase changes, we use a conservative approach to trigger a *micro-experiment* even if one of the PMU types out of the three detects a phase change. This is because failing to detect endogenous phase changes will significantly reduce the accuracy in estimating IPC of solo execution. On the other hand, predicting a non-existent phase change causes only negligible overheads when the occurrence of such mispredictions is low.

3.4.3 Putting It All Together

As discussed, the final objective of Caliper is to estimate the slowdown of an application during runtime accurately. Caliper performs *micro-experiments*, a short-lived experiment to collect a measurement of interest, by opportunistically pausing the execution of co-running applications for a small amount of time so that resource contention can be temporarily eliminated in the system. The result of such a micro-experiment represents an accurate estimate of the solo performance for the application in that small period.

Performing *micro-experiments* frequently causes huge execution overheads. Hence, it is essential to identify when micro-experiments need to be triggered. In this study,

Processor	Microarchitecture	Kernel	Hypervisor
Intel Xeon E5-2630 @2.4 GHz	Sandy Bridge-EP	3.8.0	KVM-QEMU v2.0
Intel Xeon E3-1420 @3.7 GHz	Haswell	3.8.0	KVM-QEMU v2.0

Table 3.3: Experimental platforms

we overcome this challenge by utilizing phase boundaries as triggers for conducting micro-experiments. This is because the execution behavior of applications does not drastically change within a single phase. Hence a single micro-experiment for a phase is sufficient to characterize the execution behavior of an application for that phase. Adding to that, the number of phase changes is not many in most applications. We utilize Performance Monitoring Units (PMUs) to detect phase changes during runtime.

3.5 Evaluation

3.5.1 Methodology

Infrastructure. We evaluate Caliper on two commodity multicore systems summarized in Table 5.2. We use Linux KVM as the hypervisor and run applications on virtual machines (VMs) [65] because running virtual machines is a standard way for cloud providers to isolate infrastructure among different customers. Hence our infrastructural setup consists of co-locating multiple virtual machines (VMs) where each VM belongs to a different user.

Each virtual machine has 4GB of main memory and 16GB disk. We use the Ubuntu 12.04 distribution as guest operating systems with Linux kernel 3.11.0. There is no change in the execution characteristics of the applications while executing them using virtualized environments. We take advantage of `perf` tool to collect hardware performance monitors while observing applications.

Applications. To evaluate the effectiveness of our technique, we use the bench-

Benchmarks	Class of applications	AWS use cases [7]
Sirius Suite	Machine learning	NTT Docomo (voice recognition) [8]
DjiNN & Tonic	Deep neural network	PIXNET (facial recognition) [10]
SPEC 2006	General purpose & Scientific	Penn State [9]
NPB	Parallel computing workloads	NASA NEX [13]

Table 3.4: Benchmark used in evaluation

marks from *SPEC CPU 2006* [49] with `ref` inputs, *NPB - NAS Parallel benchmarks* [14]. In addition to that, we execute emerging applications from *SiriusSuite* [45] and *DjiNN&Tonic suite* [44] in batch mode. Sirius suite and DjiNN & Tonic suite contain a class of applications which implement state-of-the-art machine learning and computer vision algorithms. It has been a common trend to execute such applications in modern public clouds where multiple applications are oversubscribed in the same server [7, 9, 10, 8]. We can clearly see that the benchmark suites that we have utilized to evaluate Caliper are similar to the applications that are being executed in state-of-the-art public cloud computing environments (e.g., Amazon web services [122]). Table 3.4 enumerates the applications, their description, input, application domain and the respective suite from which the benchmarks are obtained. Also, *SiriusSuite* [45] and *DjiNN&Tonic suite* [44] have stemmed into a startup that builds conversational artificial intelligence systems for banking sector [2].

3.5.2 Caliper – Accuracy and Overhead

In this section, we evaluate the efficacy of Caliper. We discuss the accuracy in estimating slowdown by Caliper and its overhead experimentally. Accuracy calculated by comparing the estimated slowdown from our runtime system with the actual slowdown, a metric that is consistently followed by existing literature that focuses on estimating slowdown [22, 30, 31, 102].

Fig 3.6 shows the accuracy when Caliper is trying to estimate slowdown when 4 applications are co-located on a single server. The experimental setup here consists

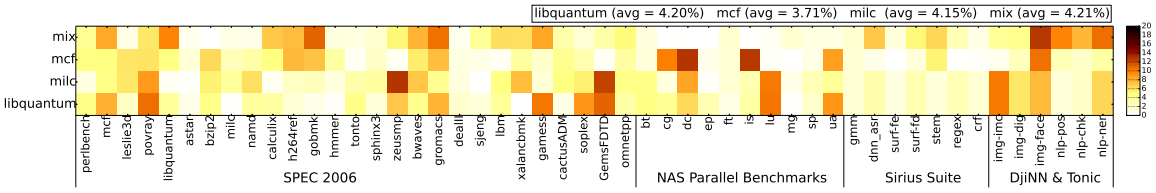

Figure 3.6: Accuracy (in percentage error) of SPEC CPU2006, NAS Parallel Benchmarks, Sirius Suite and Djinn&Tonic suite while estimating slowdown when 4 applications are co-located.

of four broad execution scenarios each based on the type of co-running application that we have taken into consideration represented in the y-axis of Fig 3.6.

Single vCPU. The single-threaded benchmarks from SPEC CPU 2006, Sirius Suite, Djinn&Tonic are evaluated where for each experiment the observed application executes in a single VM pinned to a single vCPU. The PMU-based measurements are collected from the vCPU at which the application is executing which directly corresponds to the performance of the application.

Multiple vCPU. The multi-threaded benchmarks from NPB are evaluated where for each experiment the observed application executes in a single VM pinned to two vCPUs. Here, the performance of the application is the cumulative values of the PMU-based measurements obtained from each vCPUs at which the application is executing.

Individual cells in Fig 3.6 present the difference (error) in the estimated slowdown versus the actual slowdown (Light is good and dark is bad). For each experiment, we execute 3 instances of a single type of co-runner `libquantum`, `mcf` and `milc`, simultaneously along with 1 instance of the application on the x-axis. The mix co-runner is a mix of 3 different co-runners, `libquantum`, `mcf`, and `milc`, alongside the applications on the x-axis. We have used `libquantum`, `mcf` and `milc` as co-runners as from our experiments and through prior work [107], we found out that these were the top 3 applications that exhibit significant activities towards shared

architectural resources including last-level cache and memory bandwidth. Hence, accurately estimating slowdown during the presence of such co-runners was a big challenge for us[107]. Our experiments to estimate the accuracy of slowdown and runtime overhead takes into account all the 4 applications executing in the system. We run each benchmark three times and take the mean to minimize run to run variability. We check to see if there is any phase change every second owing to the observation that phases are consistent for a few seconds. During every phase change, micro-experiments are performed for 75ms to eliminate resource contention during observation. We obtain the value 75ms empirically by performing a sweep for different quantities optimizing for reduced overhead and increased accuracy. Details will be discussed later.

Accuracy. From Fig 3.6, we can see that Caliper shows very low error rates across all the applications even when running with multiple instances of cache contentious co-runners like `libquantum`. The average error rate when co-locating with such contentious co-runners is around 4%. We observe that 95% of our applications have errors less than 10% and the worst case error is 12% in our technique, whereas the worst case error of prior techniques is up to 60% (details presented in Section 3.5.3 of evaluation). We also observe that the error in estimating interference using Caliper remains consistent regardless of the nature of the co-runners. This is indicative of two things (1) accuracy with respect to detecting phases (2) precision of micro-experiments in detecting per phase interference. In the next section, we discuss the importance of having a robust phase detection methodology and its impact on the accuracy of of estimating interference.

Overhead. To enable Caliper on production systems, we have to achieve low overheads so as to minimize the interference to running application on the servers. Table 3.5 indicates the overhead that is incurred by Caliper while estimating slowdown. We evaluate the overhead at the same experimental setup under which we had eval-

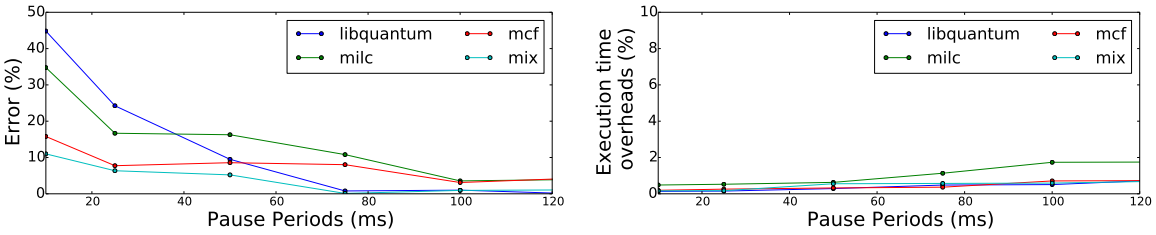

(a) Accuracy (b) Overheads

Figure 3.7: Accuracy and overheads for Caliper under different pause periods.

	SPEC		NPB		Sirius	
	Overhead (%)	Phase changes (per min)	Overhead (%)	Phase changes (per min)	Overhead (%)	Phase changes (per min)
main-app	0.65	1.58	0.35	0.38	0.25	0.20
colo-app	0.74	0.91	0.45	0.75	0.44	0.80

Table 3.5: Execution time overhead and number of phase changes

uated accuracy. From Table 3.5, we can clearly see that the overhead of the main observed application, as well as the average overhead of the co-running applications, remain less than 1% in most of the cases. On average, the overhead of Caliper's runtime system is around 0.6%. Similarly, we also see that the number of phase changes per minute is also very less. On average, there is a single phase change per minute. This indicates that each application is paused for a few hundred milliseconds every minute making the overhead extremely negligible.

Sensitivity of the pause period. Towards obtaining an optimal pause period for operating Caliper, we performed a sensitivity study. The results of this study is shown in Fig 3.7. From figures 3.7a and 3.7a, we clearly observe two trends. First, the accuracy of estimating slowdown increases as the pause periods increase up to 75ms. Then there is no benefit in increasing the pause periods. Hence we have utilized 75ms as an optimal pause period for our mechanism. Second, the overheads do not change drastically as we increase the pause periods. This is because Caliper's frequency at which it pauses the co-runners is too low causing negligible impact in the execution time overheads.

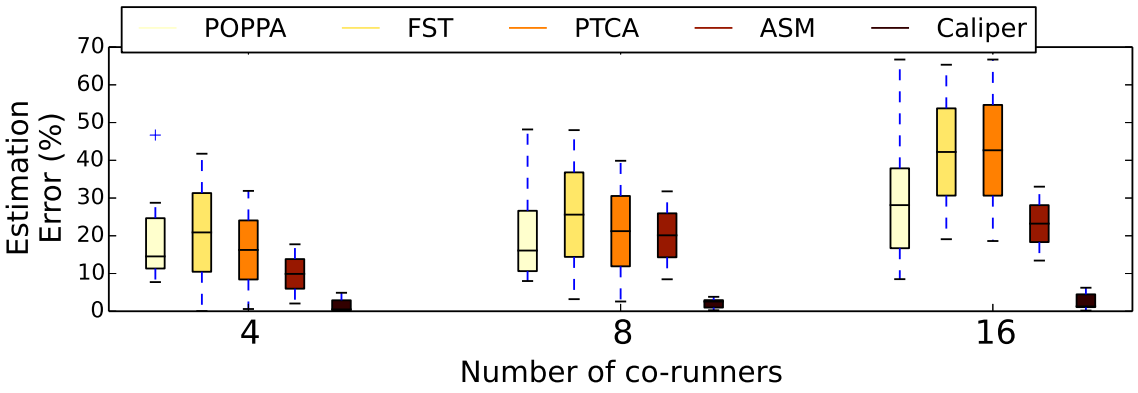

Figure 3.8: Estimation error: Caliper vs. state-of-the-art software (POPPA [22]) and hardware (FST [31], PTCA [30], ASM [102]) techniques for estimating interference

3.5.3 Comparison with Prior Work

Accuracy. Fig 3.8 shows the accuracy of Caliper as compared to the accuracy of POPPA [22], FST [31], PTCA [30], and ASM [102] for the benchmarks present in SPEC CPU 2006, NPB, Sirius suite and Djinn&Tonic suite. POPPA works by periodically pausing all co-running applications except one for a very short time at fixed time intervals. The aggregated performance of the applications during the pause periods is the key measure by which slowdown is estimated. Through these experiments, we can see that the estimation error is much lower for Caliper than POPPA [22]. The mean error of POPPA is 13.23%. On the other hand, our technique shows much lower error rates averaging around 3.77%.

It is challenging to estimate the slowdown when running with contentious co-runners as they quickly pollute the shared last-level cache and excessively use the shared memory bandwidth. One of the main reasons for POPPA's poor accuracy is that the pausing time (3.2ms) is too short to capture solo performance of an application. This is because the shared cache would not be warmed up to be containing the entire working set of the application which is to be measured. As a result, the measured application would spend most of its pausing time filling in the shared cache, giving much less time to observe how the application performs when it monopolizes

computing resources. On the other hand, Caliper performs micro-experiments which pauses co-runners only when discovering phase boundaries. This enables us to observe the solo execution performance for a longer time without worrying much about the overhead caused due to pausing for additional time. Hence, we are able to achieve high accuracy in estimating slowdown at runtime.

We also observed that the state-of-the-art hardware enabled approaches towards estimating slowdown [31, 30, 102] showed a high error rate. Just like the other software approaches, state-of-the-art hardware enabled approaches utilizes cache access rates of applications during solo execution time to determine slowdown of an application. Cache access rates of applications during solo execution is again obtained by periodically pausing co-running applications in a round robin fashion. Hence the limitations of the prior software approaches hold good for the hardware approaches too. The mean errors of POPPA, FST, PTCA, and ASM are 11.04%, 28.28%, 38.42% and 9.98% respectively. From these results, we were able to see that Caliper can outperform even the state-of-the-art hardware enabled approaches present in the literature.

Multi-tenancy. To evaluate the effectiveness of the state-of-the-art hardware or software based approaches and Caliper towards supporting multiple tenants, we increase the number of executing application contexts to 8 applications and 16 applications. Fig 3.8 shows the average accuracy of Caliper as compared to POPPA for SPEC CPU2006 and NPB when co-locating with libquantum. We can see that Caliper's accuracy is around 3.95% when co-locating with 16 applications in contrast to POPPA [22], FST [31], PTCA [30] and ASM [102] whose error is around 22%, 40%, 41% and 19% respectively. The low accuracy of the prior techniques is because as the number of co-runners increases, the shared cache becomes much more polluted due to the contention. POPPA even on such situations pauses for the same amount of time which is too less for the shared last-Level cache to warm up so as to exhibit the performance corresponding to solo execution. Hence, its slowdown estimation becomes

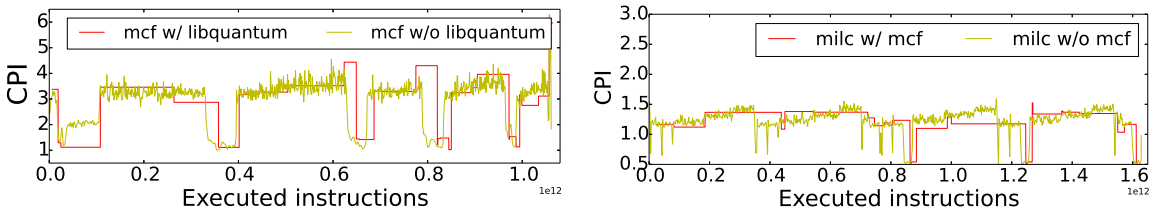

(a) `mcf` (error 0.51%) (b) `milc` (error 2.52%)

Figure 3.9: Phase level behavior of Caliper for `mcf` and `milc` when running with co-runners, 3 `libquantum` (a) and `mcf` (b), respectively. Micro-experiments are triggered effectively at phase boundaries.

highly inaccurate. Similarly, hardware techniques perform sampling in a round robin fashion using their proposed specialized hardware whose pressure increases as the number of co-running application increases. However, Caliper utilizes a phase-aware approach that performs micro-experiments at adequate amounts of time during the right time to capture the solo execution characteristics of every phase accurately.

Phase analysis. Now, we try to visualize the effectiveness at which Caliper utilizes its a robust phase detection technique in order to achieve high accuracy and low overhead in estimating slowdown. Toward illustrating this, we analyze the phase level behavior of a selected set of phasy applications to show Caliper's capability towards performing micro-experiments at every single phase change.

Firstly, we select two applications, `mcf` and `milc` to analyze the execution behaviors. These applications possess a significant number of phase changes. As co-runners, we use `libquantum` and `mcf`, respectively. Fig 3.9 (a) shows the execution behavior of `mcf` with respect to time. In each graph, the yellow line depicts the measured CPI of the application when running alone and the red line shows the CPI estimated by Caliper when the application is running with 3 instances of `libquantum` or `mcf`. We can see that Caliper can effectively trace the phase changes. The closer the red line is to the yellow line, the smaller the error. The error in estimating slowdown is 0.51% over the entire run. For `milc`, Fig 3.9 (b) presents that our technique can effectively trace all of its phase. The error while estimating slowdown is 2.52%.

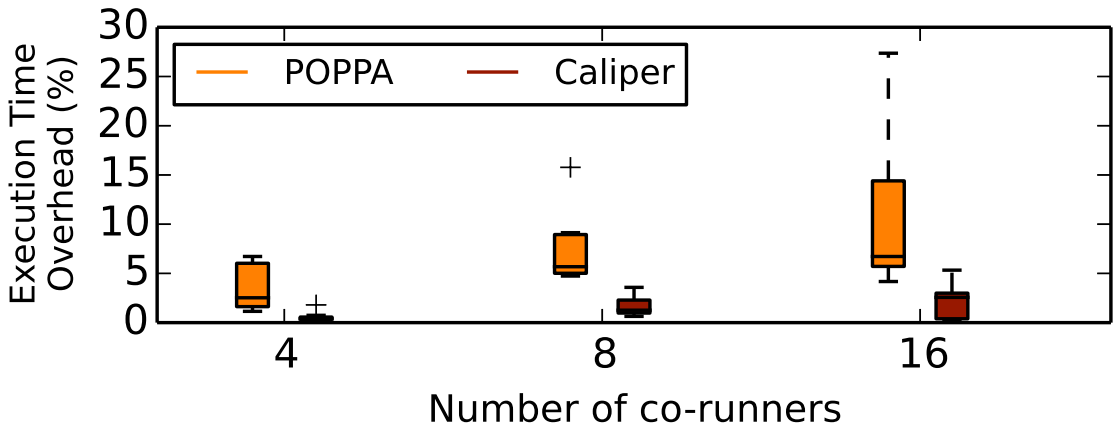

Figure 3.10: Overhead: Caliper vs. POPPA

Overhead. Fig 3.10 compares the overhead up to 16 application contexts for Caliper and the state-of-the-art software approach POPPA. We can clearly see that as the number of application context increases, the overhead of Caliper increases negligibly. However, this is not the case for other software approaches. This is due to the fact that, POPPA performs periodic pauses. As more applications are co-located, the effective time for which applications are paused increases as POPPA need to pause every application for the same amount of time for each of the co-runner. However, Caliper pauses applications only during phase changes (which are comparatively infrequent). Hence, the overhead incurred by Caliper's runtime system is lesser by an order of magnitude.

Fig 3.11 illustrates the reasons behind POPPA's higher execution time overhead. Fig 3.11 (a) compares the performance of POPPA and Caliper in an environment without any slowdown estimation runtime system. We can clearly see that the increased execution time overhead of POPPA is due to the spikes present in CPI due to frequent pausing of co-runners periodically by POPPA to estimate slowdown. However, Caliper performs micro-experiments rarely (once every phase). Hence, there are no periodic spikes as seen in POPPA. Caliper's execution time overhead also is negligible.

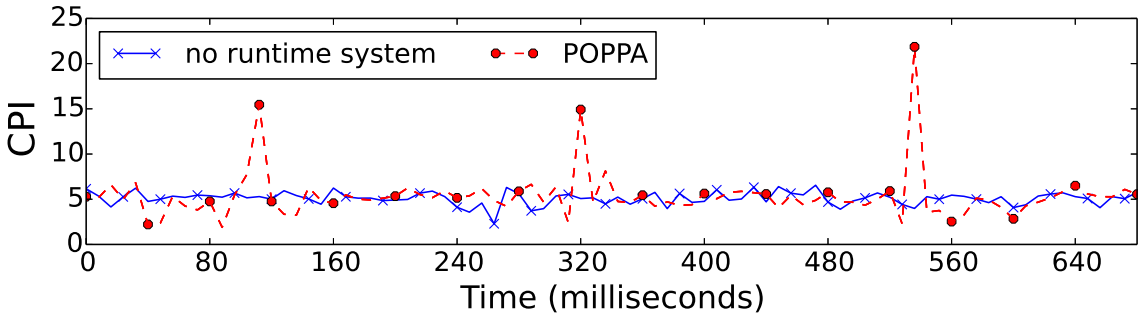

(a) Execution performance - 10.5% increase in execution time due to POPPA's runtime system

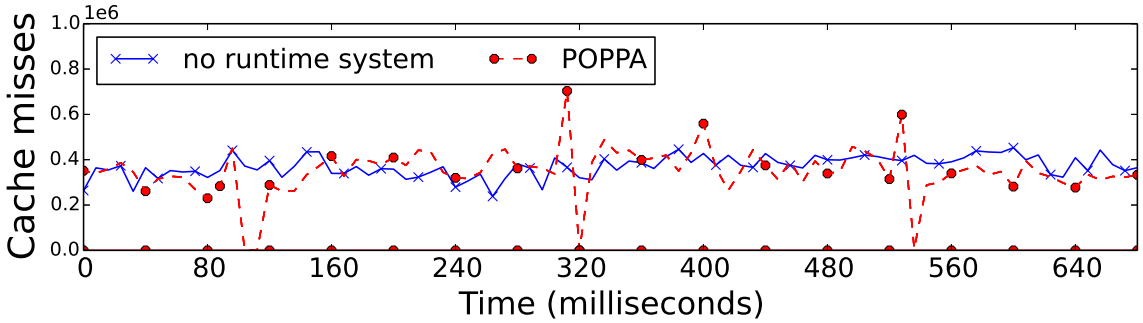

(b) Cache misses – 11.6% increase in cache misses due to POPPA's runtime system

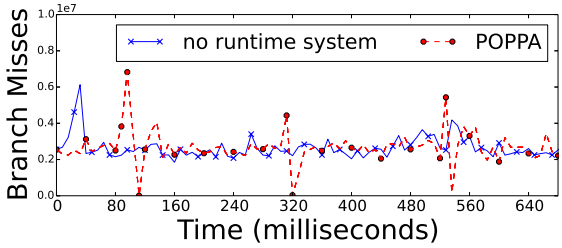

(c) Branch misses – 5.7% increase in branch misses due to POPPA's runtime system.

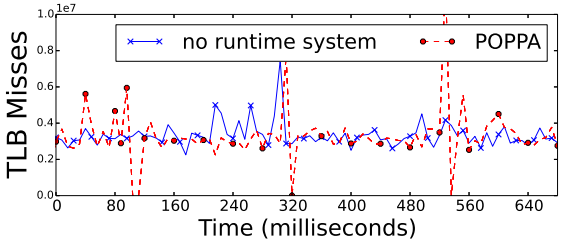

(d) TLB misses – 7% increase in TLB misses due to POPPA's runtime system

Figure 3.11: Performance of micro-architectural entities when POPPA's runtime systems are being executed

	milc (4)	gobmk(1)	hmmer(1)	perbench(1)	astar(7)	namd(1)	pos(1)	chk(1)	calculix(118)	dealII(132)
libquantum	0	0	0	0	2	0	0	0	257	49
mcf	6	0	2	0	3	1	1	1	412	98
milc	5	0	1	0	2	0	0	0	353	33
mix	2	0	1	0	2	0	1	1	251	98

Table 3.6: Number of false positives incured in Caliper runtime system. First row contains the benchmarks and the respective number of endogenous phases present in them. For example milc (8) means milc has 8 endogenous phases. First colunm contains co-runners.

We have experimentally verified the reasons for the increased overhead and is clearly shown in Fig 3.11 (b), (c), and (d), respectively. As POPPA performs periodic pauses, it incurs addition warmup overheads for the micro-architectural components present in the system. At the end of every pause period, the system refills the micro-architectural components (cache, branch target buffer, TLB etc.) that would have been flushed during its pause period. This gets translated directly into increased execution time overhead.

Fig 3.11 (b), (c), and (d) illustrate the underlying causes for this phenomenon. From Fig 3.11 (b), we can see that the cache misses increases whenever POPPA pauses co-runners in the system. However, it remains on unaffected for Caliper reasoning out its negligible overhead. Similarly, from Fig 3.11 (c) and (d), we can see that when POPPA frequently pauses applications, branch misses and TLB (transition look aside buffers) misses increases. This in on similar lines that micro-architectural components like branch target buffer (BTB), TLBs are flushed out frequently during pausing by POPPA. We can see that frequent pauses by POPPA increases the cache misses, TLB misses and branch misses by 11.6%, 5.7% and 7% respectively thereby increasing the runtime overhead of the execution of an application up to 10.5%. However, Caliper's overhead, as well as misses at the micro-architectural structures, remains less than 0.5%.

Table 3.6 illustrates the number of falsely detected phase changes by Caliper's runtime system. The first row in Table 3.6 shows the benchmarks for which we

have evaluated this experiment. We have shown only ten benchmarks in this table in the interest of space constraints. The numbers present in the bracket after the benchmarks show the endogenous phase counts (true positives). The first column shows the co-runners along which the benchmarks present in the first row have been evaluated. Each cell in table 3.6 illustrates the number of falsely detected phases by Caliper's runtime system. From our experiments, we observed that the results for most of the benchmarks were similar to `gobmk`, `hmmer`, `namd`, `pos`, `chk`. There was just one phase, and Caliper was able to detect that phase. Additionally, detecting false phases were a rare occurrence consuming negligible overheads. However, we had a few interesting observations for the benchmarks `calculix` and `dealII`. The phases of these applications are very irregular and contain spikes once every few seconds. Each of these situations where spikes occur triggers a phase change resulting in a larger number of false positives. Additionally, another interesting observation from our experiments was that there were more false positives when mcf was a co-runner. This is because mcf has many phase changes introducing many more false positives due to co-phase interference. However, the frequency at which Caliper's runtime system triggers phase changes is so low that our overhead remains lesser than 1% for most of the time.

3.5.4 Leveraging Caliper for Fair Pricing in Datacenters

Infrastructure-as-a-service (IaaS) clouds primarily use a pay-as-you-go pricing model that charges users a flat hourly fee for running their applications on shared servers. Customers renting IaaS public clouds now have the capability to choose resource fragments at varying granularity in terms of the number of virtual CPUs, the amount of memory and storage size. Cloud service providers rely on virtualization to isolate resource fragments belonging to each customer. However, in light of significant potential for parallelism, cloud service providers co-locate applications belonging

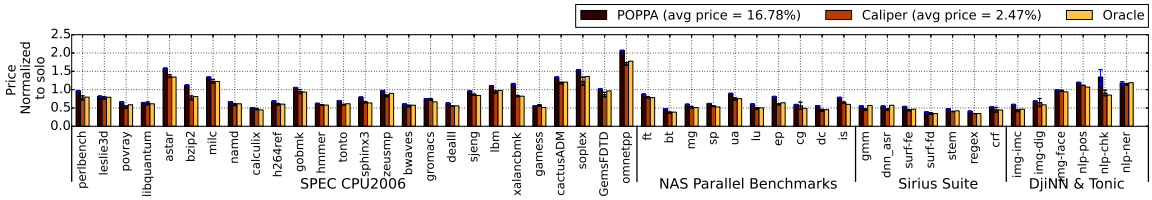

Figure 3.12: Comparison of fairness in pricing by *Caliper* with *POPPA*

to different users. Since the last-level cache and DRAM bandwidth remain shared among applications running within a single server, applications are slowed down as compared to when they run alone on the system. This increased execution time that the application is subjected to reflects directly on the price paid by the users under the pay-as-you-go scheme creating an unfair pricing scenario.

To enable fair pricing in public clouds, it is essential to estimate the performance impact that co-running applications have on an application. Identifying slowdown at runtime would be a very useful information in this regard as it would be an appropriate indicator of influence of co-runners on an application. Hence, such a scheme can be used as a critical substrate upon which any pricing scheme can be built. However, such a scheme is highly dependent on the accuracy at which fairness is estimated. Hence, achieving high accuracy in estimating slowdown becomes critical.

We compare the unfairness that is present while utilizing the hardware enabled approaches for pricing with our approach. We define unfairness as the price by which users are overcharged when they are executing their applications in IaaS public clouds. We use the pricing model proposed by Toosi et al. [114] and apply the slowdown estimation techniques along with it so as to calculate the resultant price. From Fig 3.12, we can see that is able to price applications with $5X$ more fairness while pricing users using their slowdown model as compared to the POPPA technique proposed in Breslow et al. [22]

CHAPTER IV

Proctor – Detecting and Investigating Performance Interference in Shared Datacenters

Enterprise datacenters like VMWare, Microsoft, and Amazon often house thousands of servers to service large-scale cloud applications across the globe. Cloud computing is becoming more common every day and so improving utilization is of critical importance in terms of improving cost and reducing the footprint of the datacenters [117, 11, 67].

Over past few years, datacenter operators have switched to *virtualization*, a technique that encapsulates and abstracts applications from the physical hardware by creating Virtual Machines (VM), that assists sharing of physical hardware by scheduling multiple VMs on the same physical machine. State-of-the-art VM monitors, also known as hypervisors, like Xen, Hyper-V and ESXi [124, 118] reserve fragments of the physical server resources (like CPU core, DRAM storage etc) for each application separately in a virtualized environment. This abstraction leads to better hardware utilization, as multiple VMs can now be easily scheduled on the same physical machine.

However, virtualization does not provide complete performance isolation as VMs still compete for non-reservable shared resources (like caches, network, I/O bandwidth etc.), resulting in performance interference between the VMs, which can have signif-

icant and unpredictable effects on the application performance. This unpredictable performance is particularly problematic for user-facing applications that have strict Quality of Service (QoS) requirements, forcing the datecenter operators to disable co-location, reducing datacenter utilization. Therefore, data center operators need to achieve the best of both worlds - satisfy strict QoS requirements while also keeping server utilization high.

A suitable solution to mitigate the interference problem so that it can take corrective measures later to meet QoS requirement while achieving good server utilization, needs to perform two major tasks at *runtime – Detection* and *Investigation*. First, when a performance intrusive VM is colocated with an application having strict QoS requirement and negatively impacts its performance, the technique should be able to **detect** this performance degradation. Second, once this performance intrusion is detected, it is necessary to **investigate** the source of this contention (both the performance-intrusive VM and the contended shared resource) to undertake useful remediation.

In order to detect contention and mitigate the effect of interference, we present *Proctor* [62], a runtime system that continuously monitors, automatically detects and investigates a wide range of performance issues directly affecting the Quality of Service of VMs running in a cloud scale datacenter, with high accuracy and low performance overhead. For Detection, Proctor employs a Performance Degradation Detector (PDD), that continuously monitors the performance metric of the executing VMs, looking for abrupt changes in the QoS. PDD uses state-of-the-art noise removal technique (median filtering algorithm) and step detection to detect a performance anomaly, as opposed to previous work that requires a priori knowledge. For Investigation, Proctor employs Performance Degradation Investigator (PDI), that identifies the source of contention for a performance anomaly at runtime using online statistical correlation analysis. The challenge here lies in performing investigation quickly as this

process is laborious and requires querying a database consisting of large amounts of VM monitoring data. To tackle this challenge, PDD uses a robust sub-sampling technique that reduces the amount of the data that needs to be queried while *accurately* detecting the source of contention.

We perform a thorough evaluation of our platform on real systems across a wide range of applications and commonly contended shared resources, demonstrating its effectiveness in diagnosing performance issues at runtime, improving the performance of the applications running in datacenter by up to 2.2×.

4.1 Background and Motivation

In this section, we provide the background for the performance interference for different sources of contention, followed by the limitations of the prior work in solving the problem of mitigating interference.

4.1.1 Sources of Contention

Although virtualization reserves fragments of machine resources for each application individually, the VMs can still experience performance interference when multiple VMs are colocated on the same physical machine. This happens because there are a number of non-reservable resources that can be shared among VMs, that can have significant and unpredictable effect on the VM performance. In datacenters, there are mainly four such shared resources - *I/O*, *CPU core*, *Network* and *Last Level Cache*.

As an example, I/O contention can occur when guest operating system within each VM is oblivious to the virtual nature of underlying disk and the existence of neighboring VMs on the same machine. Under such situations, a single badly behaved application that continuously issues frequent I/O requests to a disk array can disrupt the latency/throughput of every other application running over that array, negatively impacting the performance of other VMs. Similarly, such performance

intrusive behavior can happen at other hardware resources like CPU core, Network and Last Level Cache.

4.1.2 Limitations of Prior Work

There exists several prior approaches that are specifically designed to mitigate the effects of contention when multiple VMs are consolidated in a shared datacenter. However, these approaches have some limitations that restrict their deployability in a commercial datacenter. We have broadly classified them under the following three categories based on their limitations towards solving the Detection and Investigation problems.

1. **Require A Priori Application Profile.** Prior approaches like Bubble-Up and Cuanta [37, 72] have been shown to be effective at generating a precise estimation of performance degradation at co-located execution scenarios. However, these techniques require a priori knowledge of application behavior restricting their deployability in datacenters that encounter unknown applications on a regular basis (for eg., private datacenters and public clouds). Additionally, these techniques are incapable of investigating the root cause of performance intrusion. Therefore, this category is unsuitable to perform Detection and Investigation tasks in datacenters that encounter unknown applications.

2. **Incapable of Investigating Root Cause.** Second category of prior approaches [103, 38], that do not require a priori knowledge, focus on investigating a particular source of contention, unable to detect and mitigate the performance interference caused by other shared resources. In addition, the overhead incurred by these techniques in detecting performance degradation is high because their methodology perturbs the execution of VMs periodically for brief periods of time in order to profile application execution. Therefore, this

class of prior work is also unsuitable because of its high overhead in performing Detection task and their disability to execute the Investigation task.

3. **Performs VM Migration/Cloning.** A third class of approaches, identifies performance intrusion as well as its root causes. However, these techniques perform frequent VM migration and cloning, resulting in many drawbacks. First, copying huge data across machines is time consuming and introduces additional contention on the computing resources. Second, the overhead with respect to the number of additional servers required to perform these techniques is very high. Therefore, this category of prior work is also not suitable in shared datacenters as they incur high overheads while executing the Detection and Investigation tasks.

4.2 Overview of the Proposed Approach

To this end, we present Proctor [62], a runtime system that utilizes a two step methodology to solve the Detection and Investigation tasks respectively. In this section, we provide a high level overview of our technique along with the challenges in designing Proctor components.

4.2.1 Goals and Challenges

Performing Detection. Proctor utilizes *Performance Degradation Detector (PDD)* for this purpose. In contrast to prior approaches which affect the execution of application by utilizing synthetic benchmarks like smashbench, PDD is an extremely low overhead continuous monitoring infrastructure that observes individual VM QoS metric to detect drastic variation in the numerical range of the QoS metrics. This change would be an indication of an event that signifies performance degradation of the application. To detect drastic variation in numerical range of metrics, we employ

step detection – a signal processing technique that is utilized to find abrupt changes in time series signals [85].

Challenges and Approach – However, the time series data obtained from system software tools and performance counters is highly corrupted due to noise. The most straightforward solution for such problems is to perform curve smoothing. However, the most commonly used curve smoothing techniques, like exponential moving average and Kalman filter [121], are not effective in highlighting drastic changes in the time series data. This is because they project drastic changes in QoS measurements as a slow cumulatively occurring event, making it hard to detect the abrupt changes. Hence, we used a technique called *median filtering* designed specifically to cater to the step detection problem.

Performing Investigation. Once, PDD establishes the existence of performance degradation, we utilize the *Performance Degradation Identifier (PDI)* to pinpoint the exact source of contention (both VM and the shared resource the applications are competing for). PDI uses correlation analysis for this purpose, finding correlation between the hardware counter metrics of all the co-running VMs and the primary QoS metric of the affected VM (as detected by PDD). High value of correlation co-efficient for a particular metric provides sufficient evidence that the co-running VM and the resource corresponding to that metric is the root cause of performance degradation.

Challenges and Approach – However, performing correlation analysis on large amounts of HW performance counter data, which is collected at a second level granularity, is computationally intensive, resulting in high performance overhead. To tackle this problem, we sub-sample the performance counter data, reducing the amount of data that is to be utilized to find the source of contention. A random sub-sampling method can be utilized for this purpose. However, it becomes crucial that the obtained sample should be a good representation of the population from which it is drawn, as biased samples can lead to inaccuracy in performing Investigation. To address this challenge,

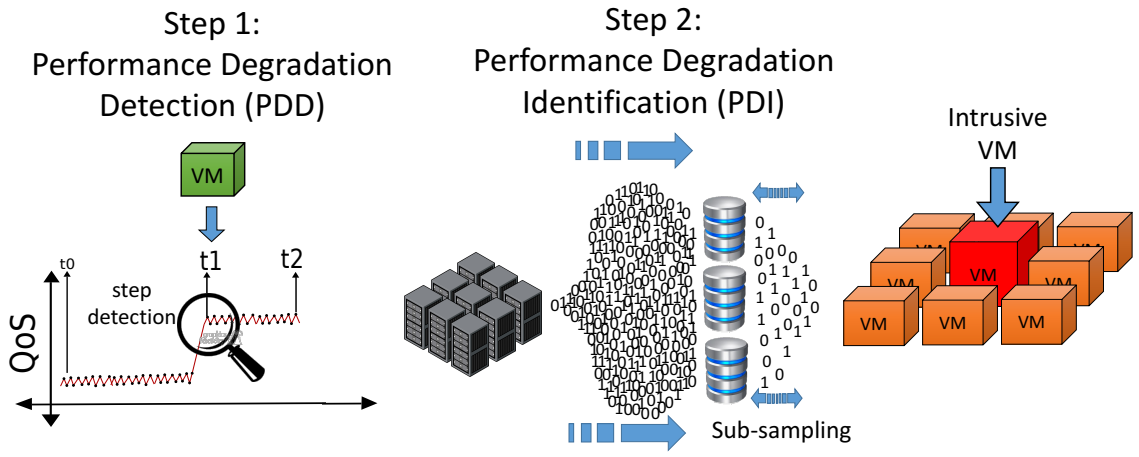

Figure 4.1: Proctor System Architecture - a two-step process performing Detection and Investigation to identify the root cause of performance interference [62]

we validate each sample by utilizing hypothesis testing techniques. As our time series measurements do not follow the guassian curve, we use a non-parametric statistical hypothesis testing technique called χ^2 test to ensure that the sub-sampled data is a good representation of the original performance counter data [130].

4.3 Proctor Architecture

Proctor is a dynamic runtime system that automatically detects performance intrusive VMs in the datacenters, their victims and the shared resource that is causing contention, with high accuracy and low overhead. In order to achieve this, Proctor utilizes a two step approach as shown in Figure 4.1. The first step, PDD, detects performance degradation caused due to performance intrusive VMs. The second step PDI, pinpoints the root cause by identifying the exact VM that is responsible for the performance intrusion and the corresponding metric for which there is contention. This section elaborates in detail the key components present in Proctor's design.

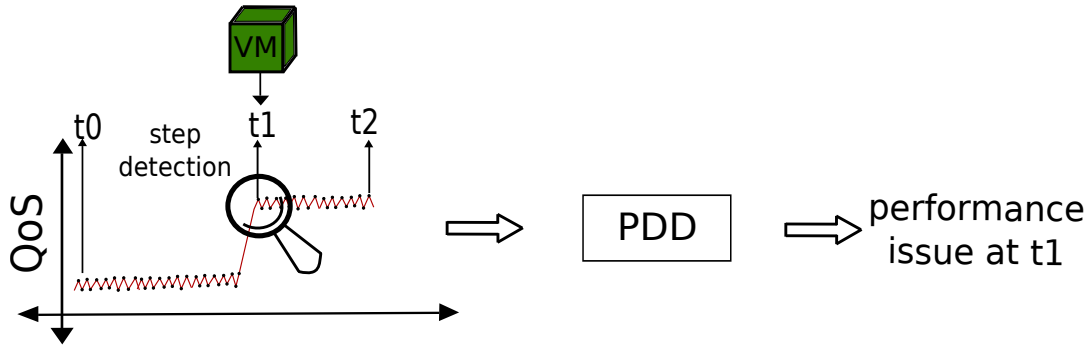

Figure 4.2: PDD detects abrupt performance variations in the application telemetry data

4.3.1 Performance Degradation Detector

Proctor utilizes (PDD) that operates in parallel with applications, continuously monitoring and looking for performance anomalies in the dataceters at runtime. It utilizes time series measurements of the primary QoS metric of each application executing inside a VM to detect drastic variation in the numerical range of metrics. This drastic variation acts as an indication of an event that the performance of the application has degraded significantly.

PDD employs a signal processing technique called *step detection* to detect these abrupt changes in the application performance [85, 93]. However, time series performance data of an application has high amount of noise, causing many false alarms if step detection is applied naively. We use *Median filtering* algorithm [23] to reduce the noise in the telemetry data, making PDD accurate in detecting performance anomalies. In the next two subsections, we will elaborate on the step detection and median filtering techniques.

4.3.1.1 Step Detection

Step detection is a process of finding abrupt changes in a time series signal [85, 93]. Using the time series measurements of the primary QoS metrics, we try to identify

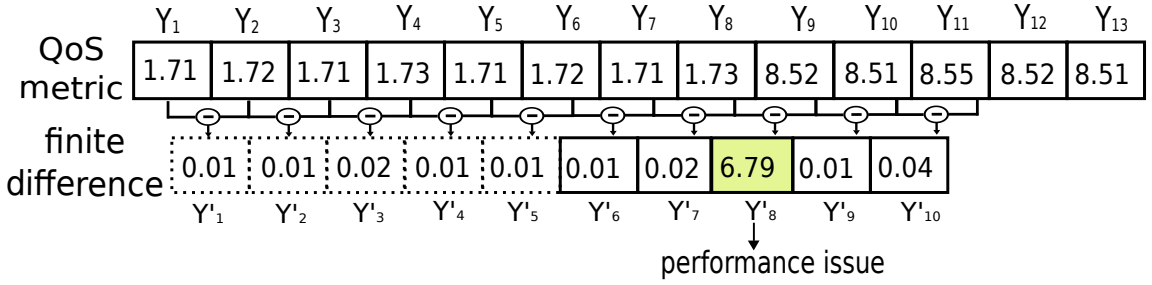

Figure 4.3: PDD Step Detection using Finite Difference Method

the exact timestamp at which abrupt changes occur in the numerical quantity of primary QoS metric. An abrupt change is statistically defined as a point in time where the statistical properties before and after this time point differ significantly. This is clearly illustrated by Figure 4.2 where we can see a sharp increase in the QoS metric at time t1. The role of PDD here is to detect such abrupt changes at runtime and identify the exact timestamp at which such abrupt changes occur. We utilize *finite difference method* for this purpose.

The fundamental hypothesis of finite difference method towards identifying abrupt changes is based on the fact that the absolute difference between subsequent time series measurements is very high at the exact point where the abrupt changes occur. This can be utilized to highlight the timestamp at which these abrupt changes occur.

Mathematically, finite difference of a time series signal is the rate of change in the individual elements in the time series. We implement finite difference method by performing pair wise difference of subsequent elements present in the time series using the following formula :-

$$Y' = \frac{Y_{j+1} - Y_j}{2\Delta T} \qquad\qquad Y'_j = Y_j \ (for\ 1 < j < n-1)$$

where Y_j is the j^{th} points present in the time series, n being the number of points, ΔT being the difference between the X values of adjacent data points (difference in

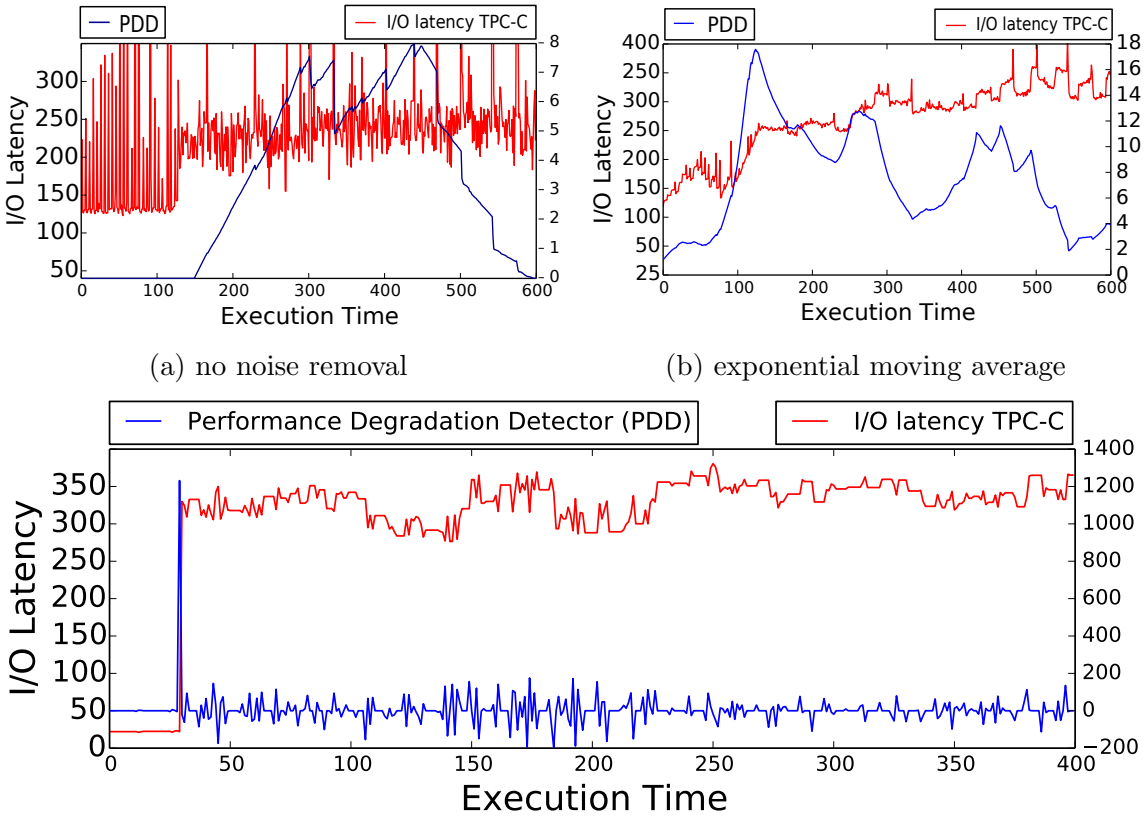

(a) no noise removal

(b) exponential moving average

(c) median filtering

Figure 4.4: Comparison of detection accuracies (a) without noise removal, (b) with exponential moving average and (c) with median filtering for the application TPC-C. Median filtering algorithm detects abrupt changes in performance

the number of timestamps for time series values). The result highlights the drastic change by showcasing a high value for Y'. This is clearly illustrated by Figure 4.3 where we can see a sharp increase in the QoS metric at time t1 at the point Y_9. Its corresponding finite differential value is very high at point Y'_9, which is utilized to indicate performance degradation at that timestamp t1.

4.3.1.2 Noise Reduction

Naively applying step detection leads to large number of false positives because of the noise in the time series measurements of QoS metric. For example, we directly apply the step detection algorithm for TPC-C benchmark and show the detected

performance anomalies in Figure 4.4a. The figure shows that there are large number of false alarms.

In order to eliminate the noise present in the raw time series measurements, we tried to utilize the state-of-the-art curve smoothing techniques like exponential moving average and kalman filter [66]. However, these techniques still show significantly high number of false positives. This is because these techniques end up smoothing out drastic changes in time series measurements, projecting them as a slow and cumulatively occurring event as shown in Figure 4.4b, failing to detect the drastic performance degradation.

To tackle this problem, we use *median filtering* for noise reduction as this technique preserves drastic changes. Our implementation of median filter consists of a moving window that selectively discard elements that are significantly higher than the median within that window. This preserves drastic changes while also removing noise from the time series measurement. Finally, Figure 4.4c shows the effectiveness of applying median filtering for noise reduction, reducing number of false alarms and making PDD highly accurate.

4.3.1.3 Obtaining QoS Measurements

The presence of virtualization in datacenter infrastructures introduces challenges towards obtaining application specific QoS metrics. Applications often run as performance black-boxes and adaptive services must infer application performance from low-level information or rely on system-specific ad hoc methods. Although this is not a challenge for CPU intensive batch applications and I/O intensive applications as their respective QoS metrics can be obtained through performance counters and system software tools, a class of user facing latency critical applications that run as performance black-boxes, provide very little information about their current performance and no information about their performance goals (eg. 99th percentile tail

Name	Description
load	Input load of application
CPU util	CPU utilization of app
page-faults	Page faults per sec of app
context-switches	Context switches per sec of app
n/w throughput	Total bytes sent and received by network
cache-misses	Total cache misses (L1,L2 and LLC)
I/O requests	Total I/O requests (read + write)
branch-misses	No. of branch mispredictions of app

Table 4.1: List of metrics utilized for performing correlation with the primary QoS metric to identify source of contention

latency). The primary goal in such situations is to offload the responsibility of providing time series measurements corresponding to the QoS metrics of an application to the user. For this purpose we utilize the the Application Heartbeats framework [50] which provides a simple, standardized way for applications to report their performance/goals to external observers. These are enabled through API calls consisting of a few functions that can be called from applications or through system software. This is being utilized to track the progress of any executing application which is fed into our proposed PDD for identifying performance intrusion during runtime.

4.3.2 Performance Degradation Investigator

Once PDD establishes the existence of performance degradation, *Performance Degradation Investigator* (PDI) is invoked for further analysis which pinpoints performance intrusive VMs and the major server resource that is causing the performance degradation.

4.3.2.1 Correlation Based Root Cause Identification

PDI identifies performance intrusive VMs and the major server resource causing contention by utilizing a correlation based root cause identification technique. The primary objective of correlation based root cause identification is to highlight the root

cause VM and the metrics corresponding to it that correlate highly with the primary QoS metric of the affected VM. In order to obtain that, PDI utilizes the time series measurements from each low level metric corresponding to the co-running VM and tries to correlate them with the time series measurements of the affected VM's primary QoS metric. The metrics having the highest value of correlation coefficient are the most highly likely indicators of resource contention and its corresponding VMs are the most likely culprits for creating performance intrusion. The list of metrics that we try to correlate is enumerated in Table 4.1. Our implementation of correlation tries to obtain Pearson's correlation coefficient [17]. However, performing correlation analysis on the complete telemetry data causes high performance overhead. Therefore, we sub-sample the complete dataset and reduce the time to find the source of contention.

4.3.2.2 Real Time Sub-sampling

One of the key challenges faced by Proctor while realizing a real time solution is the large amount of telemetry data that needs to be queried, resulting in high performance overhead. Hence, instead of performing correlation analysis on full telemetry data, we utilize a sub-sampling technique where a sample from a large data is utilized as input to PDI.

The key objective to be satisfied while realizing a sub-sampling technique is that the statistical characteristics of the sample should be consistent with that of the population. For example, measurements obtained from system software tools are bound to contain extreme values (spikes) at a very low frequency. The sub-sample that we collect should include these events as well. To ensure that, we perform a hypothesis testing to check whether the random sample that we select is representative enough of the population. If not, our hypothesis testing techniques repeats the process by randomly selecting a sample till it is representative enough of the population.

Most widely used hypothesis testing techniques assume population to be normally

distributed. However, based on our experiments we have observed that measurements that come from system software tools and performance counters are highly deviated from being normally distributed. Therefore, widely used parametric hypothesis testing techniques like t-test and F-test are not suitable for our purpose.

Hence, we use non-parametric hypothesis testing approaches that are capable of testing samples irrespective of their nature (being normally distributed). Unlike parametric statistics which primarily utilize mean and variance for this purpose, non-parametric statistics make no such assumptions on the probability distributions of the variables being assessed. Therefore, we utilize Pearson's Chi-Squared test for testing whether a sample is representative of a population [128].

Chi-square χ^2 test is a statistical test used to examine differences within categorical variables [128]. For time series data, we have taxonomized categories as numerical ranges within which measurements from system software tools and performance counters can fall into. In other words, we segregate the population data into different categories where each category refers to a specific range of numerical quantities. Subsequently, we classify the sample data also into the same categories as the population. We now obtain the frequency of elements present in each category for both the sample and population data. For the sample data to be acceptable, the frequency of elements of the sample data in each category should be close to the frequency of elements of the population data in the same category. Chi squared test, compares the frequency of elements of sample and population data in every category to determine the sample's acceptability

Input. Frequencies of population measurements and sample measurements lying in each range.

Output. Accept/Reject sample to be representative of a population.

Methodology. We undertake the following steps to perform Chi-square χ^2 test.

1. We identify the frequency of entities that belong to every range for the sample

Processor	Microarchitecture	Kernel	Hypervisor
Intel Xeon E5-2630 @2.4 GHz	Sandy Bridge-EP	3.8.0	KVM-QEMU v2.0
Intel Xeon E3-1420 @3.7 GHz	Haswell	3.8.0	KVM-QEMU v2.0

Table 4.2: Experimental platform where Proctor is evaluated

distribution.

2. To compare the frequency per range of the sample and population distribution, we adopt the following methodology.

   Null Hypothesis H_0: Sample and Population distributions are similar

   Hypothesis Test:

   $$\chi^2 = \frac{(Population - Sample)^2}{Sample}$$

3. We assess the significance level based on the size of the sample to accept/reject the null hypothesis. Hence, if the null hypothesis is rejected we repeat the same test with a different sample.

4.4 Evaluation

4.4.1 Methodology

Infrastructure. We evaluate Proctor on two commodity multicore processors summarized in Table 5.2. We use system software tools `iostat` and `netstat` to obtain network and disk specific performance metrics and linux `perf` tool to measure HW counters. Performance telemetry is collected at a second level granularity using HW counters.

Applications. Table 4.3 enumerates the applications, their description, input, application domain and the respective suite from which they is obtained. We evaluate Proctor on *workloads*, where each workload is a mix of 5 applications. We design these

	Application	Description	Benchmark Suite	QoS Metric
CPU / LLC	lbm	Fluid Dynamics	SPEC CPU2006	IPC
	libquantum	Quantum Computing		
	omnetpp	Discrete Event Simulation		
	sphinx3	speech recognition		
CPU / LLC	Naive Bayes	Big data classification	Big Data Bench	IPC
	Sort	Sort words from text		
	Grep	Search words from text		
	Word Count	Count words from text		
	Kmeans	Processing facebook network		
I/O	YCSB	Querying from Yahoo dataset	OLTP bench	I/O latency and throughput
	TPC-C	Querying from retail database		I/O latency
	TPC-H	Querying from business database		I/O latency
	Twitter	Querying from tweets		I/O latency and throughput
Network	Redis	Key value store	Redis	Tail Latency
	netperf	Network packet generator	netperf	network throughput

Table 4.3: Benchmarks which have been used to evaluate Proctor and its descriptions

workloads in a careful manner to study different types of resource contention. 4 out of 5 applications in a workload are chosen in a manner that they put stress on the four shared resources - I/O, network, CPU core and LLC. Once these four applications are executing, arrival of fifth application now causes contention for the resource it uses heavily. Table 4.4 illustrates the workload mixes that we have considered in our evaluation. Workloads are executed for a period of one hour where each application

	Work Load ID	App 1 - Main app	App 2 - Colo app	App 3 - Colo app	App 4 - Colo app	App 5 - problematic app
Network	WL1	Redis	Search	lbm	Sort	netperf
Disk I/O	WL2	Twitter	lbm	Redis	Sort	YCSB
	WL3	TPC - C	libquantum	Redis	Grep	Random I/O
	WL4	YCSB	sphinx3	Redis	Word Count	TPC - H
	WL5	TPC - H	lbm	Redis	K-Means	YCSB
CPU	WL6	Naive Bayes	libquantum	Redis	lbm	Page Rank
	WL7	Grep	TPC-C	Redis	sphinx3	Sort
	WL8	lbm	TPC-H	Redis	Sort	libquantum
LLC	WL9	omnetpp	TPC-H	Redis	Word Count	lbm
	WL10	libquantum	Random I/O	Redis	Grep	povray
	WL11	Redis	povray	Redis	povray	libquantum

Table 4.4: Workload scenarios that have been created from the benchmarks to evaluate Proctor

is introduced after a period of 12 mins.

4.4.2 Proctor Accuracy

We first evaluate end to end accuracy of Proctor in detecting and investigating the source of contention. In this experiment, we execute all the workloads and check whether Proctor is able to detect and identify the source of contention correctly. The findings of this experiment are presented in Figure 4.5, showing the true positive and the false positive rates across our workloads.True positives are the situations during which Proctor identifies performance intrusion when it exists. False positives are the situations during which Proctor identifies performance intrusion when there aren't any. In this graph, false positives represent the percentage of falsely identified metrics compared to the total number of metrics present.

We observe that Proctor detects the interference and investigates its root cause for all the workloads, whenever a performance intrusive VM is introduced into the system, as shown by 100% true positives. In additional, Proctor shows low false positive rate with an average of 8% across our workloads. This experiment show that Proctor is *accurate* in detecting and investigating the source of a performance

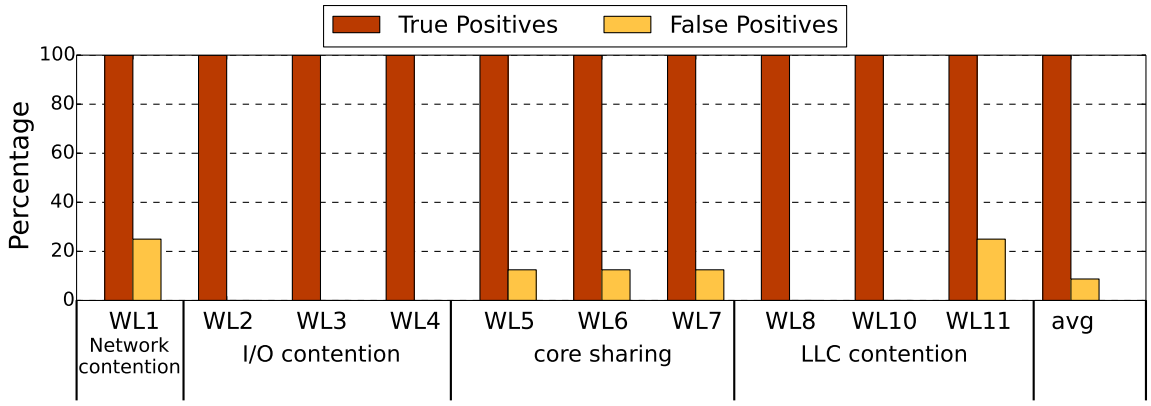

Figure 4.5: Percentage of true and false positives while utilizing Proctor to detect performance issue and identify its root cause.

anomaly, and is fully capable of guiding the remediation techniques for mitigating the performance interference. We now show evaluate the two components of Proctor in more detail.

4.4.3 Detection of Performance Interference

In this section, we evaluate the accuracy and performance of Proctor Performance Degradation Detector (PDD).

Accuracy. One of the main reasons for Proctor's accuracy is its robustness in performing the Detection task by PDD. The median filtering technique is highly effective in minimizing the false positives in detecting performance intrusion. Here, we compare the false positive rate for median filtering against state-of-the-art exponential moving average curve smoothing technique. In this experiment, we measure the false positives for both the techniques just for detecting the performance anomaly across all our workloads. The findings of this experiment are presented in Figure 4.6, showing the number of false positives for both the techniques.

The figure shows that the average number of false positives is around 10× lesser for median filtering as compared to exponential moving average. This is because exponential moving averages are highly affected by extreme values, as described in

Section 4.3.1.2, misinterpreting such noisy events as the performance degradation events. However, median filtering discards such extreme values, thereby reducing the error rate.

Performance. The computational time required for PDD is extremely negligible. The functionalities can be broken down into performing two tasks :- 1) a single subtraction per second per VM for performing step detection and 2) sorting and discarding outliers once in every 30 seconds per VM for performing median filtering. Therefore, PDD has minimal performance impact on VM performance.

4.4.4 Investigating the Performance Degradation

In this section, we evaluate the efficiency of Proctor's Performance Degradation Investigator, in pinpointing the root cause of performance degradation, towards identifying both the VM causing the performance degradation (referred to as contentious VM) and the shared resource for which the applications are competing. In this experiment, we execute each workload with the Proctor runtime system, enabling PDI to investigate performance anomalies. Here, we first show how the QoS metric of VMs affected on the arrival of a contentious VM. The QoS metric of the contentious VM would correlate with the QoS metric of the affected VM. Second, we enumerate the correlation coefficients obtained from correlating the HW performance counter measurements of the contentious VM and the QoS metric of the affected VM. Due to lack of space, we show the results for only 4 workloads, covering the four shared resources most commonly contended in datacenters - Network, I/O, CPU and Last level cache (LLC). The findings of this experiment are presented in 4.7. We show all the five applications only for workload WL1, but show only the contentious and affected VMs for the rest of the workloads for clarity. We now present the evaluation for each source of contention in detail.

Network Contention. We use setup present in WL1 to study network contention,

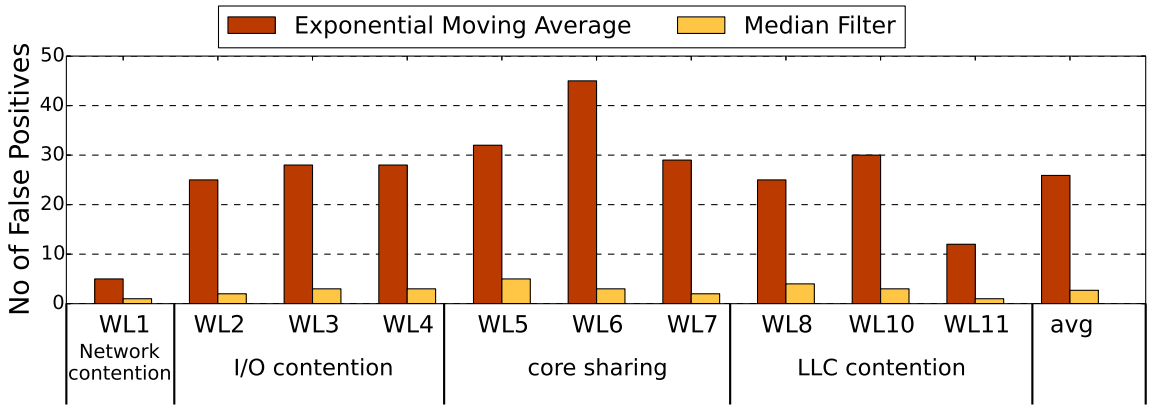

Figure 4.6: Number of falsely identified performance degradation scenarios when exponential moving average/median filtering is utilized to remove noise before step detection

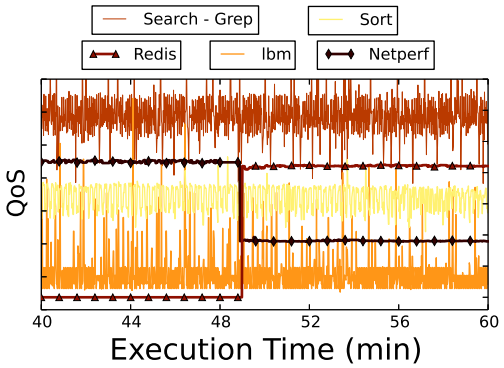

(a) WL1 – Root cause corr 0.97, others corr 0.13

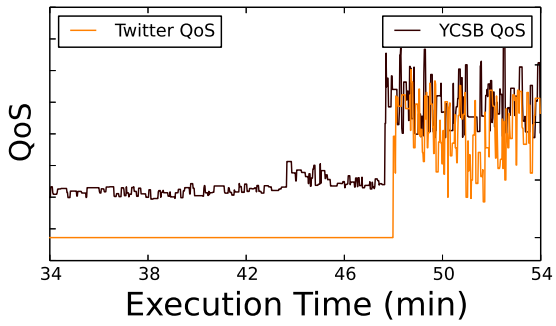

(b) WL2 – Root cause corr 0.87

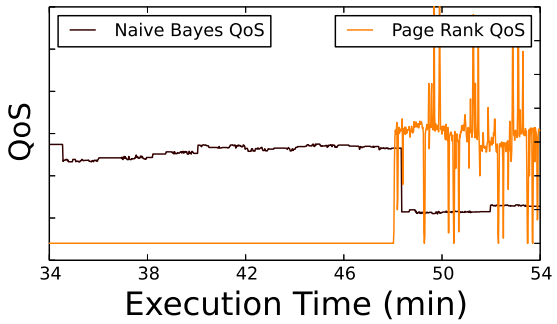

(c) WL6 – Root cause corr 0.83

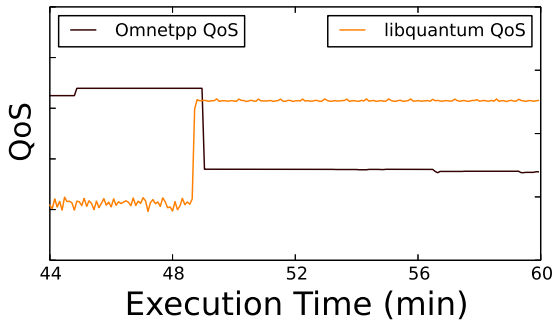

(d) WL9 – Root cause corr 0.93

Figure 4.7: Correlation between primary QoS of affected VM and other co-running VMs

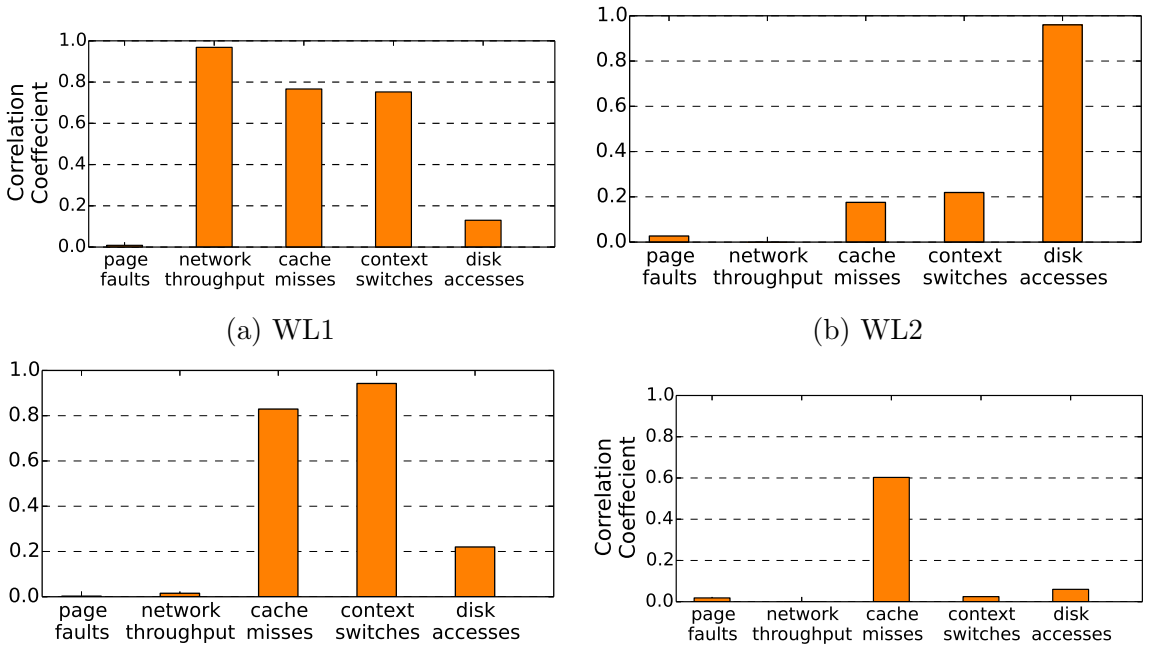

(a) WL1

(b) WL2

(c) WL6

(d) WL9

Figure 4.8: Root cause metrics identified by Proctor.

where contentious VM is executing netperf and the affected VM is executing the application redis. Therefore, we expect a high correlation between the QoS metric of VMs executing redis and netperf. Figure 4.7a illustrates this correlation, showing the QoS metrics for all the five applications in the workload. We observe that the QoS lines represented by Redis and netperf are highly correlated having a correlation coefficient of 0.97, while the correlation coefficient of the QoS metric of redis with other the QoS metric of the other CPU bound applications is very low.

Further, Figure 4.8a shows the correlation coefficients obtained by correlating the QoS metric of redis, the affected VM with HW performance counter measurements collected for the contentious VM netperf. Since netperf puts significant stress on the network, we observe that the correlation coefficient for network throughput is highest, giving substantial evidence that network is the shared resource for which the two VMs are competing for.

Interestingly, we also observe high correlation for the cache misses and the context

switches. Upon further investigation, we found the when netperf starts executing, its CPU based telemetry like cache misses and context switches start giving non-zero measurements compared to zero measurements when it was idle. This directly correlates with the primary QoS metric of the affected VM. As Proctor only looks at the most correlated metric (network throughput in this case), these false positives are ignored while performing the investigation.

I/O Contention. We use the scenario exhibited by WL2 to study Disk I/O contention. Here, Twitter, an I/O latency critical application, is being affected and Yahoo Cloud Serving Benchmark (YCSB) is the contentious application both running in virtualized environments. Therefore, we expect the QoS metric of YCSB to correlate with QoS metric of Twitter application.

We show this correlation in Figure 4.7b. YCSB, being an I/O intensive application, increases the latency of the Twitter drastically. This is because the I/O requests of the throughput intensive I/O applications pollute the I/O queue present in the disk, increasing the access time of the latency critical I/O applications. Therefore, we observe high correlation coefficient of 0.87 between the QoS metrics of YCSB and Twitter application.

Since both are I/O critical applications, sending a large number of disk requests, we expect the I/O to the be shared resource that VMs are competing for. Figure 4.8b shows this investigation where the disk accesses are highly correlated with the QoS of the Twitter application. In this manner, PDI correctly identifies the contentious VM and the shared resource for I/O intensive applications.

CPU Core Sharing. We use the setup present in WL6 for studying contention due to CPU core sharing. In this workload, Naive Bayes is the affected VM and Page Rank is the contentious VM. When a VM executing Naive Bayes is consolidated with a VM executing Google Page Rank in the same physical core, the IPC of Naive Bayes is affected as both of them are CPU intensive and end up time sharing the CPU core.

In this case, we expect a high correlation between the QoS metrics of Naive Bayes and Page Rank applications. We illustrate this interference in Figure 4.7c, showing a high correlation between the QoS metric of Naive Bayes and Google Page Rank. We observe a correlation coefficient of 0.83 in this case.

Similarly, Figure 4.8c shows the metrics correlating with Naive Bayes' QoS when it shares the CPU core with Page Rank algorithm. We observe that context switches, a by-product of CPU core contention, show high correlation.

Interestingly, we also observe that the cache misses show high correlation. This is because when VMs share physical cores, in addition to core resources, they share all private and shared caches as well. This leads to a high correlation between primary QoS of the affected VM with the cache misses of the contentious VM. Again, PDI only looks at the shared resource with the highest correlation and ignore cache misses.

LLC Contention. We use the experimental setup present in WL9 to study LLC contention, where omnetpp is the affected application and lbm is the contentious application. In this scenario, both the applications are cache sensitive and compete for last level cache. Figure 4.7d shows the effect of the arrival of lbm on the QoS of omnetpp application. We observe that when omnetpp is consolidated with a VM executing libquantum in the same server, its primary QoS metric (IPC) drops substantially, resulting in a very high correlation coefficient of 0.93.

Further, we use PDI to investigate the source of contention. Figure 4.8d shows that cache misses of contentious VM have a high correlation with the QoS of affected VM. This is expected as both the applications are cache intensive. PDI's correlation coefficient is able to tell that the cache misses of LLC for libquantum correlates with primary QoS metric of omnetpp.

No Contention. Another interesting experimental setup was conducted to verify if PDD is successful in disregarding false positives when there is no contention. WL10 illustrates a scenario where all the applications do not interfere with each other's

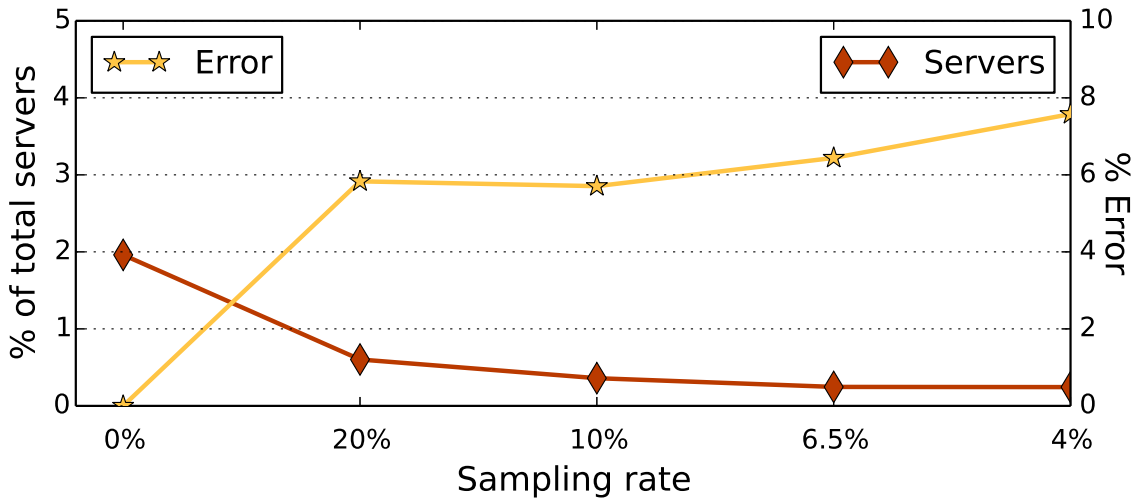

Figure 4.9: No. of Proctor servers required to handle 12800 VMs

performance. In such scenarios, PDD did not trigger a performance degradation at all. This shows the robustness of our technique in disregarding false positives.

These experiments show that PDI is accurate in investigating the source of contention across a wide range of shared resources.

4.4.5 Scalability

One of the key goals of Proctor is to provide a datacenter wide solution towards identifying performance intrusion. In this section, we study how Proctor scales in a large datacenter. In particular, we evaluate the benefits of subsampling when scaled and show that there is a minimal loss in the accuracy of detecting performance intrusive VMs when a sub-sampled data is utilized by Proctor.

For this evaluation, we simulate an environment similar to a datacenter setup capable of executing up to 12800 VMs simultaneously while utilizing 2560 nodes. For this experiment, we collect telemetry data obtained from multiple executions runs for the workload scenarios enumerated in 4.3. We then extrapolate the telemetry to obtain data nearly equivalent to the amount of data that is being collected at large-scale data centers. PDI then queries the large-scale telemetry data to identify the

source of contention. In this experiment, we start with no sampling and then increase the rate of subsampling, calculating the number of servers required to address the PDI requests from 12800 VMs. The findings of this experiment are presented in Figure 4.9, showing the impact of subsampling on datacenter resources (left y-axis).

Our baseline utilizes live telemetry (no sampling) to investigate the root cause of performance intrusion. We observe that the size of telemetry data for 12800 VMs that have been executing for an hour is around 91 GB. The baseline requires 50 servers (2% of production datacenters) to keep up with the requests of 12800 VMs. To reduce the amount of data required for the investigation, PDI uses a robust subsampling technique, that significantly reduces the server resource requirements. As shown in the figure, Proctor at 20% sampling requires only 15 machines, as compared to 50 machines with no sampling. This number reduces to just 6 machines with 4% sampling.

However, aggressive sampling can result in inaccurate results. We show the effect of sampling rate on accuracy error in Figure 4.9 (right y-axis), where accuracy error is measured from the difference between the correlation coefficients obtained by querying the sampled data and corrletaion coefficient obtained from the original data. As shown in the Figure, no sampling has zero error. We observe that subsampling results in low error in the investigation process, increasing the error to just 5% and 8% for 20% and 4.5% samples respectively. In addition, this error gets masked because the VM or the metric having maximum correlation coefficient stays the same before and after sampling. We observe diminishing benefits with more aggressive sub-sampling rate. Hence, we utilize 6.5% sampling as a final parameter for our experiments as it was the sweet spot optimizing for low error and server count overhead.

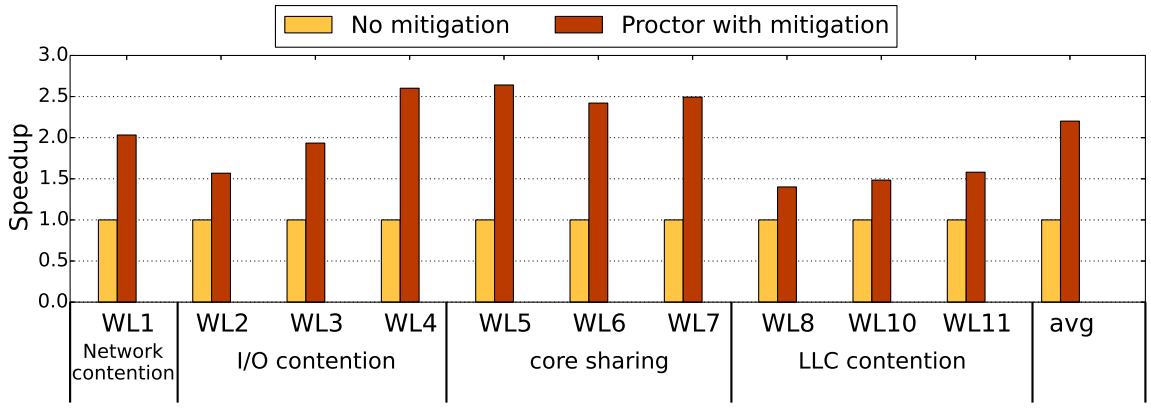

Figure 4.10: Performance improvement due to Proctor runtime system

4.4.6 Putting It All Together

The key use case of Proctor's detection and investigation technique is mitigate VMs that are subjected to performance intrusion. In this section, we demonstrate the benefits brought by Proctor towards this regard. For this study, we couple Proctor's detection and investigation methodology with a simple mitigation technique that migrates the contentious application to another core/physical disk/network channel if Proctor detects a performance anomaly. Our baseline is a system with no performance degradation detection and identification mechanism. Speedup is calculated as the ratio of QoS of the application when its performance is degraded with the QoS of the application after Proctor mitigates the performance intrusive VM at the point when PDD detects intrusion. The findings of this experiment are presented in Figure 4.10, showing the speedup achieved by Proctor for the affected VM as compared to baseline.

We are able to see that in every situation, the presence of Proctor is able to improve the QoS of the affected VMs. For example, Proctor improves the performance of I/O and network intensive workloads on an average of about 2×. This is due to the fact that the latency of I/O intensive workloads are highly affected in many cases due to intrusion. In situations when CPU cores are being shared, IPC is affected minimum 2×. This is primarily due to context switch overhead when two applications share the

same CPU core. On an average, we observe that the presence of Proctor improves the performance of datacenters by 2.2×.

CHAPTER V

GrandSLAm: Guaranteeing SLAs for Jobs at Microservices Execution Framework

Multi-tenant execution has been explored actively in the context of traditional datacenters and cloud computing frameworks towards improving resource utilization [71, 126, 28, 104]. Prior studies have proposed to co-locate high priority latency-sensitive applications with other low priority batch applications [71, 126]. However, multi-tenant execution in a microservice based computing framework would operate on a fundamentally different set of considerations/assumptions since resource sharing can now be viewed at a micro-service granularity rather than at an entire application granularity.

Figure 5.1b illustrates an example scenario in which an end-to-end intelligent personal assistant (IPA) application shares microservice instances with an image based querying application. Each of these applications is constructed as an amalgamation of different microservices (or stages). In such a scenario, requests corresponding to both the IPA and image querying applications share the natural language understanding (Stage 2) and question answering (Stage 3) microservices. As a result, the execution load in these particular microservices increases, thereby causing the latency of query execution in stages 2 and 3 to increase. This increase in latency at specific stages affects the end-to-end latency of the IPA application, thereby violating service level

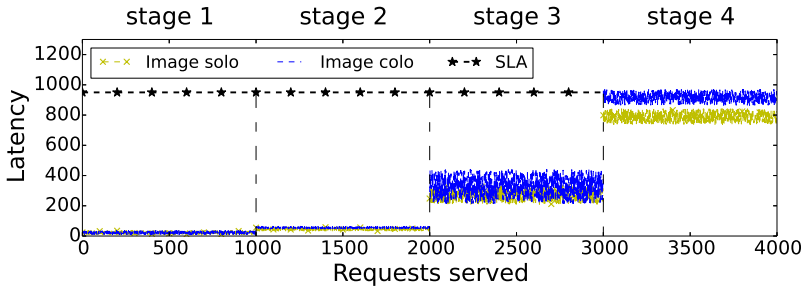

(a) Image application SLA not violated

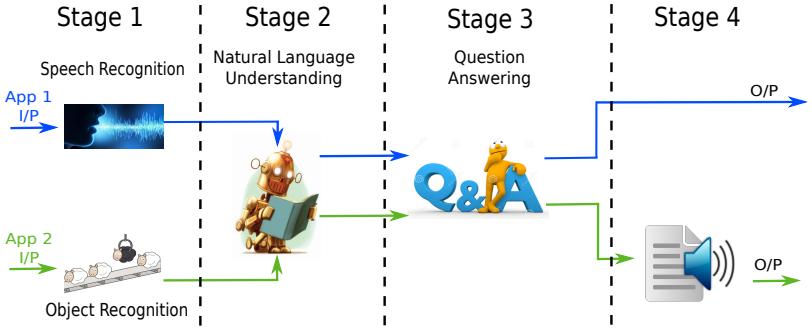

(b) Sharing NLU and QA

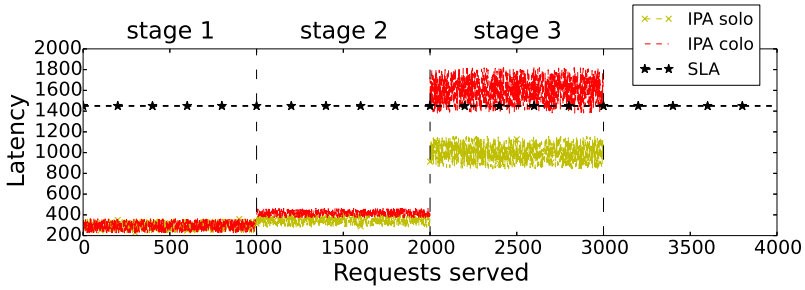

(c) IPA application SLA violated

Figure 5.1: Sharing microservice instances between Image Querying and Intelligent Personal Assistant applications using microservices execution framework

agreements. This phenomenon is illustrated by Figures 5.1c and 5.1a. The x-axis represents the number of requests served while the y-axis denotes latency. Horizontal dotted lines separate individual stages. As can be seen, the QoS violation for the image querying application 5.1a is small, whereas the IPA application suffers heavily from QoS violation. However, our understanding of resource contention need not stop at such an application granularity, unlike traditional private data centers. It can rather be broken down into contention at the microservice granularity, which makes resource contention management a more tractable problem.

This fundamentally different characteristic of microservice environments motivates us to rethink the design of runtime systems that drive multi-tenancy in microservice execution frameworks. Specifically, even in virtualized private data centers, consolidation of multiple latency critical applications is limited as such scenarios can be performance intrusive. In particular, the tail latency of these latency critical applications could increase significantly due to the inter-application interference from sharing the last level cache (LLC) capacity and memory bandwidth [71, 126, 132, 73]. Even in a private datacenter, there is limited visibility into application specific behavior and QoS which makes it hard to even determine the existence of such performance intrusion. As a result, cloud service providers would not be able to meet SLAs in such execution scenarios that co-locate multiple latency critical applications. In stark contrast, the execution flow of requests through individual microservices is much more transparent.

We observe that this visibility creates a new opportunity in a microservice-based execution framework and can enable high throughput from consolidating the execution of multiple latency critical jobs, while still employing fine grained task management to prevent SLA violations. In this context, satisfying end-to-end QoS merely becomes a function of meeting disaggregated partial SLAs at each microservice stage through which requests belonging to individual jobs propagate. However, focusing on each microservice stage's SLAs standalone misses a key opportunity, since we observe that there is significant variation in the request level execution slack among individual requests of multiple jobs. This stems from the variability that exists with respect to user specific SLAs, which we seek to exploit.

In this study, we propose GrandSLAm [61], a holistic runtime framework that enables consolidated execution of requests belonging to multiple jobs in a microservice-based computing framework. GrandSLAm does so by providing a prediction based on identifying `safe` consolidation to simultaneously deliver satisfactory QoS (la-

tency) while maximizing throughput. GrandSLAm exploits the microservice execution framework and the visibility it provides, to build a model that can estimate the completion time of requests at different stages of a job with high accuracy. It then leverages the prediction model to estimate per-stage SLAs using which it 1) ensures end-to-end job latency by reordering requests to prioritize those requests with low computational slack, 2) batches multiple requests to the maximum extent possible to achieve high throughput under the user specified latency constraints. It is important to note that employing each of these techniques standalone does not yield effective QoS and SLA enforcement. An informed combination of request re-ordering with a view of end-to-end latency slack and batching is what yields effective QoS enforcement, as we demonstrate later in the paper.

Our evaluations on a real system deployment of a 6 node CPU cluster coupled with graphics processing accelerators demonstrates GrandSLAm's capability to increase throughput of a datacenter by up to 3× over the state-of-the-art request execution schemes for a broad range of real-world applications. We perform scale-out studies as well that demonstrate increase throughput while meeting SLAs.

5.1 Analysis of Microservices

This section investigates the performance characteristics of applications utitlizing microservice execution frameworks. By utilizing the findings of our investigation, we develop a methodology that can accurately estimate completion time for any given request at each microservice stage prior to its execution. This information becomes beneficial towards safely enabling fine-grained request consolidation when microservices are shared among different applications under varying latency constraints.

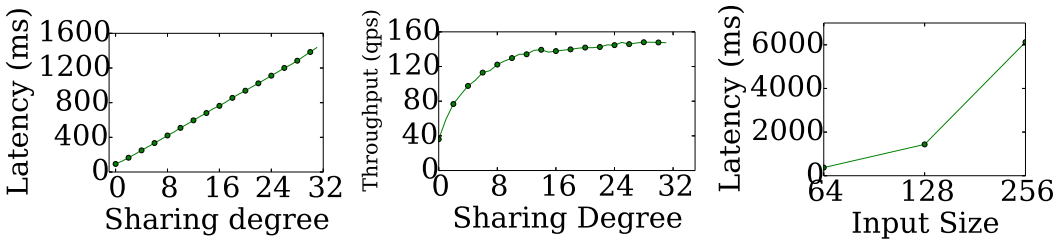

(a) Latency (b) Throughput (c) Input size

Figure 5.2: Increase in latency/throughput/input size as the sharing degree increases

5.1.1 Performance of Microservices

In this section, we analyze three critical factors that determine the execution time of a request at each microservice stage: **(i) Sharing degree (ii) Input size (iii) Queuing Delay**. For this analysis, we select a microservice that performs image classification (IMC).

Sharing Degree. Sharing degree defines the granularity at which requests belonging to different jobs/applications are batched together for execution. A sharing degree of one means that the microservice processes only one request at a time. This situation arises where a microservice instance restricts sharing its resources among requests belonging to other jobs. Requests under this scheme can achieve low latency at the cost of low resource utilization. On the other hand, a sharing degree of thirty indicates that the microservice merges thirty requests into a single batch. Increasing the sharing degree has demonstrated to increase the occupancy/throughput of the underlying computing platform (especially for GPU implementations). However, it has a direct impact on the latency of the executing requests as the first request arriving at the microservice would end up waiting until the arrival of the 30th request (when the sharing degree is 30). Figures 5.2a and 5.2b illustrate the impact of sharing degree on latency and throughput. The inputs that we have used for studying this effect is a set of images of dimension 128x128. The horizontal axes on both figures 5.2a and 5.2b represent the sharing degree. The vertical axis in figure 5.2a and figure 5.2b represents

latency in milliseconds and throughput in requests per second respectively. From figures 5.2a and 5.2b we can clearly see that the sharing degree improves throughput. However, it affects the latency of execution of individual requests as well.

Input size. Second, we observe changes in the execution time of a request by varying its input size. As the input size increases, additional amounts of computation would be performed by the microservices. Hence input sizes play a key role in determining the execution time of a request. To study this using the image classification (IMC) microservice, we obtain request execution times for different input sizes of images from 64x64 to 256x256. The sharing degree is kept constant in this experiment. Figure 5.2c illustrates the findings of our experiment. We observe that as input sizes increase, execution time of requests increase. We also observed similar performance trends for other microservice types.

Queuing delay. The last factor that affects execution time of a requests is queuing delay. This is experienced by requests waiting on previously dispatched requests to be completed.

From our analysis, we observe that there is a linear relationship between the execution time of a request, sharing degree and input size respectively. Queuing delay can be easily calculated at runtime based on execution sequences of requests and the estimated execution time of the preceding requests. From these observations, we conclude that there is an opportunity to build a highly accurate performance model for each microservice that our microservice execution framework can leverage to enable sharing across jobs. Further, we also provide capabilities that can control the magnitude of sharing at every microservice instance. These attributes can be utilized simultaneously for preventing SLA violations due to microservice sharing while optimizing for datacenter throughput.

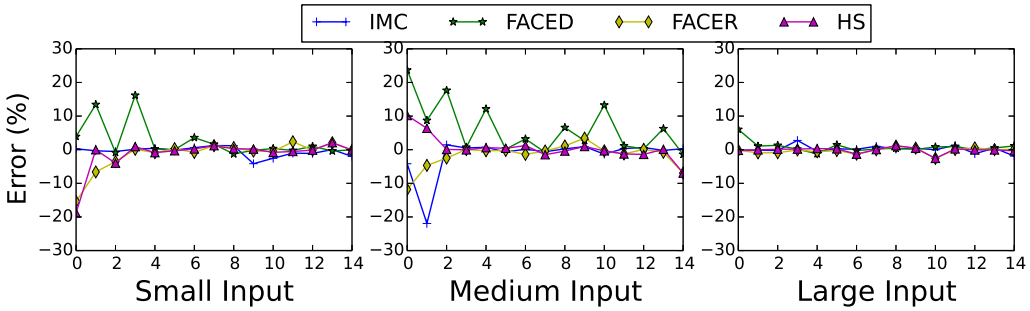

Figure 5.3: Error(%) in predicting ETC for different input sizes with increase in the sharing degree (x-axis)

5.1.2 Execution Time Estimation Model

Accurately estimating the execution time of a request at each microservice stage is a crucial as it drives the entire microservice execution framework. Towards achieving this, we try to build a model that calculates the estimated time of completion (ETC) for a request at each of its microservice stages. The ETC of a request is a function of its compute time on the microservice and its queuing time (time spent waiting for the completion of requests that are scheduled to be executed before the current request).

$$ETC = T_{queuing} + T_{compute} \tag{5.1}$$

We use a linear regression model to determine the $T_{compute}$ of a request, for each microservice type and the input size, as a function of the sharing degree.

$$Y = a + bX \tag{5.2}$$

where X is the sharing degree (batch size) which is an independent variable and Y is the dependent variable that we try to predict, the completion time of a request. b and a are the slope and intercepts of the regression equation. $T_{queuing}$ is determined as the sum of the execution times of the previous requests that need to be completed before the current request can be executed on the microservice which can directly be

determined at runtime.

Data normalization. A commonly followed approach in machine learning is to normalize data before performing linear regression so as to achieve high accuracy. Towards this objective, we rescale the raw input data present in both dimensions in the range of [0, 1], normalizing with respect to the min and max, as in the equation below.

$$x' = \frac{x - min\,(x)}{max\,(x) - min\,(x)} \tag{5.3}$$

We trained our model for sharing degrees following powers of two to create a predictor corresponding to every microservice and input size pair. We cross validated our trained model by subsequently creating test beds and comparing the actual values with the estimated time of completion by our model. Figure 5.3 shows the error rate that exists in predicting the completion time, given a sharing degree for different input sizes. For the image based microservices, the input sizes utilized are images of dimensions 64, 128 and 256 for small, medium and large inputs, respectively. These are standardized inputs from publicly available datasets whose details are enumerated in Table 5.1. As can be clearly observed from the graph, the error in predicting the completion time from our model is around 4% on average. This remains consistent across other microservices too whose plots are not shown in the figure to avoid obscurity.

The estimated time of completion (ETC) obtained from our regression models is used to drive decisions on how to distribute requests belonging to different users across microservice instances. However, satisfying application-specific SLAs becomes mandatory under such circumstances. For this purpose, we seek to exploit the variability in the SLAs of individual requests and the resulting slack towards building our request scheduling policy. Later in section 5.2.2 and 5.2.3, we describe in detail the methodology by which we compute and utilize slack to undertake optimal request

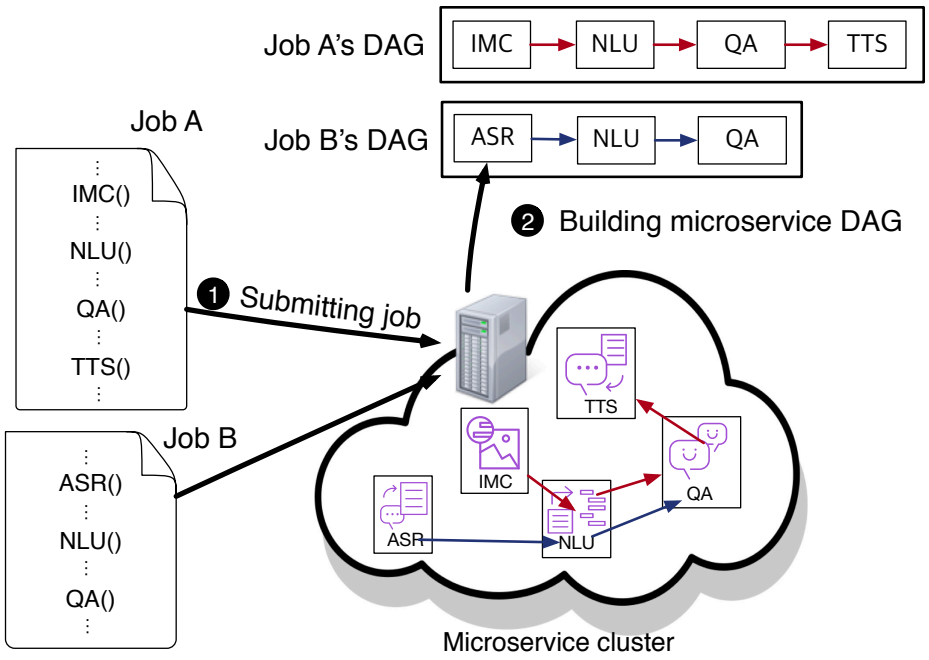

Figure 5.4: Extracting used microservices from given jobs in the microservice cluster

distribution policies.

5.2 GrandSLAm Design

This section presents the design and architecture of GrandSLAm [61], our proposed runtime system for moderating request distribution at microservice execution frameworks. The goal of GrandSLAm is to enable high throughput at microservice instances without violating application specific SLAs. GrandSLAm leverages the execution time predictions from ETC to determine the amount of execution slack different jobs' requests possess at each microservice stage. We then exploit this slack information for efficiently sharing microservices amongst users to maximize throughput while meeting individual users' Service Level Agreements (SLAs).

5.2.1 Building Microservice Directed Acyclic Graph

The first step in GrandSlam's execution flow is to identify the pipeline of microservices present in each job. For this purpose, our system takes the user's job written in a high-level language such as Python, Scala, etc. as an input ❶ in Figure 5.4 and converts it into a directed acyclic graph (DAG) ❷ of microservices. Here, each vertex represents a microservice and each edge represents communication between two microservices (e.g., RPC call). Such DAG based execution models have been widely adopted in distributed systems frameworks like Apache Spark [129], Apache Storm [51] etc. Building a microservice DAG is an offline step that needs to be performed once before GrandSLA's runtime system starts distributing requests across microservice instances.

5.2.2 Calculating Microservice Stage Slack

The end-to-end latency of a request is a culmination of the completion time of the request at each individual microservice stage. Therefore, in order to design a runtime mechanism that provides end-to-end latency guarantees for requests, we take a disaggregated approach. We calculate the partial deadlines at each microservice stage which every request needs to meet at so that end-to-end latency targets are not violated. We define this as microservice stage slack. In other words, microservice stage slack is defined as the maximum amount of time a request can spend at a particular microservice stage. Stage slacks are allocated offline after building the microservice DAG, prior to the start of the GrandSLAm runtime system.

Mathematically slack at every stage is determined by calculating the proportion of end-to-end latency that a request can utilize at each particular microservice stage.

$$slack = \frac{L_m}{L_a + L_b \cdots + L_m + \ldots} \times SLA \tag{5.4}$$

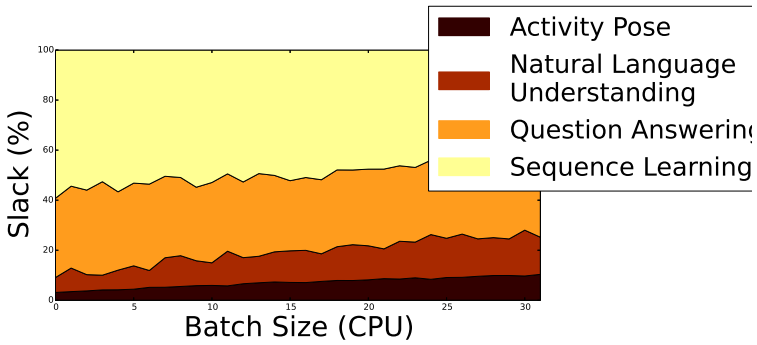

Figure 5.5: Microservice stage slack corresponding to different microservices present in Pose Estimation for Sign Language application

where L_m is the latency of job at stage m and L_a, $L_b \ldots$ are the latency of the same job at the other stages $a, b \ldots$ respectively. Figure 5.5 illustrates the proportion of time that should be allocated at each microservice stage for varying batch sizes, for a real world application called Pose Estimation for Sign Language. We can clearly see from figure 5.5 that the percentage of time a request would take to execute the Sequence Learning stage is much higher than the percentage of time the same request would take to execute the Activity Pose stage. Hence, requests are allocated stage level execution slacks proportionally.

5.2.3 Dynamic Batching with Request Reordering

GrandSLAm's final step is orchestrating requests at each microservice stage based on two main objective functions (i) meeting end-to-end latency (ii) maximizing throughput. For this purpose, GrandSLAm tries to execute every request that is queued up at a microservice stage in a manner at which it simultaneously maximizes the sharing degree while meeting end-to-end latency guarantees. Here, GrandSLAm undertakes two key optimizations: ❶ Request Reordering and ❷ Dynamic batching as depicted in Figure 5.6. GrandSLAm through these optimizations tries to maximize throughput. However, it keeps a check on the latency of the executing job by comparing slack possessed by every request (calculated offline as described at 5.2.2) with its execution

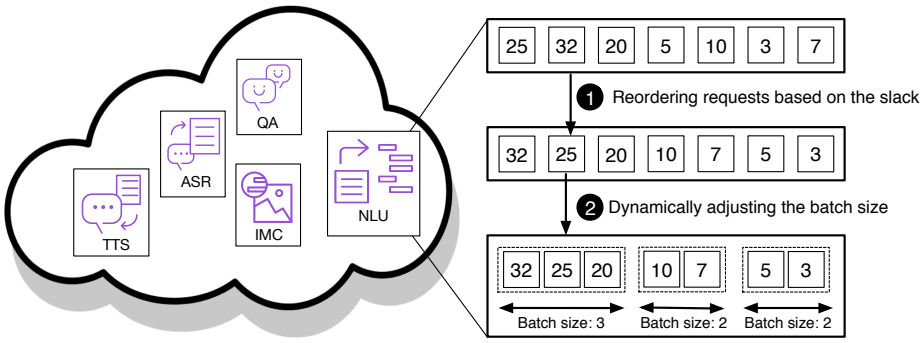

Figure 5.6: Request reordering and dynamic batching mechanism

time estimates obtained from the model described at Section 5.1.2.

Request reordering. Slack based request reordering is performed at each microservice instance by our runtime system. The key objective of our request reordering mechanism is to prioritize the execution of requests with lower slack as they possess much tighter completion deadlines. Hence, our GrandSLAm runtime system reorders requests at runtime that promotes requests with lower slack to the head of the execution queue. The request reordering mechanism in Figure 5.6 illustrates this with an example. Each rectangle is a request present in the microservice execution and the number in each rectangle illustrates its corresponding slack value. On the left, it shows the status before reordering and on the middle, it shows the status after reordering.

Algorithm 1 Dynamic batching algorithm

```
1: procedure DynBatch(Q)                                  ▷ Queue of requests
2:     startIdx = 0
3:     Slack_q = 0
4:     executed = 0
5:     len = length(Q)
6:     while executed ≤ QSize do                          ▷ All are not batched
7:         window = 0
8:         partQ = Q[startidx : length]
9:         window = getMaxBatchSizeUnderSLA(partQ, Slack_q)
10:        startIdx = startIdx + window
11:        Slack_q = Slack_q + latency
12:        executed = executed + window
13:    end while
14: end procedure
```

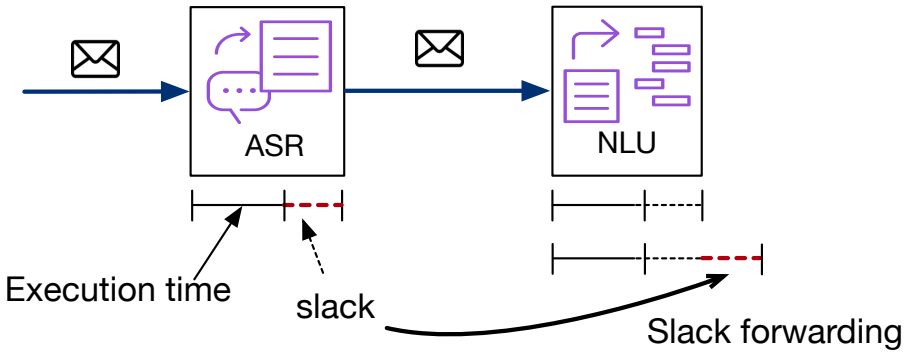

Figure 5.7: Forwarding unused slack in the ASR stage to the NLP stage

Dynamic batching. At each microservice, once the requests have been reordered using slack, we identify the largest sharing degree (actual batch size during execution) that can be employed such that each request meets its stage level SLAs. Such a safe identification of the largest sharing degree is done by comparing the allocated slack obtained by the process described in Section 5.2.2 with the slack estimation model described in Section 5.1.2.

Algorithm 1 summarizes the dynamic batching approach that we employ. The input to the algorithm is a queue of requests sorted by their respective slack values. Starting from the request possessing the lowest slack value we traverse through the queue increasing the batch size. We perform this until increasing batch size violates the sub-stage SLA of individual requests present in the queue. We repeat the request reordering and dynamic batching process continuously as new incoming requests arrive from time to time. Figure 5.6 shows how the dynamic batching is used in our system from the middle part to the right part.

5.2.4 Slack Forwarding

While performing slack based request scheduling in multi-stage jobs, we encounter a common scenario. At the end of each microservice stage, there is some slack that remains unused for a few requests. We reutilize this remaining slack, by performing slack forwarding, wherein we carry forward the unused slack on to the subsequent mi-

Type	Application	Input Sizes	Output	Network	Type	Layers	Parameters
Image Services	Image Classification (IMC)	64X64, 128X128 and 256 X 256 images	Probability of an object	Alexnet	CNN	8	15M
	Face Detection (FACED)		Facial Key Points	Xception	CNN	9	58K
	Facial Recognition (FACER)		Probability of a person	VGGNet	CNN	14	40M
	Human Activity Pose (AP)		Probability of a pose	deeppose	CNN	8	40M
	Human Segmentation (HS)		Presence of a body part	VGG16	CNN	16	138M
Speech Services	Speech Recognition (ASR)	52.3KB, 170.2KB audio	Raw text	NNet3	DNN	13	30M
	Text to Speech (TTS)		Audio output	WaveNet	DNN	15	12M
Text Services	Part-of-Speech Tagging (POS)	text containing 4-70 words per sentence	Words part of speech eg. Noun	SENNA	DNN	3	180K
	Word Chuncking (CHK)		Label Words as begin chunk etc.	SENNA	DNN	3	180K
	Name Entity Recognition (NER)		Labels words	SENNA	DNN	3	180K
	Question Answering (QA)		Answer for question	MemNN	RNN	2	43K
	Sequence Learning (SL)		Translated text	seq2seq	RNN	3	3072
General Purpose Services	NoSQL Database (NoSQL)	Directory input	Output of Query	N/A	N/A	N/A	N/A
	Web Socket Programmig (WS)	Text, image	Data communication	N/A	N/A	N/A	N/A

Table 5.1: Summary of microservices and their funcationality

CPU/GPU config	Microarchitecture
Intel Xeon E5-2630 @2.4 GHz	Sandy Bridge-EP
Intel Xeon E3-1420 @3.7 GHz	Haswell
Nvidia GTX Titan X	Maxwell
GeForce GTX 1080	Pascal

Table 5.2: Experimental platforms

croservice stages. In many scenarios, such a technique ends up deprioritizing requests that had higher priorities in previous stages. This shuffles the queueing time across requests, as they propagate through the execution stages. By the time requests reach the last stage, their cumulative compute and queuing delay (end-to-end delay) becomes fairly consistent meeting the microservice-specific SLA. Figure 5.7 exemplifies the case where the unused slack in the ASR stage can be forwarded into the next microservice stage.

5.3 Evaluation

In this section, we evaluate GrandSLAm's policy and also demonstrate its effectiveness in meeting service level agreements (SLAs), while simultaneously achieving high throughput in datacenters that house microservices.

Application	Description	Microservice DAG
1. IPA-Query	Provides answers to queries that are given as input through voice.	ASR→NLP→QA
2. IMG-Query	Generates natural language descriptions of the images as output.	IMG→NLP→QA
3. POSE-Sign	Analyzes interrogative images and provides answers.	AP→NLP→QA→SL
4. FACE-Security	Scans images to detect the presence of identified humans.	FACED→FACER
5. DETECT-Fatigue	Detects in real time the onset of sleep in fatigued drivers.	HS→AP→FACED→FACER
6. Translation	Performs language translation.	SL QA NoSQL

Table 5.3: Applications used in evaluation

5.3.1 Experimental Environments

Infrastructure. We evlauate GrandSLAm on a testbed consisting of 100 docker containers. Each container has a single 2.4 GHz CPU core, 2GB of RAM and runs Ubuntu 16.10. Executing applications using accelerators has been a common trend [45, 44, 80, 25, 24, 89, 78]. Hence, we evaluate GrandSLAm on both CPU and GPU platforms as enumerated in Table 5.2. We setup a topology of services and processes according to that of **IBM Bluemix** [36]. In other words, each microservice executes on containerized execution environments. We use docker containers for this purpose.

Microservice types. Table 5.1 show the list of microservices that we have utilized in our experiments. POS, CHK and NER microservices utilize the kernels from Djinn&Tonic [43] suite which in turn uses SENNA [26]. Similarly, ASR microservice utilizes kernels from Djinn&Tonic suite [43], which in turn uses Kaldi [88]. IMC, FACED, FACER, AP, HS, QA and SL microservices are implemented using **Tensorflow framework version 1.0** [3]. Using these microservices we build a wide range of applications as shown in Table 5.3. These applications cover a variety of domains incuding Natural Language Processing, Computer Vision and Security [19, 45, 44, 99, 18, 33, 100, 20, 12].

Workload	App1	App2	App3	App4	Shared microservices
WL1	IMG-Query	FACE-Security	DETECT-Fatigue	POSE-Sign	QA, FACED, FACER, AP
WL2	IPA-Query	POSE-Sign	Translation		NLU, QA
WL3	I/O -IPA-Query	I/O-Sign	I/O-Translation		NLU, NoSQL

Table 5.4: Workload scenarios

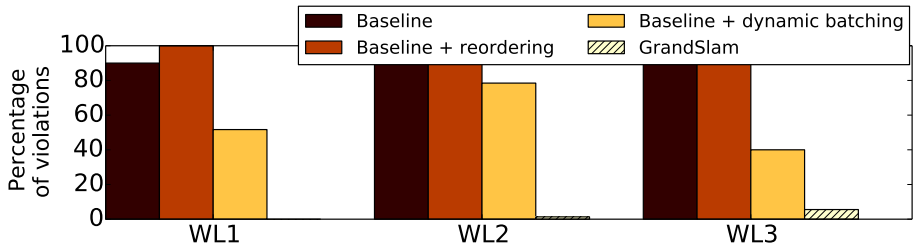

(a) Percentage of requests that violate SLA

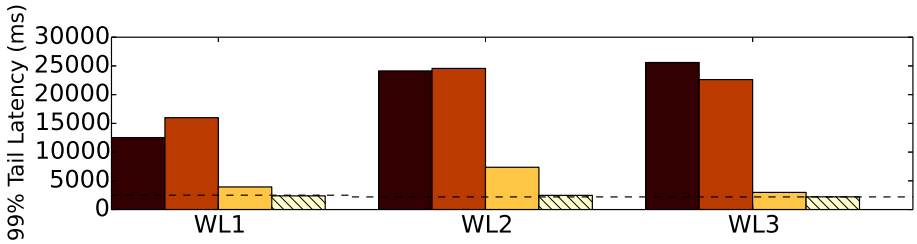

(b) 99th Percentile tail latency of each application

Figure 5.8: Comparing the effect of different components present in GrandSLAm's policy

Load generator/Input. To evaluate the effectiveness of GrandSLAm, we design a load generator that submits user requests following a **Poisson distribution** that is widely used to mimic cloud workloads [75]. The effect of performance degradation at multi-tenant execution scenarios is luminous extensively at servers handling high load. Hence, our experiments are evaluated at scenarios in datacenters where the load is high. Such a distribution has been used by several prior works on multi-stage applications [127, 116, 106]. The SLA that we use for each application is obtained and calculated from the methodology proposed by PowerChief [127]. Table 5.4 shows the workload table and the microservices that are shared when they are executed together. For each microservice request we have evaluated our methodology using inputs that correspond to data that is available from open source datasets.

5.3.2 Achieving Service Level Agreements (SLAs)

First, we evaluate the effectiveness of GrandSLAm in achieving Service Level Agreements (SLAs) for the workload scenarios enumerated in Table 5.4. For this purpose, we incrementally introduce reordering and batching over the baseline system and try to study its effects on the percentage of SLA violations.

5.3.2.1 Reducing SLA violations

For this experiment, we deployed a docker container instance for each microservice type. Communication across microservice instances within the cluster happens through web sockets. Under this experimental setup, we first obtain the % of requests violating SLA under a **baseline scheme** which executes requests (i)in a first-in-first-out (FIFO) fashion (ii)without sharing the microservices. Subsequently, we introduce a request re-ordering scheme that executes requests in an Earliest Deadline First (EDF) fashion to compare it with the baseline system. Similarly, we also execute requests in where requests share microservice instances to see how it improves performance. Lastly, we compare GrandSLAm with these schemes to instantiate its effectiveness. Our experiment keeps the input load constant at fixed Requests per Second (RPS) while comparing each policy.

Figure 5.8 shows the results of this experiment. From figure 5.8a we can clearly see that for a given workload, almost all of the requests violate SLAs under the baseline and reordering policies. However, the effect is much amortized when requests are grouped together in batches. This is because batching can improve the overall latency of a multitude of requests [43] collectively. This is clearly evident from the percentage of requests violated under baseline+dynamic batching policy. GrandSLAm utilizes best of both the policies where it ends up having a low percentage of requests that violate SLA.

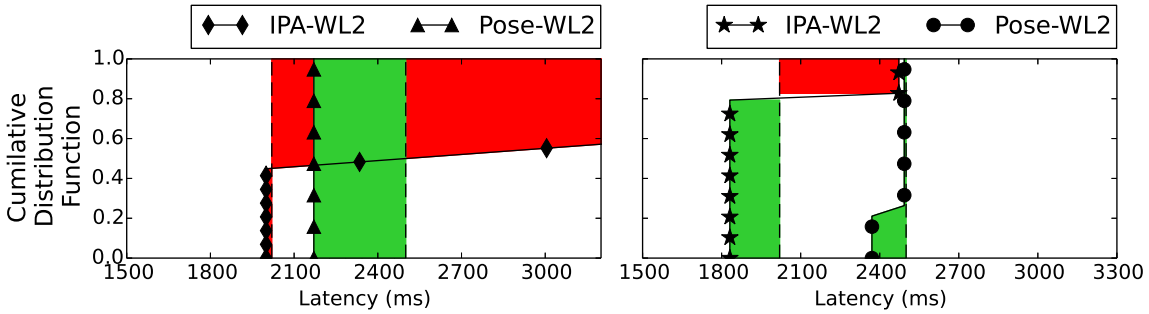

(a) EDF dynamic batching VS GrandSLAm

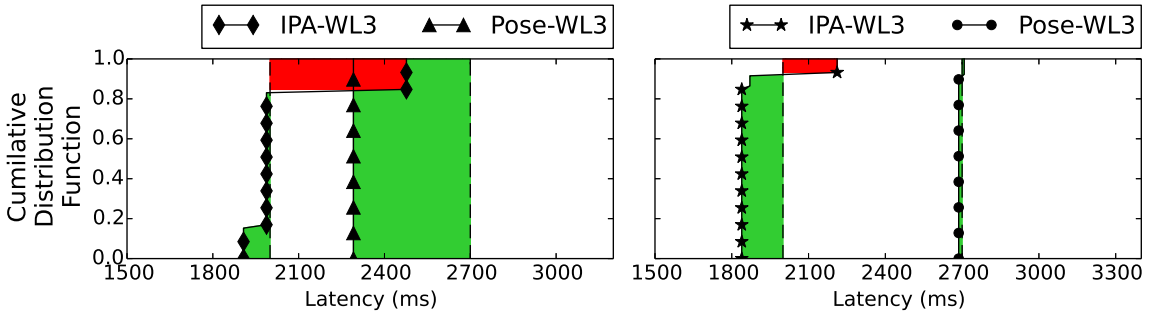

(b) EDF static batching (batch size 50) VS GrandSLAm

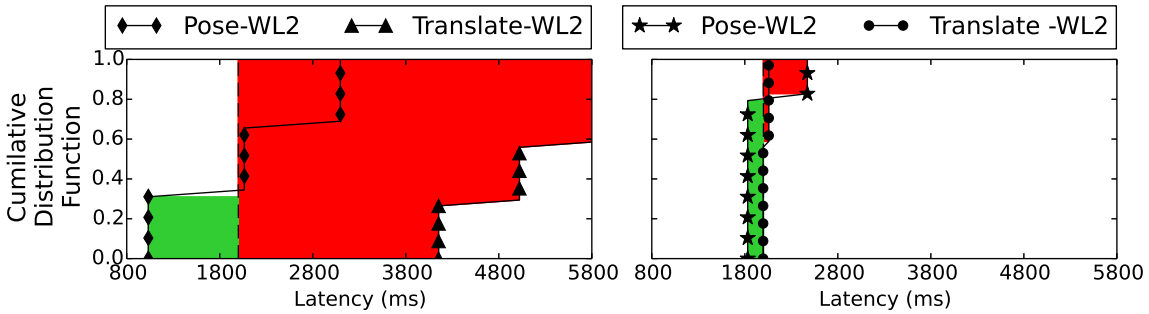

(c) ED dynamic batching VS GrandSLAm

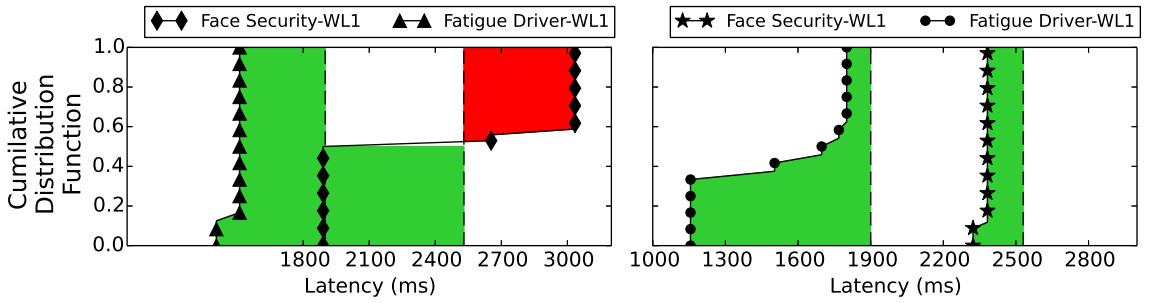

(d) ED static batching (batch size 30) VS GrandSLAm

Figure 5.9: Comparing the cumulative distribution function of latencies for prior approaches and GrandSLAm.

5.3.3 Comparing with prior techniques

Prior approaches which try to solve this problem are categorized based on their respective (i) batching policies for aggregating requests and (ii) slack calculation policies for reordering requests. Most relevant work use a **no-batching policy** where they do not batch multiple requests. Djinn&Tonic [43] utilizes a **static batching policy** where they used a fixed batch size for all applications. However, we propose a dynamic batching technique which varies the batch size based on the slack available for each request. Again, with respect to slack calculation policy, prior approaches [129, 51] utilize a **equal division slack allocation (ED)** policy which equally divides slack across individual microservice stages. Certain other approaches utilize a **first-in-first-out** policy while most approaches utilize **earliest deadline first (EDF)** slack allocation policy [116, 106]. However, we propose a slack calculation policy which allocates slack taking into account the intrinsic variation present in the execution time of different computational stages. This is clearly explained in Section 5.2.2.

We derive 4 baselines on equal division policy. **ED-NB**(equal division no batch) disables batching, **ED-30** and **ED-50** statically fix batch size to 30 and 50 respectively, and **ED-DNB**(equal division dynamic batch) utilizes the dynamic batching approach proposed by GrandSLAm along with the ED policy. We also derive 4 baselines on using earliest deadline first policy: EDF-NB, EDF-30, EDF-50 and EDF-DNB respectively. **EDF-NB** disables batching, **EDF-30** and **EDF-50** statically fix batch size to 30 and 50 while **EDF-DNB** utilizes the dynamic batching proposed by GrandSLAm. GrandSLAm's policy is abbrevated as **GS** in our graphs.

5.3.3.1 Reordering Requests based on Slack

In this subsection, we quantify the effectiveness of GrandSLAm's slack calculation and reordering policy by comparing it with ED and EDF. We illustrate this using the

cumulative distribution function (CDF) of latencies, as shown in Figure 5.9. We have used the same experimental setup where the configuration of the input load and the number of microservice instances remains constant.

Figures 5.9a, 5.9b, 5.9c and 5.9d compare the CDF of the policies EDF dynamic batch (EDF-DYN), EDF constant batch size 50 (EDF-50), ED constant batch size 50 ED-50, and ED dynamic batching (ED-DYN) respectively with GrandSLAm(GS. The horizontal axis denotes time. The vertical axis denotes the CDF of the percentage of requests executed at a particular time. The dashed lines correspond to the target SLAs that individual applications are subjected to meet. For each figure, the graph in the left portrays the CDF of the baseline techniques (EDF-DYN, EDF-50, ED-DYN, and ED-30) and the graph in the right portrays the CDF of GrandSLAm. The green shaded portion illustrates the leftover slack at the final stage when requests execute before the deadline. The red shaded portion illustrates slack violation when requests execute after the deadline has passed. In an ideal case, both green and red portions should be minimized. In other words, requests should be reordered and batched in such a way that it neither passes the deadline nor executes way ahead of the deadline. Executing way ahead of the deadline restricts requests with lower slack to stall creating a situation where other requests end up violating SLAs. In an ideal situation, slack remaining should be transferred to the requests who are about to violate slack. From these graphs, we draw the following conclusion. As shown in figures 5.9a, 5.9b, 5.9c and 5.9d requests reordering policies proposed by prior literature creates a situation where a few requests execute much before the expected deadline while other requests end up violating the SLAs.

Figures 5.9a and 5.9b compares EDF with with GrandSLAm. EDF's slack allocation policy for each request is agnostic to the intrinsic variation present in the microservice execution stages within an application. Hence, in many instances, it underestimates execution times of requests and performs aggressive batching. As a

result of this, some requests complete their execution well ahead of the latency targets while other requests end up violating SLAs. GrandSLAm, on the other hand, avoids this situation by allocating slack that is proportional to the time that would be taken at each stage. GrandSLAm performs judicious batching while limiting aggressive batching by introducing sub-stage SLAs. This is clearly illustrated in Figure 5.9a. Pose and IPA are two applications present in WL2. Under EDF's policy, we see that the requests corresponding to the Pose application complete well ahead of time (as shown in the green patch). However, a substantial number of requests corresponding to the IPA violate SLAs(as shown in the red patch). GrandSLAm, on the other hand, carefully reallocates slack among applications. Hence, the execution of requests with abundant slack is stalled until just before the deadline thereby allowing requests with less amount of slack to be executed, preventing them from violating SLAs. The can clearly be seen in figure 5.9a as the amount of green and red patches are much lesser for GrandSLAm. A similar phenomenon can be witnessed for EDF's static batching policy with batch size 50, as illustrated in Figure 5.9b.

Figures 5.9c and 5.9d compare ED dynamic and static batching with GrandSLAm. The major drawback of the ED technique lies in its inability to gauge the slack that should be allocated in each stage. This is clearly illustrated in Figures 5.9c and 5.9d. In many cases, it wrongly allocates more slack to requests that do not require it, while depriving other requests that actually need slack. This introduces additional queuing time, thereby violating the SLA for a substantial amount of requests. This could be avoided if slack is being distributed judiciously across requests. GrandSLAm is cognizant of this need and hence, predicts the appropriate amount of compute time required for each stage and allocates slack proportionally.

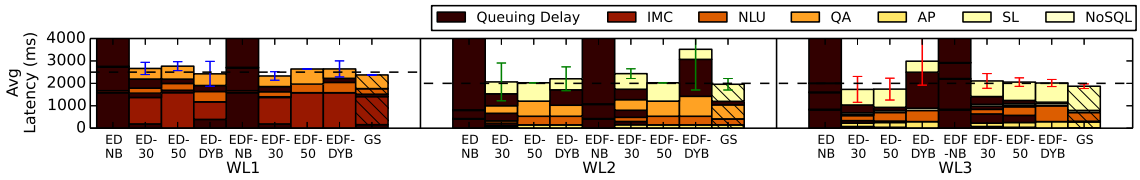

(a) Average Latency

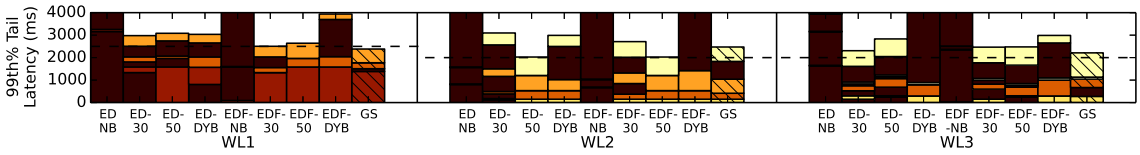

(b) 99th Percentile tail latency

Figure 5.10: Comparing the latency of workloads under different policies. GrandSLAm has the lowest average and tail latency.

5.3.3.2 Dynamic batching for latency reduction

In order to study the effects of dynamic batching, we compare GrandSLAm with all our baseline policies. Figures 5.10 and 5.11 illustrate the results of this experiment. In Each stacked bar in Figure 5.10a and 5.10b represents the average latencies and the tail latencies of the applications respectively. The policies in each figure are ordered starting from ED-NB followed by ED-30, ED-50, ED-DYN, EDF-NB, EDF-30, EDF-50, EDF-DYN concluding with GrandSLAm as GS respectively. GrandSLAm is distinctively distinguished from other bars by hatching it with slanting lines. The color in the stacked graph corresponds to either queuing latency experienced at any stage or the compute latency at individual microservice stages. The different components of this plot are stacked breaking the end-to-end latency as queuing latency or compute stage delay over time (which is why there is a queuing latency stack after each stage). As can be seen in Figure 5.10a, GrandSLAm achieves the lowest latency across all policies. GrandSLAm is able to meet the required SLA for almost every request, as compared to prior policies that violate SLAs for several of these requests. We draw the following insights into why prior policies are ineffective in meeting SLAs.

No batching techniques. The latency of requests is completely dominated by the

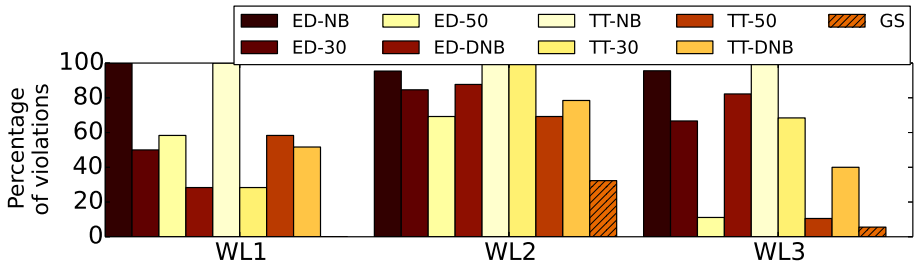

Figure 5.11: Percentage of requests violating SLAs under different schemes

queueing latency when employing techniques that don't perform batching, namely ED-NB and EDF-NB. Hench, such policies are undesirable.

Static batching techniques. In view of the clear disadvantage when requests are not batched, statically batching them is one of the simplest policies that can be employed to improve throughput. However, latencies and SLAs could be compromised if they are not batched judiciously.

Assigning a large fixed batch size for execution can critically violate the latency of many requests within that particular batch. Let us take WL1 for example. From Figure 5.10a and 5.10b we see that employing a fixed batch size (batch size 50) under EDF policy violates SLA only by a small proportion. However, it violates the SLA for most requests present in the workload. This can be seen in Figure 5.11 where the percentage of violations for WL1 under ED-50 goes up to 60%. This is caused because of using a large batch size resulting in a situation where every request ends up violating the SLA especially at the last stage of the application. This is because a fixed batch size is not aware of the latencies and slack of requests that are executing at a point in time. This is an unfavorable outcome especially for applications that require strict latency targets.

To remediate this, employing smaller batch sizes could be viewed as a favorable solution. However, smaller batch sizes can be conservative, thereby not being able to exploit the potential opportunities where aggressive batching can increase throughput while still meeting the latency constraints. Furthermore, small batch sizes could

also cause excessive queuing. Specifically, when requests are grouped with small batch sizes, the first few batches might have low queuing delays. However subsequent batches of requests would end up waiting for a substantial period of time for the execution of prior batches of requests to complete, thereby affecting the end-to-end latency. This increase in queueing latency at the later stages can be clearly seen in situations created by WL2 (from figure 5.10a and 5.10b) where policies ED-30 and EDF-30 violates SLAs both in terms of average latencies as well as tail latencies. Additionally, many requests also violate SLAs as queuing becomes a huge problem due to large batch sizes. This can be seen in figure 5.11. These observations strongly motivate a dynamic batching policy where batch sizes are determined online, during runtime, depending upon each application's latency constraints.

Dynamic batching. Equal Division dynamic batching, Earliest Deadline First dynamic batching and Grand Slam determines appropriate batch sizes during runtime. The difference between these three policies is the way by which they compute slack. Once slack is computed, the largest batch size which accommodates all the requests without violating its slack is obtained during runtime. For Equal Division dynamic batching, slack for each request is a fair share from the SLA for each stage in the end-to-end pipeline. For instance, for an application consisting of 3 stages, each request of that application is estimated to have a slack of 33% of the SLA at each stage. Earliest Deadline first approach, however, undertakes a greedy approach wherein the slack for each request of an application at each stage is the remaining time the request possesses before it would end up violating the SLA. GrandSLAm is unique and distinct from all these mechanisms. We adopt the methodology elaborated in Section 5.2.2 that is cognizant of the volume of computation each individual stage performs.

In Figures 5.10a and 5.10b we clearly see that both Equal Division dynamic batching and Earliest Deadline First dynamic batching perform poorly. This is due to the following reasons. First, the policy that Earliest Deadline First (EDF) utilizes to

determine the appropriate batch size for a set of requests is a greedy policy. EDF dynamically selects batch sizes for the requests aggressively until there is remaining slack. Although this can be beneficial for traditional datacenter applications where execution can only be thought of as single stage and monolithic, such an approach performs poorly at microservice execution framework that possesses multistage execution pipelines. This is due to the fact that when requests reach the final stages of execution, they have a limited amount of slack, which in turn restricts the amount of batching possible to avoid potential SLA violations due to excessive batching. Such a policy has two key downsides, First, it increases the queuing time for subsequent requests thereby increasing the of those requests. This has a negative impact especially on the tail latency of applications as shown in figure 5.10b. Second, it becomes difficult to identify the exact individual stage that was the causing this bottleneck. As a result, the command center will perform non-optimal remediations where unwanted instances would be scaled up leading to high resource utilization. This is experimentally validated in section 5.3.4.2. Third, equal division dynamic batching introduces a fair share of sub-stage SLA for each stage. This can restrict microservices from batching aggressively at a single stage. It can also identify the exact microservice instance that was responsible for end-to-end SLA violation. Such a policy, on the one hand, can address the high tail latency problem that exists in the Earliest Deadline First's aggressive and greedy dynamic batching approach. However, on the other hand, it neglects the fact that the computation time at each stage is very different. Hence, in many scenarios, it does not exploit the full benefits of batching for stages that have high slack. For example, during the final stage in WL2 shown in figure 5.10a and figure 5.10b, if all the requests have been batched, the percentage of requests that would have violated slack would be much lower. However, the equal division policy cannot exploit this opportunity resulting in an increased latency of requests.

GrandSLAm. Our technique, on the other utilizes a hybrid approach by exploiting

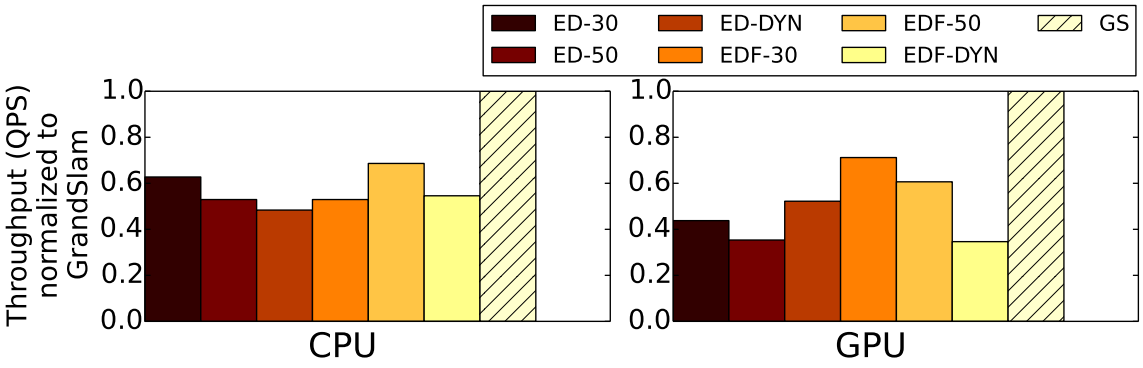

Figure 5.12: Throughput gains from GrandSLAm

the advantages of dynamic batching as well as enabling sub stage cut off slacks. GrandSLAm utilizes a weighted sub-stage SLA slack based on the computational requirements of each stage and an online dynamic batching technique. As a result, GrandSLAm is able to outperform all prior approaches and achieve a much lower average and tail latency as shown in figures 5.10a and 5.10b.

5.3.4 GrandSLAm Performance

In this section, we evaluate GrandSLAm's capability in increasing datacenter throughput and server utilization, while guaranteeing Service Level Agreements (SLAs) for the workload scenarios enumerated in Table 5.4.

5.3.4.1 Throughput Increase

In this section, we demonstrate the throughput benefits of GrandSLAm, as compared to the state-of-the-art techniques at scale-out environments. We compare the different execution policies by constructing a real-time simulational experimental setup consisting of a 1000 node CPU and GPU enabled cluster. As executing AI applications in accelerator platforms is becoming more common, we try to evaluate our technique at both CPU and GPU platforms. For GPU based experiments the executing workloads do not utilize the CPU and are executed only in the GPU de-

vice and vice versa. Additionally, to mimic scale out execution scenarios, we collect performance telemetry of workload scenarios for multiple execution runs. We then extrapolate the performance telemetry to obtain data nearly equivalent to the amount of data being collected at large scale datacenter. On top of that, we build a simulation infrastructure that mimics GrandSLAm's execution model at a larger scale. We also we fix our application specific SLA, instance count and the server configuration across experimental runs. We ensure that every request executing across the end-to-end pipeline meets the latency constraints. Under such situations, we observe the throughput gains corresponding to each execution policy.

Figure 5.12 illustrates the throughput gains of GrandSLAm compared to state of the art execution policies. Each bar represents the average number of Requests executed per Second (RPS) across all the applications and workload scenarios enumerated in Table 5.4, normalized to the average QPS of GrandSLAm. We normalize with respect to GrandSLAm since the best prior technique is different for the CPU and GPU systems. We clearly see that GrandSLAm outperforms other execution policies. The graph on the left is the average throughput for executing the workloads on a CPU cluster while the graph on the right illustrates the results of the same experiment on a GPU platform. An interesting observation consistent across both CPU and accelerator platforms is that the static batching techniques consistently outperform the dynamic batching techniques. This is because, dynamic batching, for instance, in the context of time trader, aggressively batches requests initially. However, requests get stalled during the terminal stages resulting in decreased throughput. On the contrary, equal division misjudges the proportion of slack that is to be allocated. As a result, the policy restricts aggressive batching during scenarios where latency does not take a hit. This results in low throughput. On an average we obtain up to 3× performance on the GPU platform and around 2.2× performance on the CPU server cluster, over the best prior mechanism.

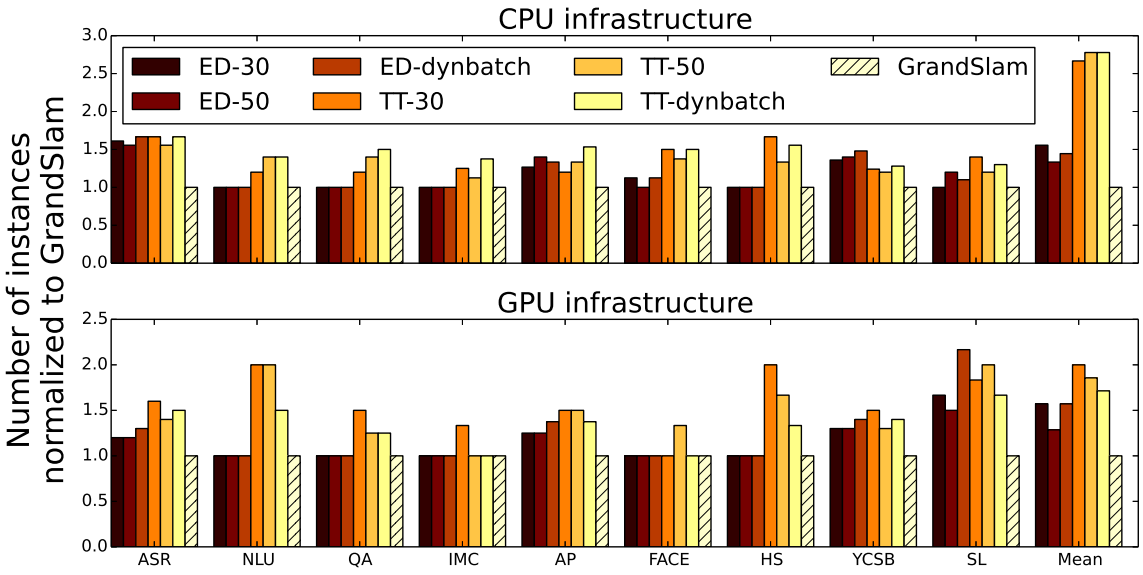

Figure 5.13: Decrease in number of servers due to GrandSLAm

5.3.4.2 Reduced Overheads due to Decreased Instance Propagation

In this section, we illustrate the decrease in the number of microservice instances when employing GrandSLAm's execution policy. Under fixed latency and throughput constraints, we try to obtain the number of microservice instances of each type that is required for executing the workloads enumerated in Table 5.4 in a scale-out fashion similar to section 5.3.4.1.

Figure 5.13 compares the instance count for GrandSLAm and prior works. The top graph corresponds to CPU performance while the bottom graph corresponds to GPU performance. We can see that GrandSLAm reduces instance count significantly on both the CPU and GPU platforms. Additionally, GrandSLAm's instance count reduction is higher on the GPU platform. This is intuitive as GPUs are devices that are optimized to provide high throughput. Overall, we conclude that GrandSLAm is able to effectively meet SLAs while achieving high throughput at low instance counts.

CHAPTER VI

Conclusion

Cloud-scale datacenter management systems utilize virtualization in multi-tenant execution scenarios to provide performance isolation while maximizing the utilization of the underlying hardware infrastructure. However, virtualization does not provide complete performance isolation as Containers/Virtual Machines (VMs) still compete for non-reservable shared resources. This becomes highly challenging to address in datacenter environments housing tens of thousands of VMs, causing degradation in application performance. This dissertation tries to address this problem for production datacenters by providing solutions based on the type of datacenter and the requirements of the tenants that are utilizing the datacenter.

First, I conduct an analysis of performance interference in a multi-core datacenter server to characterize the impact in performance due to sharing of architectural resources. Based in that I designed a runtime system to estimate performance degradation of applications running in datacenter servers. Second, I compartmentalize performance interference based on the type of architectural resource for which applications are contending. Subsequently, I design a mechanism that can detect and identify the source of interference at a tenant level and at the specific resource level. Lastly, I explore and identify an important problem due to multi-tenant execution in microservice execution framework. With that, I design a runtime system to guarantee

SLAs among applications utilizing microservices in a serverless computing platform. This has proved to be useful especially for microservices executing DNN based machine learning algorithms in serverless framework.

BIBLIOGRAPHY

BIBLIOGRAPHY

[1] Private vs public clouds which one to choose. http://www.logicworks.net/blog/2015/03/difference-private-public-hybrid-cloud-comparison/. Accessed: 2015.

[2] Dec 2018.

[3] M. Abadi, A. Agarwal, P. Barham, E. Brevdo, Z. Chen, C. Citro, G. S. Corrado, A. Davis, J. Dean, M. Devin, et al. Tensorflow: Large-scale machine learning on heterogeneous distributed systems. *arXiv preprint arXiv:1603.04467*, 2016.

[4] M. K. Aguilera, J. C. Mogul, J. L. Wiener, P. Reynolds, and A. Muthitacharoen. Performance debugging for distributed systems of black boxes. In *Proceedings of the Nineteenth ACM Symposium on Operating Systems Principles*, SOSP '03, pages 74–89, New York, NY, USA, 2003. ACM.

[5] P. Aguilera, K. Morrow, and N. S. Kim. Fair share: Allocation of gpu resources for both performance and fairness. In *Computer Design (ICCD), 2014 32nd IEEE International Conference on*, pages 440–447. IEEE, 2014.

[6] J. Ahn, C. Kim, J. Han, Y.-R. Choi, and J. Huh. Dynamic virtual machine scheduling in clouds for architectural shared resources. In *Proceedings of the 4th USENIX Conference on Hot Topics in Cloud Ccomputing*, HotCloud'12, pages 19–19, Berkeley, CA, USA, 2012. USENIX Association.

[7] Amazon. Amazon web services User Case Studies. https://aws.amazon.com/solutions/case-studies/. Accessed: 2015-08-12.

[8] Amazon. AWS Case Study: NTT Docomo. http://aws.amazon.com/solutions/case-studies/ntt-docomo/. Accessed: 2015-08-12.

[9] Amazon. AWS Case Study: Penn State. http://aws.amazon.com/solutions/case-studies/penn-state/. Accessed: 2015-08-12.

[10] Amazon. AWS Case Study: PIXNET. http://aws.amazon.com/solutions/case-studies/pixnet/. Accessed: 2015-08-12.

[11] Amazon Inc. Amazon Elastic Compute Cloud(EC2).

[12] S. Avireddy, V. Perumal, N. Gowraj, R. S. Kannan, P. Thinakaran, S. Ganapthi, J. R. Gunasekaran, and S. Prabhu. Random4: An application specific randomized encryption algorithm to prevent sql injection. In *2012 IEEE 11th International Conference on Trust, Security and Privacy in Computing and Communications*, pages 1327–1333, June 2012.

[13] AWS Case Study. NASA/JPL's Desert Research and Training Studies: https://aws.amazon.com/solutions/case-studies/nasa-jpl/.

[14] D. H. Bailey, E. Barszcz, J. T. Barton, D. S. Browning, R. L. Carter, L. Dagum, R. A. Fatoohi, P. O. Frederickson, T. A. Lasinski, R. S. Schreiber, H. D. Simon, V. Venkatakrishnan, and S. K. Weeratunga. The nas parallel benchmarks—summary and preliminary results. In *Proceedings of the 1991 ACM/IEEE Conference on Supercomputing*, Supercomputing '91, pages 158–165, New York, NY, USA, 1991. ACM.

[15] H. Ballani, D. Gunawardena, and T. Karagiannis. Network sharing in multi-tenant datacenters. Technical report, February 2012.

[16] P. Barham, B. Dragovic, K. Fraser, S. Hand, T. Harris, A. Ho, R. Neugebauer, I. Pratt, and A. Warfield. Xen and the art of virtualization. In *ACM SIGOPS operating systems review*, volume 37, pages 164–177. ACM, 2003.

[17] J. Benesty, J. Chen, Y. Huang, and I. Cohen. Pearson correlation coefficient. In *Noise reduction in speech processing*, pages 1–4. Springer, 2009.

[18] C. F. Benitez-Quiroz, R. Srinivasan, Q. Feng, Y. Wang, and A. M. Martinez. Emotionet challenge: Recognition of facial expressions of emotion in the wild. *arXiv preprint arXiv:1703.01210*, 2017.

[19] C. F. Benitez-Quiroz, R. Srinivasan, and A. M. Martinez. Facial color is an efficient mechanism to visually transmit emotion. *Proceedings of the National Academy of Sciences*, page 201716084, 2018.

[20] F. Benitez-Quiroz, R. Srinivasan, and A. M. Martinez. Discriminant functional learning of color features for the recognition of facial action units and their intensities. *IEEE transactions on pattern analysis and machine intelligence*, 2018.

[21] S. Blagodurov, S. Zhuravlev, M. Dashti, and A. Fedorova. A case for numa-aware contention management on multicore systems. In *Proceedings of the 2011 USENIX Conference on USENIX Annual Technical Conference*, USENIXATC'11, pages 1–1, Berkeley, CA, USA, 2011. USENIX Association.

[22] A. D. Breslow, A. Tiwari, M. Schulz, L. Carrington, L. Tang, and J. Mars. Enabling fair pricing on high performance computer systems with node sharing. *Scientific Programming*, 22(2):59–74, 2014.

[23] D. R. K. Brownrigg. The weighted median filter. *Commun. ACM*, 27(8):807–818, Aug. 1984.

[24] Q. Chen, H. Yang, M. Guo, R. S. Kannan, J. Mars, and L. Tang. Prophet: Precise qos prediction on non-preemptive accelerators to improve utilization in warehouse-scale computers. *SIGOPS Oper. Syst. Rev.*, 51(2):17–32, Apr. 2017.

[25] Q. Chen, H. Yang, J. Mars, and L. Tang. Baymax: Qos awareness and increased utilization for non-preemptive accelerators in warehouse scale computers. *SIGPLAN Not.*, 51(4):681–696, Mar. 2016.

[26] R. Collobert, J. Weston, L. Bottou, M. Karlen, K. Kavukcuoglu, and P. P. Kuksa. Natural language processing (almost) from scratch. *CoRR*, abs/1103.0398, 2011.

[27] C. Delimitrou and C. Kozyrakis. Paragon: Qos-aware scheduling for heterogeneous datacenters. In *Proceedings of the Eighteenth International Conference on Architectural Support for Programming Languages and Operating Systems*, ASPLOS '13, pages 77–88, New York, NY, USA, 2013. ACM.

[28] C. Delimitrou and C. Kozyrakis. Paragon: Qos-aware scheduling for heterogeneous datacenters. In *Proceedings of the Eighteenth International Conference on Architectural Support for Programming Languages and Operating Systems*, ASPLOS '13, pages 77–88, New York, NY, USA, 2013. ACM.

[29] A. S. Dhodapkar and J. E. Smith. Comparing program phase detection techniques. In *Proceedings of the 36th Annual IEEE/ACM International Symposium on Microarchitecture*, MICRO 36, pages 217–, Washington, DC, USA, 2003. IEEE Computer Society.

[30] K. Du Bois, S. Eyerman, and L. Eeckhout. Per-thread cycle accounting in multicore processors. *ACM Trans. Archit. Code Optim.*, 9(4):29:1–29:22, Jan. 2013.

[31] E. Ebrahimi, C. J. Lee, O. Mutlu, and Y. N. Patt. Fairness via source throttling: A configurable and high-performance fairness substrate for multi-core memory systems. In *Proceedings of the Fifteenth Edition of ASPLOS on Architectural Support for Programming Languages and Operating Systems*, ASPLOS XV, pages 335–346, New York, NY, USA, 2010. ACM.

[32] S. Elnikety, E. Nahum, J. Tracey, and W. Zwaenepoel. A method for transparent admission control and request scheduling in e-commerce web sites. In *Proceedings of the 13th international conference on World Wide Web*, pages 276–286. ACM, 2004.

[33] C. Fabian Benitez-Quiroz, R. Srinivasan, and A. M. Martinez. Emotionet: An accurate, real-time algorithm for the automatic annotation of a million facial expressions in the wild. In *Proceedings of the IEEE Conference on Computer Vision and Pattern Recognition*, pages 5562–5570, 2016.

[34] E. Forbes, R. Basu, R. Chowdhury, B. Dwiel, A. Kannepalli, V. Srinivasan, Z. Zhang, T. Belanger, S. Lipa, E. Rotenberg, W. R. Davis, and P. D. Franzon. Experiences with two fabscalar-based chips, 2015.

[35] E. Forbes, Z. Zhang, R. Widialaksono, B. Dwiel, R. B. R. Chowdhury, V. Srinivasan, S. Lipa, E. Rotenberg, W. R. Davis, and P. D. Franzon. Under 100-cycle thread migration latency in a single-isa heterogeneous multi-core processor. In *2015 IEEE Hot Chips 27 Symposium (HCS)*, pages 1–1, Aug 2015.

[36] A. Gheith, R. Rajamony, P. Bohrer, K. Agarwal, M. Kistler, B. L. W. Eagle, C. A. Hambridge, J. B. Carter, and T. Kaplinger. Ibm bluemix mobile cloud services. *IBM Journal of Research and Development*, 60(2-3):7:1–7:12, March 2016.

[37] S. Govindan, J. Liu, A. Kansal, and A. Sivasubramaniam. Cuanta: Quantifying effects of shared on-chip resource interference for consolidated virtual machines. In *Proceedings of the 2Nd ACM Symposium on Cloud Computing*, SOCC '11, pages 22:1–22:14, New York, NY, USA, 2011. ACM.

[38] A. Gulati, I. Ahmad, and C. A. Waldspurger. Parda: Proportional allocation of resources for distributed storage access. In *Proccedings of the 7th Conference on File and Storage Technologies*, FAST '09, pages 85–98, Berkeley, CA, USA, 2009. USENIX Association.

[39] A. Gulati, A. Holler, M. Ji, G. Shanmuganathan, C. Waldspurger, and X. Zhu. Vmware distributed resource management: Design, implementation, and lessons learned. *VMware Technical Journal*, 1(1):45–64, 2012.

[40] A. Gupta, J. Sampson, and M. Taylor. Quality time: A simple online technique for quantifying multicore execution efficiency. In *Performance Analysis of Systems and Software (ISPASS), 2014 IEEE International Symposium on*, pages 169–179, March 2014.

[41] F. Guthrie, S. Lowe, and K. Coleman. *VMware vSphere Design*. SYBEX Inc., Alameda, CA, USA, 2nd edition, 2013.

[42] G. Hamerly, E. Perelman, J. Lau, and B. Calder. Simpoint 3.0: Faster and more flexible program phase analysis. *J. Instruction-Level Parallelism*, 7, 2005.

[43] J. Hauswald, Y. Kang, M. A. Laurenzano, Q. Chen, C. Li, R. Dreslinski, T. Mudge, J. Mars, and L. Tang. Djinn and tonic: Dnn as a service and its implications for future warehouse scale computers. In *Proceedings of the 42nd Annual International Symposium on Computer Architecture (ISCA)*, ISCA '15, New York, NY, USA, 2015. ACM. Acceptance Rate: 19

[44] J. Hauswald, Y. Kang, M. A. Laurenzano, Q. Chen, C. Li, T. Mudge, R. G. Dreslinski, J. Mars, and L. Tang. Djinn and tonic: Dnn as a service and its implications for future warehouse scale computers. In *Proceedings of the 42Nd*

Annual International Symposium on Computer Architecture, ISCA '15, pages 27–40, New York, NY, USA, 2015. ACM.

[45] J. Hauswald, M. A. Laurenzano, Y. Zhang, C. Li, A. Rovinski, A. Khurana, R. G. Dreslinski, T. Mudge, V. Petrucci, L. Tang, and J. Mars. Sirius: An open end-to-end voice and vision personal assistant and its implications for future warehouse scale computers. In *Proceedings of the Twentieth International Conference on Architectural Support for Programming Languages and Operating Systems*, ASPLOS '15, pages 223–238, New York, NY, USA, 2015. ACM.

[46] Y. He, S. Elnikety, J. R. Larus, and C. Yan. Zeta: scheduling interactive services with partial execution. In *SoCC*, 2012.

[47] S. Hendrickson, S. Sturdevant, T. Harter, V. Venkataramani, A. C. Arpaci-Dusseau, and R. H. Arpaci-Dusseau. Serverless computation with openlambda. *Elastic*, 60:80, 2016.

[48] S. Hendrickson, S. Sturdevant, T. Harter, V. Venkataramani, A. C. Arpaci-Dusseau, and R. H. Arpaci-Dusseau. Serverless computation with openlambda. In *8th USENIX Workshop on Hot Topics in Cloud Computing (HotCloud 16)*, Denver, CO, 2016. USENIX Association.

[49] J. L. Henning. Spec cpu2006 benchmark descriptions. *SIGARCH Comput. Archit. News*, 34(4):1–17, Sept. 2006.

[50] H. Hoffmann, J. Eastep, M. D. Santambrogio, J. E. Miller, and A. Agarwal. Application heartbeats: A generic interface for specifying program performance and goals in autonomous computing environments. In *Proceedings of the 7th International Conference on Autonomic Computing*, ICAC '10, pages 79–88, New York, NY, USA, 2010. ACM.

[51] M. H. Iqbal and T. R. Soomro. Big data analysis: Apache storm perspective. *International journal of computer trends and technology*, 19(1):9–14, 2015.

[52] C. Isci and M. Martonosi. Phase characterization for power: evaluating control-flow-based and event-counter-based techniques. In *HPCA*, pages 121–132, 2006.

[53] V. Jalaparti, P. Bodik, S. Kandula, I. Menache, M. Rybalkin, and C. Yan. Speeding up distributed request-response workflows. *SIGCOMM Comput. Commun. Rev.*, 43(4):219–230, Aug. 2013.

[54] V. Jalaparti, P. Bodík, S. Kandula, I. Menache, M. Rybalkin, and C. Yan. Speeding up distributed request-response workflows. In *SIGCOMM*, 2013.

[55] V. Jeyakumar, M. Alizadeh, D. Mazières, B. Prabhakar, C. Kim, and A. Greenberg. Eyeq: Practical network performance isolation at the edge. *REM*, 1005(A1):A2, 2013.

[56] A. Jog, E. Bolotin, Z. Guz, M. Parker, S. W. Keckler, M. T. Kandemir, and C. R. Das. Application-aware memory system for fair and efficient execution of concurrent gpgpu applications. In *Proceedings of Workshop on General Purpose Processing Using GPUs*, GPGPU-7, pages 1:1–1:8, New York, NY, USA, 2014. ACM.

[57] J. Jose, M. Li, X. Lu, K. C. Kandalla, M. D. Arnold, and D. K. Panda. Sr-iov support for virtualization on infiniband clusters: Early experience. In *Cluster, Cloud and Grid Computing (CCGrid), 2013 13th IEEE/ACM International Symposium on*, pages 385–392. IEEE, 2013.

[58] E. Kalyvianaki, M. Fiscato, T. Salonidis, and P. Pietzuch. Themis: Fairness in federated stream processing under overload. In *Proceedings of the 2016 International Conference on Management of Data*, pages 541–553. ACM, 2016.

[59] S. Kanev, J. P. Darago, K. Hazelwood, P. Ranganathan, T. Moseley, G.-Y. Wei, and D. Brooks. Profiling a warehouse-scale computer. In *Proceedings of the 42Nd Annual International Symposium on Computer Architecture*, ISCA '15, pages 158–169, New York, NY, USA, 2015. ACM.

[60] S. Kanev, K. Hazelwood, G. Y. Wei, and D. Brooks. Tradeoffs between power management and tail latency in warehouse-scale applications. In *2014 IEEE International Symposium on Workload Characterization (IISWC)*, pages 31–40, Oct 2014.

[61] R. S. Kannan, L. , Subramanian, A. Raju, J. Ahn, L. Tang, and J. Mars. Grandslam: Guaranteeing slas for jobs at microservices execution framework. In *Proceedings of the Fourteenth EuroSys Conference*, EuroSys '19, 2019.

[62] R. S. Kannan, A. Jain, M. A. Laurenzano, L. Tang, and J. Mars. Proctor: Detecting and investigating interference in shared datacenters. In *Performance Analysis of Systems and Software (ISPASS), 2018 IEEE International Symposium on*, pages 76–86. IEEE, 2018.

[63] M. P. Kasick, J. Tan, R. Gandhi, and P. Narasimhan. Black-box problem diagnosis in parallel file systems. In *Proceedings of the 8th USENIX Conference on File and Storage Technologies*, FAST'10, pages 4–4, Berkeley, CA, USA, 2010. USENIX Association.

[64] O. Kayiran, N. C. Nachiappan, A. Jog, R. Ausavarungnirun, M. T. Kandemir, G. H. Loh, O. Mutlu, and C. R. Das. Managing gpu concurrency in heterogeneous architectures. In *2014 47th Annual IEEE/ACM International Symposium on Microarchitecture*, pages 114–126, Dec 2014.

[65] A. Kivity, Y. Kamay, D. Laor, U. Lublin, and A. Liguori. kvm: the linux virtual machine monitor. In *Proceedings of the Linux Symposium*, volume 1, pages 225–230, Ottawa, Ontario, Canada, June 2007.

[66] A. J. Lawrance and P. A. W. Lewis. An exponential moving-average sequence and point process (ema1). *Journal of Applied Probability*, 14(1):98?113, 1977.

[67] H. Li. *Introducing Windows Azure*. Apress, Berkely, CA, USA, 2009.

[68] L. Liu, Y. Li, Z. Cui, Y. Bao, M. Chen, and C. Wu. Going vertical in memory management: Handling multiplicity by multi-policy. In *Proceeding of the 41st Annual International Symposium on Computer Architecuture*, ISCA '14, pages 169–180, Piscataway, NJ, USA, 2014. IEEE Press.

[69] M. Liu and T. Li. Optimizing virtual machine consolidation performance on numa server architecture for cloud workloads. In *Proceeding of the 41st Annual International Symposium on Computer Architecuture*, ISCA '14, pages 325–336, Piscataway, NJ, USA, 2014. IEEE Press.

[70] J. Mars and L. Tang. Whare-map: Heterogeneity in "homogeneous" warehouse-scale computers. In *Proceedings of the 40th Annual International Symposium on Computer Architecture*, ISCA '13, pages 619–630, New York, NY, USA, 2013. ACM.

[71] J. Mars, L. Tang, R. Hundt, K. Skadron, and M. L. Soffa. Bubble-up: Increasing utilization in modern warehouse scale computers via sensible co-locations. In *Proceedings of the 44th Annual IEEE/ACM International Symposium on Microarchitecture (MICRO)*, MICRO-44, pages 248–259, New York, NY, USA, 2011. ACM.

[72] J. Mars, L. Tang, R. Hundt, K. Skadron, and M. L. Soffa. Bubble-up: Increasing utilization in modern warehouse scale computers via sensible co-locations. In *Proceedings of the 44th Annual IEEE/ACM International Symposium on Microarchitecture*, MICRO-44, pages 248–259, New York, NY, USA, 2011. ACM.

[73] S. Marston, Z. Li, S. Bandyopadhyay, J. Zhang, and A. Ghalsasi. Cloud computing - the business perspective. *Decis. Support Syst.*, 51(1):176–189, Apr. 2011.

[74] J. C. McCullough, J. Dunagan, A. Wolman, and A. C. Snoeren. Stout: An adaptive interface to scalable cloud storage. In *Proceedings of the 2010 USENIX Conference on USENIX Annual Technical Conference*, USENIXATC'10, pages 4–4, Berkeley, CA, USA, 2010. USENIX Association.

[75] D. Meisner and T. F. Wenisch. Dreamweaver: Architectural support for deep sleep. *SIGARCH Comput. Archit. News*, 40(1):313–324, Mar. 2012.

[76] O. Mutlu and T. Moscibroda. Stall-time fair memory access scheduling for chip multiprocessors. In *Proceedings of the 40th Annual IEEE/ACM International Symposium on Microarchitecture*, MICRO 40, pages 146–160, Washington, DC, USA, 2007. IEEE Computer Society.

[77] K. Nagaraj, C. Killian, and J. Neville. Structured comparative analysis of systems logs to diagnose performance problems. In *Proceedings of the 9th USENIX Conference on Networked Systems Design and Implementation*, NSDI'12, pages 26–26, Berkeley, CA, USA, 2012. USENIX Association.

[78] V. Nagarajan, R. Hariharan, V. Srinivasan, R. S. Kannan, P. Thinakaran, V. Sankaran, B. Vasudevan, R. Mukundrajan, N. C. Nachiappan, A. Sridharan, K. P. Saravanan, V. Adhinarayanan, and V. V. Sankaranarayanan. Scoc ip cores for custom built supercomputing nodes. In *2012 IEEE Computer Society Annual Symposium on VLSI*, pages 255–260, Aug 2012.

[79] V. Nagarajan, K. Lakshminarasimhan, A. Sridhar, P. Thinakaran, R. Hariharan, V. Srinivasan, R. S. Kannan, and A. Sridharan. Performance and energy efficient cache system design: Simultaneous execution of multiple applications on heterogeneous cores. In *2013 IEEE Computer Society Annual Symposium on VLSI (ISVLSI)*, pages 200–205, Aug 2013.

[80] V. Nagarajan, V. Srinivasan, R. Kannan, P. Thinakaran, R. Hariharan, B. Vasudevan, N. C. Nachiappan, K. P. Saravanan, A. Sridharan, V. Sankaran, V. Adhinarayanan, V. S. Vignesh, and R. Mukundrajan. Compilation accelerator on silicon. In *2012 IEEE Computer Society Annual Symposium on VLSI*, pages 267–272, Aug 2012.

[81] A. A. Nair and L. K. John. Simulation points for spec cpu 2006. In *Computer Design, 2008. ICCD 2008. IEEE International Conference on*, pages 397–403. IEEE, 2008.

[82] R. Nathuji, A. Kansal, and A. Ghaffarkhah. Q-clouds: Managing performance interference effects for qos-aware clouds. In *Proceedings of the 5th European Conference on Computer Systems*, EuroSys '10, pages 237–250, New York, NY, USA, 2010. ACM.

[83] K. J. Nesbit, N. Aggarwal, J. Laudon, and J. E. Smith. Fair queuing memory systems. In *Proceedings of the 39th Annual IEEE/ACM International Symposium on Microarchitecture*, MICRO 39, pages 208–222, Washington, DC, USA, 2006. IEEE Computer Society.

[84] D. Novaković, N. Vasić, S. Novaković, D. Kostić, and R. Bianchini. Deepdive: Transparently identifying and managing performance interference in virtualized environments. In *Proceedings of the 2013 USENIX Conference on Annual Technical Conference*, USENIX ATC'13, pages 219–230, Berkeley, CA, USA, 2013. USENIX Association.

[85] E. S. Page. A test for a change in a parameter occurring at an unknown point. *Biometrika*, 42(3/4):523–527, 1955.

[86] H. Park, S. Baek, J. Choi, D. Lee, and S. H. Noh. Regularities considered harmful: Forcing randomness to memory accesses to reduce row buffer conflicts for

multi-core, multi-bank systems. In *Proceedings of the Eighteenth International Conference on Architectural Support for Programming Languages and Operating Systems*, ASPLOS '13, pages 181–192, New York, NY, USA, 2013. ACM.

[87] N. Partitioning and SR-IOV. Nic partitioning and sr-iov, technology brief by cavium.

[88] D. Povey, A. Ghoshal, G. Boulianne, L. Burget, O. Glembek, N. Goel, M. Hannemann, P. Motlicek, Y. Qian, P. Schwarz, et al. The kaldi speech recognition toolkit. In *IEEE 2011 workshop on automatic speech recognition and understanding*, number EPFL-CONF-192584. IEEE Signal Processing Society, 2011.

[89] A. Putnam, A. Caulfield, E. Chung, D. Chiou, K. Constantinides, J. Demme, H. Esmaeilzadeh, J. Fowers, J. Gray, M. Haselman, S. Hauck, S. Heil, A. Hormati, J.-Y. Kim, S. Lanka, E. Peterson, A. Smith, J. Thong, P. Y. Xiao, D. Burger, J. Larus, G. P. Gopal, and S. Pope. A reconfigurable fabric for accelerating large-scale datacenter services. In *Proceeding of the 41st Annual International Symposium on Computer Architecuture (ISCA)*, pages 13–24. IEEE Press, June 2014.

[90] M. K. Qureshi and Y. N. Patt. Utility-based cache partitioning: A low-overhead, high-performance, runtime mechanism to partition shared caches. In *Proceedings of the 39th Annual IEEE/ACM International Symposium on Microarchitecture*, MICRO 39, pages 423–432, Washington, DC, USA, 2006. IEEE Computer Society.

[91] J. Rao, K. Wang, X. Zhou, and C. zhong Xu. Optimizing virtual machine scheduling in numa multicore systems. In *High Performance Computer Architecture (HPCA2013), 2013 IEEE 19th International Symposium on*, pages 306–317, Feb 2013.

[92] G. Ren, E. Tune, T. Moseley, Y. Shi, S. Rus, and R. Hundt. Google-wide profiling: A continuous profiling infrastructure for data centers. *IEEE Micro*, 30(4):65–79, July 2010.

[93] B. M. Sadler and A. Swami. Analysis of multiscale products for step detection and estimation. *IEEE Transactions on Information Theory*, 45(3):1043–1051, Apr 1999.

[94] T. Sherwood, S. Sair, and B. Calder. Phase tracking and prediction. In *Proceedings of the 30th Annual International Symposium on Computer Architecture*, ISCA '03, pages 336–349, New York, NY, USA, 2003. ACM.

[95] A. Shieh, S. K, A. Greenberg, C. Kim, and B. Saha. Sharing the data center network. In *In NSDI*, 2011.

[96] A. Shieh, S. Kandula, A. G. Greenberg, and C. Kim. Seawall: Performance isolation for cloud datacenter networks. In *HotCloud*, 2010.

[97] J. Y. Shin, M. Balakrishnan, T. Marian, and H. Weatherspoon. Gecko: Contention-oblivious disk arrays for cloud storage. In *Presented as part of the 11th USENIX Conference on File and Storage Technologies (FAST 13)*, pages 285–297, San Jose, CA, 2013. USENIX.

[98] L. Soares, D. Tam, and M. Stumm. Reducing the harmful effects of last-level cache polluters with an os-level, software-only pollute buffer. In *Proceedings of the 41st Annual IEEE/ACM International Symposium on Microarchitecture*, MICRO 41, pages 258–269, Washington, DC, USA, 2008. IEEE Computer Society.

[99] R. Srinivasan, J. D. Golomb, and A. M. Martinez. A neural basis of facial action recognition in humans. *Journal of Neuroscience*, 36(16):4434–4442, 2016.

[100] R. Srinivasan and A. M. Martinez. Cross-cultural and cultural-specific production and perception of facial expressions of emotion in the wild. *IEEE Transactions on Affective Computing*, 2018.

[101] V. Srinivasan, R. B. R. Chowdhury, E. Forbes, R. Widialaksono, Z. Zhang, J. Schabel, S. Ku, S. Lipa, E. Rotenberg, W. R. Davis, and P. D. Franzon. H3 (heterogeneity in 3d): A logic-on-logic 3d-stacked heterogeneous multi-core processor. In *2017 IEEE International Conference on Computer Design (ICCD)*, pages 145–152, Nov 2017.

[102] L. Subramanian, V. Seshadri, A. Ghosh, S. Khan, , and O. Mutlu. The application slowdown model: Quantifying and controlling the impact of inter-application interference at shared caches and main memory. In *Proceedings of the 48th Annual IEEE/ACM International Symposium on Microarchitecture*, MICRO-48. IEEE Computer Society, 2015.

[103] L. Subramanian, V. Seshadri, A. Ghosh, S. Khan, and O. Mutlu. The application slowdown model: Quantifying and controlling the impact of inter-application interference at shared caches and main memory. In *2015 48th Annual IEEE/ACM International Symposium on Microarchitecture (MICRO)*, pages 62–75, Dec 2015.

[104] L. Subramanian, V. Seshadri, A. Ghosh, S. Khan, and O. Mutlu. The application slowdown model: Quantifying and controlling the impact of inter-application interference at shared caches and main memory. In *Proceedings of the 48th International Symposium on Microarchitecture*, MICRO-48, pages 62–75, New York, NY, USA, 2015. ACM.

[105] G. E. Suh, S. Devadas, and L. Rudolph. A new memory monitoring scheme for memory-aware scheduling and partitioning. In *Proceedings of the 8th International Symposium on High-Performance Computer Architecture*, HPCA '02, pages 117–, Washington, DC, USA, 2002. IEEE Computer Society.

[106] L. Suresh, P. Bodik, I. Menache, M. Canini, and F. Ciucu. Distributed resource management across process boundaries. In *Proceedings of the 2017 Symposium on Cloud Computing*, SoCC '17, pages 611–623, New York, NY, USA, 2017. ACM.

[107] L. Tang, J. Mars, and M. L. Soffa. Contentiousness vs. sensitivity: Improving contention aware runtime systems on multicore architectures. In *Proceedings of the 1st International Workshop on Adaptive Self-Tuning Computing Systems for the Exaflop Era*, EXADAPT '11, pages 12–21, New York, NY, USA, 2011. ACM.

[108] L. Tang, J. Mars, W. Wang, T. Dey, and M. L. Soffa. Reqos: Reactive static/dynamic compilation for qos in warehouse scale computers. In *Proceedings of the Eighteenth International Conference on Architectural Support for Programming Languages and Operating Systems*, ASPLOS '13, pages 89–100, New York, NY, USA, 2013. ACM.

[109] S. Tang, B. He, S. Zhang, and Z. Niu. Elastic multi-resource fairness: Balancing fairness and efficiency in coupled cpu-gpu architectures. In *SC16: International Conference for High Performance Computing, Networking, Storage and Analysis*, pages 875–886, Nov 2016.

[110] E. Thereska, H. Ballani, G. O'Shea, T. Karagiannis, A. Rowstron, T. Talpey, R. Black, and T. Zhu. Ioflow: a software-defined storage architecture. In *Proceedings of the Twenty-Fourth ACM Symposium on Operating Systems Principles*, pages 182–196. ACM, 2013.

[111] P. Thinakaran, J. R. Gunasekaran, B. Sharma, M. T. Kandemir, and C. R. Das. Phoenix: a constraint-aware scheduler for heterogeneous datacenters. In *Distributed Computing Systems (ICDCS), 2017 IEEE 37th International Conference on*, pages 977–987. IEEE, 2017.

[112] P. Thinakaran, D. Guttman, M. Kandemir, M. Arunachalam, R. Khanna, P. Yedlapalli, and N. Ranganathan. *Visual Search Optimization*, volume 2, pages 191–209. Elsevier Inc., United States, 7 2015.

[113] P. Thinakaran, J. Raj, B. Sharma, M. T. Kandemir, and C. R. Das. The curious case of container orchestration and scheduling in gpu-based datacenters. In *Proceedings of the ACM Symposium on Cloud Computing*, pages 524–524. ACM, 2018.

[114] A. N. Toosi, R. N. Calheiros, R. K. Thulasiram, and R. Buyya. Resource provisioning policies to increase iaas provider's profit in a federated cloud environment. In *High Performance Computing and Communications (HPCC), 2011 IEEE 13th International Conference on*, pages 279–287, Sept 2011.

[115] T. Ueda, T. Nakaike, and M. Ohara. Workload characterization for microservices. In *2016 IEEE International Symposium on Workload Characterization (IISWC)*, pages 1–10, Sept 2016.

[116] B. Vamanan, H. B. Sohail, J. Hasan, and T. N. Vijaykumar. Timetrader: Exploiting latency tail to save datacenter energy for online search. In *Proceedings of the 48th International Symposium on Microarchitecture*, MICRO-48, pages 585–597, New York, NY, USA, 2015. ACM.

[117] VMware. Vmware.

[118] VMWare. Vmware esxi and esx.

[119] H. J. Wang, J. C. Platt, Y. Chen, R. Zhang, and Y.-M. Wang. Automatic misconfiguration troubleshooting with peerpressure. In *Proceedings of the 6th Conference on Symposium on Opearting Systems Design & Implementation - Volume 6*, OSDI'04, pages 17–17, Berkeley, CA, USA, 2004. USENIX Association.

[120] L. Wang, M. Li, Y. Zhang, T. Ristenpart, and M. Swift. Peeking behind the curtains of serverless platforms. In *2018 USENIX Annual Technical Conference (USENIX ATC 18)*, pages 133–146, Boston, MA, 2018. USENIX Association.

[121] G. Welch and G. Bishop. An introduction to the kalman filter. Technical report, Chapel Hill, NC, USA, 1995.

[122] Wikipedia. Amazon Elastic Compute Cloud. `https://en.wikipedia.org/wiki/Amazon_Elastic_Compute_Cloud`. Accessed: 2015-08-10.

[123] Wikipedia. Hyper-converged infrastructure — wikipedia, the free encyclopedia, 2017. [Online; accessed 5-May-2017].

[124] D. E. Williams. *Virtualization with Xen(Tm): Including XenEnterprise, XenServer, and XenExpress: Including XenEnterprise, XenServer, and XenExpress*. Syngress Publishing, 2007.

[125] W. Xu, L. Huang, A. Fox, D. Patterson, and M. I. Jordan. Detecting large-scale system problems by mining console logs. In *Proceedings of the ACM SIGOPS 22Nd Symposium on Operating Systems Principles*, SOSP '09, pages 117–132, New York, NY, USA, 2009. ACM.

[126] H. Yang, A. Breslow, J. Mars, and L. Tang. Bubble-flux: Precise online qos management for increased utilization in warehouse scale computers. In *Proceedings of the 40th Annual International Symposium on Computer Architecture*, ISCA '13, pages 607–618, New York, NY, USA, 2013. ACM.

[127] H. Yang, Q. Chen, M. Riaz, Z. Luan, L. Tang, and J. Mars. Powerchief: Intelligent power allocation for multi-stage applications to improve responsiveness on

power constrained cmp. In *Proceedings of the 44th Annual International Symposium on Computer Architecture*, ISCA '17, pages 133–146, New York, NY, USA, 2017. ACM.

[128] F. Yates. Contingency tables involving small numbers and the χ 2 test. *Supplement to the Journal of the Royal Statistical Society*, 1(2):217–235, 1934.

[129] M. Zaharia, R. S. Xin, P. Wendell, T. Das, M. Armbrust, A. Dave, X. Meng, J. Rosen, S. Venkataraman, M. J. Franklin, A. Ghodsi, J. Gonzalez, S. Shenker, and I. Stoica. Apache spark: A unified engine for big data processing. *Commun. ACM*, 59(11):56–65, Oct. 2016.

[130] X. Zhang, E. Tune, R. Hagmann, R. Jnagal, V. Gokhale, and J. Wilkes. Cpi2: Cpu performance isolation for shared compute clusters. In *Proceedings of the 8th ACM European Conference on Computer Systems*, EuroSys '13, pages 379–391, New York, NY, USA, 2013. ACM.

[131] X. Zhang, E. Tune, R. Hagmann, R. Jnagal, V. Gokhale, and J. Wilkes. Cpi2: Cpu performance isolation for shared compute clusters. In *Proceedings of the 8th ACM European Conference on Computer Systems*, EuroSys '13, pages 379–391, New York, NY, USA, 2013. ACM.

[132] Y. Zhang, Z. Zheng, and M. Lyu. Exploring latent features for memory-based qos prediction in cloud computing. In *Reliable Distributed Systems (SRDS), 2011 30th IEEE Symposium on*, pages 1–10, Oct 2011.

[133] S. Zhuravlev, S. Blagodurov, and A. Fedorova. Addressing shared resource contention in multicore processors via scheduling. In *Proceedings of the Fifteenth Edition of ASPLOS on Architectural Support for Programming Languages and Operating Systems*, ASPLOS XV, pages 129–142, New York, NY, USA, 2010. ACM.

[134] S. Zhuravlev, S. Blagodurov, and A. Fedorova. Addressing shared resource contention in multicore processors via scheduling. *SIGPLAN Not.*, 45(3):129–142, Mar. 2010.